VIL ENGINEERING STUDIES

STRUCTURAL RESEARCH SERIES NO. 86

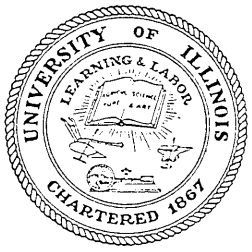

SHEAR DEFLECTION OF WIDE FLANGE STEEL BEAMS IN THE PLASTIC RANGE

By

W. J. HALL

Approved by

N. M. NEWMARK

Technical Report

to

WRIGHT AIR DEVELOPMENT CENTER

UNITED STATES AIR FORCE

Contract No. AF 33(616)-170

Expenditure Order No. R 449-37 AW-7

UNIVERSITY OF ILLINOIS

URBANA, ILLINOIS

SHEAR DEFLECTION OF WIDE FLANGE STEEL BEAMS IN THE PLASTIC RANGE

By

W. J. Hall

Approved by

N. M. Newmark

Technical Report

to

Wright Air Development Center
United States Air Force

Contract No. AF 33(616)-170

Expenditure Order No. R 449-37 AW-7

University of Illinois
Urbana, Illinois
November 1954

TABLE OF CONTENTS

TABLE OF CONTENTS (Continued)

LIST OF TABLES

LIST OF FIGURES

LIST OF FIGURES (Continued)

LIST OF FIGURES (Continued)

SHEAR DEFLECTION OF WIDE FLANGE STEEL BEAMS IN THE PLASTIC RANGE

I. INTRODUCTION

1. Introductory Remarks

The utilization of the reserve plastic strength of steel in structural design applications is a subject which has merited considerable attention in the literature in recent years. Basically there are two different approaches to the design problem, the difference between the two concepts being distinguished by the limiting "failure" criterion which is to be adopted. The conventional elastic design approach considers the theoretical beginning of inelastic action to be the limiting criterion, while the plastic or limit design approach considers the maximum capacity load to be the limiting criterion. In both cases the working value of the load or stress is obtained by dividing the limiting value by a factor, commonly called a safety factor in the former case and a load factor in the latter case. In either instance the working load or stress value normally will fall within the theoretical elastic range.

However, the loads or stresses are not the only considerations to be taken into account. Deflections must be considered in both cases, and often may be the controlling factor in design. Thus it is imperative that it be possible to calculate or at least make an estimate of the deflections under a specified loading in the plastic as well as in the elastic range.

A review of the literature indicates that up to the present time the discussions of the deflection of structures loaded beyond the elastic limit have been restricted to bending alone. In many cases there may be good reasons for such restrictions. Nevertheless, it is important to be able to recognize when shear deflection should be considered, and also to have the concepts and data available which will allow it to be taken into consideration. Aside from mentioning the possible importance of the shear problem, an extremely small amount of work on this aspect is reported in the literature.

2. Object and Scope

The object of this investigation was to study the deformation characteristics of beams subjected to high shear forces. Insofar as possible the data obtained from these tests were correlated with those of other investigations reported in the literature. A brief evaluation of the importance of the shear aspect and its effect on the behavior of beams is presented.

A review of the literature is presented in Section 3. This report does not include a thorough review of the entire plastic design field. Only a few of the general references are cited, and primary attention is devoted to those articles dealing with the shear problem.

For the experimental portion of the investigation it was decided to use one type of beam section. Two continuous beam tests were made. Each beam had sections subjected to pure bending, bending and low shear, and bending and high shear. The tests were carried far into the plastic range. In analyzing the data, it was assumed that

the bending and shear deflections could be separated and that their combined effect could be obtained by superposition. The description of the specimens and apparatus is presented in Part II, and the results and interpretation of the test data are presented in Part III.

Two beam tests alone cannot give a complete picture of the shear problem. Rather, they should be considered as exploratory tests which show what can be expected under the test conditions used. It is hoped that these tests will be of value in plotting the direction of future test programs, if the effect of shear should be considered important. This study shows that the effect is not of great importance except for unusual loading conditions.

Section IV is devoted to a brief discussion of the shear problem. Several illustrations of the effects which high shear forces may have on the behavior of beams are presented.

3. Review of Past Work

The literature is replete with articles bearing on the subject of limit design and methods of utilizing the reserve plastic strength of steel. Since this discussion does not purport to be a survey of the field of plastic analysis as applied to design, only a brief introduction is given to the subject. The majority of the work cited deals with the question of shear and the role it plays in the problem.

Methods for calculating the maximum loads to be carried by steel beams under conditions of pure bending have long been available.

Timoshenko (14)* traces the basic assumptions and concepts for such analysis back to Saint Venant in 1864. The first real attempts at utilizing the plastic properties of mild steel in structural applications started in the 1920's in Europe. Of the pioneer work performed during the period of 1920-1936, a series of tests in Germany by Maier-Leibnitz (11) is of particular interest. The tests involved rolled steel joints, (I-shaped members of 14 cm. depth) tested as continuous beams, with loads of such a magnitude as to initiate inelastic action. Evidently this work was performed to eliminate some of the skepticism regarding beam action when strains exceeded the elastic limit and also to corroborate some of the earlier theoretical work. World War II provided added emphasis (particularly in Great Britain) to the problem of utilizing the additional load-carrying capacity of steel by providing cases for military applications. Attention was focused on the field again in 1948-49 when the well-known works of Van den Broek (15) in this country and Baker (1) in Great Britian were published. A comprehensive historical review of the behavior of mild steel beams under various loading conditions is given in a paper by Roderick and Phillipps (13). Most of the past literature dealing with structural applications of the plastic theory up to 1948 can be traced through the extensive bibliographies contained in each of the articles cited thus far.

In the United States, large-scale experimental work relative to the inelastic behavior of steel structures has been performed at

---

*Numbers in parentheses refer to items in the bibliography.

Lehigh University, and also more recently at the University of Illinois. This work has involved the testing and analysis of columns, beams, joints, and frames. The following papers published on this work are of particular interest since they are related to the subject matter of this report. In Progress Report No. 1, Luxion and Johnston (9) evaluate a number of tests of wide flange beams (8WF31, 8WF40, and 8WF67 sections) tested as simple beams under third-point loading with spans of 12 ft. and 14 ft. Progress Report No. 3 by Yang, Beedle, and Johnston (16) is devoted to a theoretical discussion of the deformation of structures in the plastic range (bending alone) and to criteria for the selection of the full load in plastic design methods. Progress Report No. 5 by Yang, Beedle, and Johnston (17) includes the results of a series of five continuous beam tests (8WF40 and 14WF30 sections with a central span of 14 ft., 7 ft. overhangs, and third-point loading), and the results are discussed on the basis of residual strain measurements. In Progress Report No. 9, Knudson, Yang, Johnston, and Beedle (7) discuss the various methods available for computing the flexural deflection of beams which are loaded into the plastic range. The theoretical and measured deflections are compared for portions of the test data presented in Progress Report No. 5 (17). In Progress Report No. 8, Johnston, Yang, and Beedle (6) evaluate plastic analysis as applied to structural design. They point out the trends in this field and many of the problems which must be considered in the application of plastic analysis.

The literature cited thus far deals with the behavior of beams in which shear forces are low or absent altogether. There is little theoretical or experimental information in the literature on the plastic deformation of structural beam sections in which high shear forces are present. The elastic shear deflection of simple beams is discussed in most strength of materials textbooks. In England the influence of shear forces on the deformation characteristics of I sections has been investigated experimentally by Baker and Roderick (2) and by Hendry (4), and theoretically by Horne (5). In the United States the subject has been mentioned in various articles. In Progress Report No. 8, Johnston, Yang, and Beedle (6) point out some of the implications of shear yielding of the web, present several pictures of beam sections in which the web yielded in shear, and indicate that consideration is being given to the subject at Cambridge and Lehigh. A recent report by Leth (8) is devoted to a theoretical treatment of the problem and for the most part amounts to an extension of Horne's (5) work.

Baker and Roderick (2) describe 14 tests made on 1-1/4 in. x 1-1/4 in. x I/8 in. H sections subjected to two-point loading and tested as simple beams. The distance between the symmetrical loads was kept at 5 in. and the over-all span was varied between 13.5 in. and 7.0 in. in order to increase the shear-moment ratio in the end portions. The beams were prestraightened by cold bending and were stress relieved. No material properties were given, the mode of failure was not described, nor was the manner of putting the load into the beams described. The data showed that as the end span decreases,

the bending moment which corresponds to the limit of proportionality of the load versus center deflection curves decreases. However, they also showed that for the section tested, the bending moment corresponding to collapse only dropped about 7 per cent as the shear increased.* This could be interpreted to mean that the shear force had only little effect on the bending moment (i.e., load-carrying capacity) at collapse.

Hendry (4) presented a summary of the data from tests of 19 simply supported I beams tested with centrally concentrated loads or with two symmetrically spaced loads. Four different cross sections were tested, ranging from 4 in. x 3 in. steel joists to a 1-1/4 in. x I in. I section fabricated by welding two tees together along the middle of the web. The spans were varied to give different shear-moment ratios. Here again no material properties, loading details, or types of failure were given. The author summarized the tests by presenting a table titled "Limits of Application of the Simple Plastic Theory." For various ratios of web area to total section area, the ratios of shear at collapse to shear at general yielding in the web were presented. The value of shear at collapse ranged from 30 per cent above to 20 per cent below that corresponding to general yielding in the web.

The theoretical treatments of the problem by Horne (5) and Leth (8) were admirable attempts to investigate theoretically the effect of shear stresses with reference to the reduction to be expected

---

*Several of the collapse values for the extremely high shear forces were estimates since the capacity of the testing apparatus was exceeded.

in the so-called fully plastic moment.* Horne treated the problem of the bending of a beam (essentially a cantilever beam with a concentrated load at the end) as one of plane stress and used Tresca's yield conditions (maximum shear stress theory) as the limiting criterion. The central elastic core was considered to carry the shear stress. From a knowledge of the stress distribution and propagation, expressions were derived which gave the reductions in moment from the fully plastic value. The results indicated that the reduction was small except for extremely short beams. For example, for an 8 in. x 4 in. RSJ cantilever beam of length L, the reduction in the fully plastic moment amounted to about 4 per cent when $\frac{L}{h} = 2$.

Leth actually extended Horne's work, and, utilizing two stress fields and one velocity field, calculated two lower and one upper bound for the collapse load of a cantilever beam undergoing plastic bending. The results of this analysis were compared with the results of Baker and Roderick and Hendry insofar as possible. For some sections analyzed in Leth's report a possible 30 per cent reduction in collapse load was indicated.

Both Horne and Leth devoted considerable space to outlining the assumptions upon which their work was based, and more particularly to outlining the limitations and shortcomings of the analyses. In short, the elasto-plastic bending of beams is so complex that at present no exact soltuions are available. In both papers it is pointed out clearly at the beginning that the solutions are stress solutions, and no consideration is given to the problem of strain compatibility.

---

*The fully plastic moment concept is discussed in more detail in Section 10 of this report.

4. Acknowledgment

The experimental portions of the work described in this report were performed in the Structural Research Laboratory, Department of Civil Engineering, University of Illinois, during the Fall of 1953 and were financed with research funds available for that purpose from the Engineering Experiment Station of the University of Illinois. The subject matter of this investigation has both a direct relationship to and supplements the static tests which were made in this laboratory as a part of a project sponsored by the Wright Air Development Center, Department of the Air Force, under Contract AF 33(616)-170.

This report has been drawn from a doctoral dissertation of the same title by W. J. Hall which was submitted to the Graduate College of the University of Illinois. The writer wishes to thank his adviser, Dr. N. M. Newmark, Research Professor of Structural Engineering, for his advice and encouragement during the course of the investigation. He also wishes to acknowledge the assistance of Mr. F. L. Howland, Research Associate in Civil Engineering and project director of AF-170, in making arrangements for the publication of this report.

II. DESCRIPTION OF BEAM SPECIMENS AND APPARATUS

5. Description of Specimens and Loading Apparatus

Two continuous beams of 8WF58 as-rolled section were tested as a part of this investigation. Selection of this section was dictated by three considerations: first, from the standpoint of bending alone, it posessed excellent rotation capacity* as attested by its low b/t and h/w values; second, from the standpoint of shear alone, it had a relatively thick web and low h/w value which was desirable for sustaining large shear deformations; third, it was on hand in the laboratory.

The setup for the continuous beam tests is shown schematically in Fig. 1. Figures 35 and 43 are photographs of the actual test setups for beams B1 and B2 respectively. The central span of 9 ft. was maintained in both tests, with the central load points being symmetrically spaced at the one-third points for beam B1 and at the one-sixth points for beam B2. Symmetrical loading was utilized in order to facilitate analysis of the data. Unsymmetrical loading would have made the analysis of the data extremely difficult. This is illustrated by the theoretical examples presented in Section 13.

Both beams were tested to simulate fixed-end beams by utilizing the end cantilever sections to maintain zero rotation at the supports. Following the testing of beam B2 as a continuous beam, the cantilevers

---

*Rotation capacity refers to the ability of a section to sustain the "hinge" moment through the required rotation without failure by local flange buckling or web buckling.

were freed and the central portion was tested in pure bending.*

Two 10WF77 sections placed side by side served as the base beam. The load was applied through a distributing beam to the two central load points by means of the 3,000,000-lb. capacity Baldwin-Southwark hydraulic testing machine in Talbot Laboratory. The distribution of load between the two load points was checked by two "load stubs" which were placed between the distributing beam and the rollers. These load stubs, which were instrumented with SR-4 strain gages, were calibrated before each test. The cantilever ends were loaded by jacks through the ends. The tie rods, which were instrumented with SR-4 strain gages and calibrated before each test, were used to obtain the end load on the cantilevers and thereby the restraining moments for the main span. A single 20-ton Simplex jack was used on each end for beam B1 and a single 50-ton Blackhawk jack was used on each end for beam B2a. The only guides for the tests were situated near the ends of the cantilevers and actually served more as a

---

*The beam descriptions used hereafter are as follows:

B1 refers to the first continuous beam test.

B2 refers to the second continuous beam when no distinction is required regarding the two separate tests performed with this beam.

B2a refers to the first test of beam B2 in which shearing action was studied.

B2b refers to the subsequent pure bending test of the central portion of beam B2.

Each beam had sections under three different types of loading, hereafter referred to as the cantilever sections, the central section, and the shear-moment sections (V-M sections). The latter refers to the portions between the central load points and the reactions.

safety device than as guides. The central portions of the beams were restrained from lateral motion to a considerable extent by the manner in which they were loaded.

The load and reaction brackets were identical, and the same type was used in both tests. Details of the loading brackets are shown in Fig. 2. The brackets were not designed to simulate any particular type of connection. They came closest to resembling a splice plate, although not in the true sense, since the beam was not cut to insert the plates but instead was continuous throughout its entire length. The load plates were slotted to fit the wide flange section and were welded completely around the beam. These load and reaction brackets showed no signs of failure in either test.

6. Instrumentation

Sixty SR-4 wire resistance strain gages were used in beam test B1, and 46 in beam test B2. Gage types A-11, A-5, AR-1, and PA-3 were used. This was the second time that post-yield gages (PA-3) had been used by the structural research group. The highest recorded strain from a post-yield gage was 6.7 per cent, with that particular gage still in service.

Deflection readings were taken at 21 points along beam B1 and at 17 points along beam B2, using Ames dial gages. These gages were mounted on a rig which was supported on the beams at the two reactions.

Measurements of permanent strains were made with Berry and direct reading gages at selected points on the beams. These mechanical strain readings served as check readings and insurance in case certain key strain gages happened to fail.

As an extension to the SR-4 rosette gage readings on the web, measurements of shear detrusion in the shear-moment sections were made by using direct reading gages and gage holes on a 2 in. square spacing. The gage holes were placed symmetrically about the longitudinal axis of the web and on both sides of the web. The lengths of the sides and diagonals were measured with direct reading Ames dial gages. These data were lost in beam test B1 due to faulty gages, but the second test provided valuable information.

The two levels which were used to maintain the end-fixity at the reactions had a sensitivity of 9 seconds per 0.1 in. division.

Whitewash was applied to more than half of the beam in each test to indicate the yielding pattern and the progression of yield zones. Pictures of the yielded portions were taken throughout the test.

7. Section and Material Properties

The section properties of beams B1 and B2 are presented in Table 1. Each beam was cut from an original 20 ft. length. A 2 ft. piece from the end of each length was used to make 9 tension test specimens of 8 in. gage length which were longitudinal with the beam. The test specimens conformed to ASTM specifications as closely as possible.

The results of these coupon tests are summarized in Table 2. The coupon tests were made in a 120,000-lb. Baldwin-Southwark hydraulic testing machine. The strains were recorded automatically with an 8 in. micro-former type strain gage to approximately 0.5 per cent strain. Then the test was momentarily stopped while a C type extensometer with SR-4 gages as the sensing element was placed on the specimen. This gage was used to approximately 10 per cent strain. For strains greater than 10 per cent, dividers were used. All tests were run at a platen speed of 0.20 in./min. which corresponds to a strain rate of approximately 0.02 in./in./min. For use in computing the theoretical moment-rotation ($M-\varphi$) relationship for each beam, a weighted stress-strain curve was calculated from the 9 coupon tests. The values were weighted in proportion to the area they represented as well as their distance from the neutral axis. This appeared to be a rational method of obtaining an over-all average stress-strain curve for the material in the beam. The stress-strain curves derived on this basis are shown in Fig. 3 and Fig. 4.

For beam B1, longitudinal residual strain measurements were made on a 10 in. portion of the beam which was 2-1/2 ft. from the end of the 20 ft. section. Gage holes of 8 in. gage length were drilled at the sections shown in the sketch accompanying Fig. 5. An 8 in. Berry gage was used for the measurements. Three SR-4 gages were applied at the beginning of the procedure as a check, and showed comparable values with those found by the Berry gage. Measurements were taken before the piece was sawed from the beam and then again after the pieces of approximately 1/2 in. thickness were sawed out. This amounted to a relaxation procedure and provided a measure of the residual strains in the longitudinal direction only.

8. Test Procedure

The load increments were selected before each test, although these were adjusted during the test when it was found desirable. The testing procedure consisted of loading with the 3,000,000-lb. machine while at the same time jacking down the ends of the cantilevers to keep the levels centered at the reaction points. When yielding occurs under constant load in the plastic range, it takes considerable time for the beam to come to rest. Under such conditions, when the beam did not come to rest in 15 to 20 minutes, the load was decreased slightly (1 to not more than 2 kips in a total load of 200 to 400 kips) to stop the beam deflection while readings were taken. In this manner it was possible to run the tests in 14 to 16 hours.

A check on the progression of the test during the loading operation was made by continuously monitoring several deflection and strain gages.

III. RESULTS AND INTERPRETATION OF TESTS

9. General Remarks

To fulfill the objectives of this investigation, two continuous beam tests were made. Neither beam had failed by the end of the test. The test of beam B1 was stopped at a load of 269 kips because of a jack failure. At that time the compression flanges inside each reaction, i.e., in the shear-moment section, were just starting to buckle. This buckling was barely visible to the eye. Beam test B2a was carried to a deflection which was thought to be sufficient to obtain the desired data, but at the same time was stopped while the central portion was still in the elastic range. This was done in order to allow the central portion to be used in a pure bending test. No failure of any portion of beam B2a was observed by the end of the test. Following the latter test the cantilever ends were freed and the central section was tested as a simple beam in pure bending. The central section failed by gradual lateral buckling as the test was carried into the strain hardening range.

The pure bending test was made in order to obtain an experimental moment-curvature relationship for comparison with that obtained from the tension test coupon data. Moreover, it was necessary to have fairly reliable moment-curvature information for the analysis of the shear-moment data.

The separate deformation concepts attributed to moment and shear are illustrated in Fig. 6. The basic hypothesis used in the reduction of the moment-shear data is that the bending and shear behavior

can be separated and treated independently in both the elastic and plastic range. In other words, superposition is assumed to hold through the range of response under study. This appears to be the best method of handling the two effects. It is believed that when the data obtained from these tests are used to compute the shear deflection of other similar beams, the predicted deflections will be reasonably accurate. Data for making an estimate of shear deflections when shear forces are high have not previously been available in the literature.

Obviously, space limitations prohibit the inclusion of every scrap of data obtained from such extensive tests. The pertinent data which are relevant to the subject matter of the report are summarized in the tables and figures. In order to make the more basic data from these tests available for study by other investigators, Tables 3, 4, 5, and 6 have been included. These tables give the center load, shear, moment, and deflections at key points for beams B1 and B2a. These data, plus the additional data summarized in the remainder of the report, should give a fairly complete picture of the tests. For the pure bending test, no additional data over and above those in the text are presented, since it is believed that this test is fairly well covered.

Deflection calculations were made by using the numerical integration procedure which is presented in a paper by N. M. Newmark (12). This is the most general procedure available and can give results as accurate as the M-φ diagram which is used. This and other procedures for computing flexural deflections of beams in the plastic range are

discussed in Progress Report No. 9 by Knudson, Yang, Johnston, and Beedle (7). The other procedures described in the latter article employ assumptions as to the propagation of the plastic regions and modifications of the M-φ diagram which tend to simplify the calculations but yield less accurate results. For many design and analysis applications the simpler procedures are admittedly preferable, whereas for most research applications the numerical integration procedure is often the most desirable.

10. Pure Bending

The theory of the pure bending of mild steel beams in the plastic range is based on three assumptions:

a. The flexural strain is distributed linearly over the cross-section of the beam, as in the elastic bending theory.

b. The stress-strain relationship in a bent beam is the same as that determined from a static tension test of a coupon of the material.

c. The stress-strain relationship is the same in compression as it is in tension.

In the elastic range the moment and curvature of a bent beam are related by the following expression:

$$\varphi = \frac{M}{EI}$$

In the plastic range the moment-curvature relationship is obtained from a consideration of the stress and strain conditions assumed to exist in a section of the member. The calculation of the

moment requires a consideration of the stress block assumed to be acting on the section. Since the strain is linearly distributed, the stress block corresponding to a given strain distribution is actually the stress-strain curve (up to the maximum strain) with the strain axis adjusted to one-half the beam depth.

The build-up of the stress block in the simple plastic theory for a mild steel beam is shown in Fig. 7. The linear strain distribution is shown in Fig. 7a. In Fig. 7b the yield point has just been reached at the top and bottom, while in Fig. 7c yielding has penetrated through the flange. In Fig. 7d, strain hardening is just impending at the top and bottom of the section. The stress block in Fig. 7e corresponds to strains well into the strain hardening region. Figure 7f represents the so-called fully plastic stress distribution. The moment corresponding to this stress distribution is called the fully plastic moment (M_{fp}). For a wide flange section the value of the fully plastic moment is very close to that value represented in Fig. 7d when strain hardening is impending. The shape factor, a term commonly encountered in the literature, is the ratio of the fully plastic moment to the moment when yielding is impending. For wide flange beams the shape factor ranges from 1.1 to 1.2. The simple plastic theory usually neglects the strain hardening regions, but to study adequately the deformation of beams which posess large rotation capacity it must be taken into account.

Methods of calculating the M-φ diagram have been presented in many articles, one being Progress Report No. 1 by Luxion and Johnston (9). Only several key values are needed to sketch adequately a M-φ

diagram, and expressions for computing these values are presented in Appendix A. The theoretical M-φ diagrams for beams B1 and B2, computed by the method outlined in Appendix A, and by using the stress-strain curves of Fig. 3 and Fig. 4, are presented in Figs. 9 through 11.

In Figs. 10 and 11 is shown the actual M-φ diagram obtained from beam test B2b, the pure bending test. The curve shown was obtained by a curve-fitting process in which the curvatures were computed so as to make the derived deflections check the measured deflections. A check was obtained by computing the curvatures from the strain gage readings. An independent check on the curve-fitting process was obtained by using the measured deflections and a second order difference equation. All the latter values fell so close to the original curve that they could not be distinguished with the scale used in Fig. 11.

The initial slope of the experimental M-φ curve in Fig. 11 corresponds to an EI value of 69.3×10^5 kip/in.^{2} With I computed to be 232 in.^{4}, E equals 29.9×10^3 kip/in.^{2}, which is reasonable.

It is noted that the experimental curve falls below the theoretical curve through the flat portion and then climbs again toward the theoretical curve in the strain hardening region. The decrease amounts to about 9 per cent of the theoretical value in the flat portion and about 3-1/2 per cent in the strain hardening region. An examination of M-φ diagrams in other publications, Progress Report No. 1 (9) and No. 5 (17) in particular, showed decreases of the same order of magnitude. The experimental M-φ diagram obtained from beam test B2b was used in all computations for beam B2. An adjusted curve (shown in Fig. 9) using the same 9 per cent and 3-1/2 per cent reduction values was used in the computations for beam B1.

A moment-strain curve from beam test B2b is shown in Fig. 24. The strains shown are the average of the top and bottom strains for the section. The curve could be converted to a M-φ diagram by dividing the strain values by one-half the depth of the beam. A moment-strain curve for the central portion of beam B1 is shown in Fig. 22. It breaks over at a moment value somewhat higher than the adjusted curve shown in Fig. 9. Since the test of beam B1 was not carried far enough to obtain higher curvature (and thereby strain values) in the central section, it was felt that the adjusted M-φ curve was satisfactory for deflection computations.

An interesting correlation was noted at this point in the investigation. Progress Report No. 8 (6) contains a comprehensive discussion on mill test tensile coupon data for mild steel, and concludes that a reasonable value of σ_{yp} to use in plastic design is 33,000 lb/sq.in. The flat portion of the experimental M-φ diagram for beam B2b is found to correspond to a σ_{yp} of 32,300 lb./sq.in.

The measured load versus center deflection curve for beam B2b is shown in Fig. 12. Also shown in the same figure is the load deflection curve corresponding to the theoretical M-φ diagram of Fig. 10. It is observed that a slight variation in the M-φ diagram for regions of pure bending can cause considerable differences in deflections. This is particularly true for long spans under pure bending.

The strain distribution at the center of beams B1 and B2b is shown in Fig. 25. It is observed that the strain increases slightly more rapidly in the top (compression) portion during the yielding phase. Apparently this can be attributed to the compressive residual strains which are present in the flanges (See Fig. 5). Later, however, as the strain hardening region is approached, the strain distribution tends to become symmetrical again. This is indicated by the tabulated values in the same figure.

Figures 41 and 42 show the cracked whitewash patterns for beam B1. Yielding (as evidenced by the flaking of the whitewash) started at the outer edges of the top flanges at a load of 206 kips (corresponding to a center moment of about 1700 kip-in.). This would be expected from a study of the residual strain patterns in Fig. 5 which show a compressive residual strain at the outer edge of the flange. At the time beam test B2a was stopped, the central section was still in the elastic range -- the moment in the center was about 1240 kip-in. -- and there was no cracked whitewash. In beam test B2b, the pure bending test, initial yielding as evidenced by the cracking of the whitewash was observed at a load of 190 kips (corresponding to a center moment of about 1710 kip-in.) in the outer edges of the top flanges. Figure 50 shows the cracked whitewash pattern at the end of beam test B2b.

11. Combined Bending and Shear Sections

Since both continuous beams were loaded symmetrically, little or no shear was present in the central sections during the tests. The cantilever sections which were used to maintain the end-fixity of the main span were of such a length that the shear was relatively low in them. Shear yielding did not occur in the web of the cantilever sections in either test. In the regions between the reaction and central load points, the shear forces were of a magnitude to cause shear yielding of the web, and large shear deflections resulted. These latter portions were of primary interest in this investigation. The behavior and analysis of the cantilever sections will be described first, to be followed by a similar treatment of the shear-moment sections.

Figures 13 and 14 show the fixed-end moment versus end deflection relationships for the cantilever sections of beams B1 and B2a. The end load (Q) for the cantilevers is shown in these figures, and can be obtained by dividing the moment by the length of the cantilever (53 in.). The dotted curves represent the deflections as computed from the adjusted M-φ diagrams described in Section 10. These dotted curves also include the component of deflection due to shear, which was elastic throughout and constitutes a practically negligible quantity. The agreement shown for beam B1 is excellent, whereas for beam B2a some discrepancy is noted. Although the reason for the discrepancy in the latter case is not definitely known, it most likely can be accounted for by the fact that the regions adjacent to the ends of the cantilever were undergoing extremely high shear deformations. These high shear deformations were

able to influence the ends of the cantilever sections because the beam was continuous through the reaction and had not been cut at that point. The difference between the deflection curves for the cantilevers (Figs. 13 and 14) and the central portion of beam B2a (Fig. 12) is quite noticeable. In the former case, due to the character of the moment diagram, strain hardening commences immediately and causes the curve to rise immediately after yielding has occurred at the fixed end. In the latter case, since the section must deflect a considerable distance before strain hardening commences, the curve has an extended flat portion.

The strain distribution near the ends of the cantilevers is shown in Fig. 26. The strain distribution is plotted for nearly every other load increment. For higher strains some typical values are tabulated opposite each diagram. These values should be self-explanatory. Both of the sections at which these strains were measured were close to the reactions, and this probably accounts to some degree for the fact that the strains show a nonlinear tendency. The top and bottom strains also were measured at several sections farther from the reactions, and at these locations the strains were nearly equal throughout the test. Moment-strain curves for the cantilever sections are shown in Figs. 21 and 23. The strain values represent the average of the top and bottom strains at a section. It will be observed that these curves have the same shape as the moment-curvature diagrams and can be converted to moment-curvature diagrams by merely dividing the strain values by half the depth of the beam. This is admissible in this case only because the shear was low and did not markedly influence the linear strain

distribution. The bending action of the cantilevers in the plastic range, as evidenced by the formation of the yield patterns in the whitewash, showed the formation of a plastic hinge in its truest sense. Figure 40 is an illustration of this and shows the end of the cantilever section for beam B1 after the test.

The moment-load relationships for the main span of beam B1 and B2a are shown in Figs. 17 through 20. The moment values corresponding to the theoretical beginning of yielding and strain hardening are indicated on the figures. These values are 1648 kip-in. and 1897 kip-in. for M_{yp} and M_{sh} respectively for beam B1, and 1701 kip-in. and 1957 kip-in. respectively for beam B2a. These values correspond to the adjusted M-ϕ curves which are discussed in Section 10. The dotted curves are the theoretical moment-load relationships which would be expected from considerations of flexure alone. The method of computing these theoretical relationships is of interest and will be described briefly. In the elastic range, the ratio between the end moment and moment at the load point was 2 to 1 for beam B1 and 5 to 1 for beam B2a. The latter ratio is recognized as an extremely steep moment gradient. Expressions for the moments in the elastic range can be obtained from any structural handbook. In the plastic range it is necessary to obtain the relationships by a trial and error procedure. This is not difficult since the beam is symmetrically loaded and there is only one unknown. Because of symmetry the slope at the ends and center of the beam must be zero. The procedure consisted of selecting the end moment and altering the moment at the load point until the slope conditions were satisfied. Since shearing deformation does

not affect the moment-load relationship in symmetrically loaded beams, the agreement between the theoretical and experimental curve is, in general, good, as would be expected. A study of the load-moment relationship reveals that there is no appreciable reduction in the resisting moments which can be traced to shear.

Figures 15 and 16, the load versus center deflection curves for beams B1 and B2a, show the effect of the high shear forces on the deflection of the main span. The additional deflection due to the shearing action is outstanding. The dotted curves represent the deflections which would be expected if the deflections were computed on the basis of flexure alone.

Methods of estimating the elastic shear deflection of beams are well known. Fife and Wilbur (3) summarize the test data from some simple beam tests. They conclude that the nominal shear stress value which should be used in the shear strain computation is obtained by dividing the shear by the gross web area (the web thickness times the depth of the beam). This value of shear stress divided by the shearing modulus of elasticity (G) gives the shear strain. The shear strain, which is in units of radians, times the length in question will give the component of deflection due to shear. This is the conventional method of computing the elastic shear deflections of structural beams and gives a reasonable answer. Many refinements can be made by considering more exact stress distributions, and these are presented in many strength of materials and theory of elasticity textbooks.

Throughout this report the web area corresponding to the web thickness times the distance between centers of the flange is used to obtain the average shear stress in the web in the elastic and plastic range. This area is denoted as A_w and is equal to $w(h-t)$.* It is felt that this area is a reasonable value, applicable to shallow beams as well as to deep beams.

One of the objectives of this investigation was to obtain data by means of which an estimate of shearing deflection could be made for wide flange beams loaded into the plastic range. In order to accomplish this aim, several methods were employed to obtain a shear versus shear strain relationship which could be used to predict shear deflections. As explained in Section 9, superposition of bending and shear deflection is assumed to hold in the plastic as well as the elastic range. The first method of obtaining a shear versus shear strain curve was to compute the deflections due to flexure alone, to subtract these deflections from the measured deflections, and to assume that the difference was due to shear. These differences in deflection were divided by the length between the deflection points to obtain a measure of the shear strain. Shear strain values were also computed from a number of rosette gage sets which were mounted symmetrically on both sides of the web of the beam. For a given symmetrical pair of rosette gages the strain readings for corresponding arms were averaged and these were used in the rosette strain analysis. In order to extend the range

---

*See the list of notation.

of the shear strain data obtained from the rosette gages, the series of gage holes described in Section 6 were placed on both sides of the web. From measurements of the lengths of the sides and diagonals of the square gage grids at various loads, the angle changes in the square grids were computed by trigonometry. Since the grids were symmetrical about the mid-line of the web, the angle changes were the shear deformations. The measurements were lost on beam test B1 due to faulty gages. The grid and deflection gage layout used in obtaining these shear strain data is illustrated in Fig. 31. Figures 27 through 33, exclusive of Fig. 31, represent the shear strain data obtained from beam tests B1 and B2a. The position of the rosette strain gages is shown in Fig. 33. These shear versus shear strain data were plotted to two different scales. The smaller scale was used to show the entire curve while the large scale was used to expand the initial portions of the curves. The shear versus shear strain diagrams obtained by the three methods show excellent agreement. A method of utilizing this information to compute the shear deflections of other beam sections is presented in Section 12.

Figures 22 and 24 show the moment-strain relationships at a section in beams B1 and B2a. The strain values shown are the average of the top and bottom strains. The break-over in the curves corresponds to the same load at which there is a sharp break in the load deflection curves for the corresponding beams (Figs. 15 and 16). These moment-strain curves have little significance. They are presented to show that a general shear yielding of the web does markedly influence the strains in the flanges. They should not be interpreted as an equivalent moment-curvature relationship for the shear-moment section since a study of

other strain data taken in this region shows a different shaped curve to exist for each section. The longitudinal strain distribution in the shear-moment sections is extremely erratic. Rather than plot the strain distribution at typical sections to show the erratic nature that can be expected, the strain values are recorded in Table 8 for one cross-section of each beam. The relaxation in some of the strain values at certain loads can be explained by noting the decrease in the moment at the section. These fluctuations in the moment values are occasioned by a change in the moment gradient as yielding occurs at the reactions and load points. If nothing else, this information tends to emphasize the fact that the strain distribution is extremely complicated in short sections. Moreover, the boundary conditions which are representative of the manner in which the load is put into the beam obviously have a large influence on the strain distribution.

The SR-4 strain gage rosettes which were placed on the web of the beam primarily to obtain shear strain data in the plastic range also provided some information on the elastic shear stress distribution. As explained previously, the strain values for individual arms of symmetrically placed gages on each side of the web were averaged and used in the computations. The shear stress values from the rosettes are tabulated in Table 7. Also tabulated are the VQ/Ib values and V/A_w values. As expected, the greatest discrepancy between the rosette and theoretical shear stress values occurs for those rosettes nearest the reaction or load points.

Figures 36 through 39 show the progression of yielding in the shear-moment section for beam B1. Flaking of the whitewash was initially observed at a load of 50.5 kips at both the reaction and load ends of the section in the web corners under compressive bending stress. This is to be expected since the residual strains in the web are of a compressive nature.

Figures 45 through 49 show the progression of shear yielding in the web of the shear-moment section of beam B2a. Here again initial yielding started at a low load (30 kips). The yield patterns were noted to be almost identically symmetrical on either side of the web. Figure 44 shows one of the shear-moment sections of beam B2a after the test. The early yielding in these compression areas was also evidenced in both beams by the rosette gages in the corresponding instrumented shear-moment sections. This is illustrated in Fig. 33 where the shear strains for the rosette sets in the compression regions deviate at a low shear (and corresponding low load) value.

12. Shear Stress-Strain Curve

To be able to use the shear versus strain data presented in Section 11 for predicting the shear deflections of other beam shapes, it is expedient to express the shear values in terms of the average shear stress in the web. The web area used in this conversion is denoted A_w, where $A_w = w(h-t)$.

From the information presented in Section 11 a representative shear versus shear strain curve was drawn. A study of this curve showed that there were three rather definite regions: the initial elastic portion; after the break-over a gently sloping portion extending to a shear strain value of about 0.020 radians; and a remaining portion which resembled the strain hardening portion of a tension stress-strain curve. A curve-fitting scheme was used to obtain expressions for the three portions of the curve in terms of V and γ, the shear and shear strain. The expressions were then divided by A_w for the 8WF58 section to reduce the shear values to average shear stress in the web.

A mean shear value at the break-over in the V-γ curves appeared to be about 69 kips, which corresponds to a shear stress of 16,500 lb./sq.in. for the 8WF58 section. This is noted to be 0.5 σ_{yp} if the yield point was 33,000 lb./sq.in. As explained in Section 10, the nominal yield point corresponding to the experimental M-φ curve shown in Fig. 10 was 32,300 lb./sq.in. A shear stress of 16,500 lb./sq.in. represents 0.51 σ_{yp} in this case. These values of shear stress are average values based on uniform distribution of shear stress across the web; nevertheless, they fall near the range of values reported by Lyse and Godfrey (10). These investigators made a number of torsion tests on specimens taken from the webs of structural beams and found that the ratio of yield point in shear to yield point in tension varied from 0.505 to 0.634.

The curve-fitting process yielded the following expressions:

$$\gamma = \tau/G = 8.70\ V/A_w \times 10^{-5} \qquad 0 < \gamma < .00143 \text{ rad.}, \quad 0 < \tau < 16.5 \text{ kips/sq.in.}$$

$$\gamma = \frac{\tau - 16.06}{307} \qquad .00143 < \gamma < .020, \quad 16.5 < \tau < 22.2$$

$$\gamma = \left(\frac{\tau}{70}\right)^{3.40} \qquad .020 < \gamma < .300, \quad 22.2 < \tau < 49.1$$

The curve based on these expressions is presented in Fig. 34. It must be remembered that this diagram is based only on data obtained from the 8WF58 section. However, there is every reason to believe that this τ-γ relationship will give reasonable estimates of the shear deflections of other mild steel wide flange sections.

To estimate the shear deflection of a beam using this curve it is first necessary to compute τ, which is equal to V/A_w. Enter the curve with τ and find γ, the shearing strain which is expressed in radians. The equations could also be used to obtain γ. The shearing strain multiplied by the length in question gives the component of deflection due to shear. This procedure has to be modified in special cases. Some of these are discussed in Section 13.

IV. SHEAR DEFORMATION AND ITS EFFECT ON BEAM BEHAVIOR

13. Theoretical Examples Illustrating the Redistribution of Slope and Moment

The purpose of this section is to illustrate some of the effects which shear deformation may have on the behavior of a beam. For symmetrically loaded beams with symmetrical boundary conditions, shear causes no readjustment of moment and slope, even in the plastic range. This was the case for the continuous beam tests which are reported in Part III of this report. However, for unsymmetrically loaded beams, there is a readjustment of moment and slope. Some of the problems which may be expected to arise in the actual testing or analysis of an unsymmetrically loaded beam are illustrated by an example which follows.

A 12WF120 beam having a span of 20 ft. with the load 4 ft. from one end was selected. The beam is treated first as a simple beam, second as a beam fixed at the short end and simply supported at the other end, and third as a beam fixed at both ends. In each case bending alone and bending and shear combined are presented for comparison.

The M-φ curve and τ-γ curve which were used in the computations are shown in Fig. 51. In order to simplify the analysis several assumptions were made with regard to the shape of the M-φ and τ-γ curves. The initial portion of the M-φ curve is assumed to be elastic up to the fully plastic moment value of 6150 kip-in. At this point the M-φ curve is assumed to break over horizontally as indicated by the solid line. The dotted curve represents the curve as it would look if computed by the methods outlined in Appendix A. Strain hardening is neglected

in most of the computations which follow, though when it is included to illustrate a certain point, the discussion indicates this fact. Neglecting strain hardening means that the deflections will be greater than if strain hardening were included. Neglecting strain hardening also allows the plastic hinge method of computing deflections to be used. This provides a further simplification in the calculations. In the plastic hinge method it is assumed that flexural yielding is limited to the cross-section which first reaches initial yield. In other words, there is no propagation of the plastic regions due to bending; the beam has elastic regions and localized plastic hinges only.

The shear stress-strain curve is taken from Fig. 34 with the exception that the second linear portion is extended beyond 0.020 radians to a shear strain of about 0.045 radians. This approximation simplifies the calculations. For the following examples the deflection at B is computed. This is not the maximum beam deflection but is near enough in magnitude to the latter to illustrate the trend.

a. Simple Beam (Fig. 52)

For the simple beam the moment increases linearly with the load. The beam remains elastic (both with regard to bending and shear) up to a load of 160 kips. The dotted portion represents the deflection due to bending alone while the solid line represents the combined deflection due to bending and shear. In accordance with the plastic hinge concept, at a load of 160 kips the beam would turn into a mechanism with a hinge at B and deflect without any increase in load. This is

represented by the solid line in Fig. 52. However, to illustrate a point regarding shear deflection, strain hardening is considered, and the deflection is now represented by the dashed lines. At a load of 185 kips, the nominal shear stress in the portion AB is 17.4 kips/sq.in. which indicates that yielding has taken place. The flexural deflection at B is 3.69 in. The shear deflection for the portion AB is computed to be 0.205 in. while that for BC is 0.072 in. This immediately indicates a lack of closure of 0.133 in. as is shown directly below the beam sketch in Fig. 52. Since the shear angle change at B is fixed and the deflections must close out, the triangle is rotated to effect the closure, which reduces the shear deflection at B to 0.178 in. The total deflection at B is then 3.69 in. plus 0.18 in., or 3.87 in. total.

The physical significance of this lack of closure and necessary adjustment of the shear deflection can be seen by realizing that the yielded portion AB wanted to deflect the full amount while the elastic portion could not and thereby held it back to some extent. This action in turn caused a slight readjustment of the slopes at the ends of the beam which can be calculated. Obviously the shear yielding of AB could have been induced while the flexural deflection was in the elastic range had the load been closer to the end of the beam.

b. Beam Fixed at A and Simply Supported at C (Fig. 53)

The beam is once indeterminate. For bending alone the relationship between M_A and P in the elastic range can be obtained from the area-moment propositions, since the deflection at C with respect

to the tangent at A must be zero. This yields:

$$M_A = \frac{Pab}{2L^2}(L + b)$$

For the example, M_A reaches the hinge value of 6150 kip-in. at a load of 178 kips with M_B being 1915 kip-in. At this point the beam becomes a simple beam with a constant resisting moment of 6150 kip-in. acting at A. The second hinge forms at B at a load of 288 kips. The dashed lines in Fig. 53 indicate the relationships for bending alone.

For bending and shear combined, the net deflection between A and C must be zero. It is assumed that the shear angle changes take place abruptly at the face of the support and at the load point. Adding the shear deflection terms to the bending terms results in the following general expression:

$$\frac{1}{EI}\left[-\frac{Pab}{6}(L + b) + \frac{M_A L^2}{3}\right] + \gamma_{AB}\, a - \gamma_{BC}\, b = 0$$

In the elastic case this reduces to

$$M_A = \frac{\frac{Pab}{6}(L + b)}{\frac{L^2}{3} + \frac{1}{K}}$$

where

$$K = \frac{A_w G}{EI}$$

Shear causes a slight redistribution of moment in the elastic range, as is shown by the solid lines in Fig. 53. At a load of 149 kips the portion AB yields in shear. This causes a marked redistribution

in moment, particularly at A which reaches the hinge value at a load of 265 kips. An increase in load causes M_B to reach the hinge moment value at a load of 288 kips. The dashed lines beyond 6150 kip-in. indicate the trend of M_A and M_B if strain hardening were to be taken into account. The effect of the shear forces on the deflection of the beam is clearly indicated.

c. Beam Fixed at A and C (Fig. 54)

This beam is twice indeterminate. In this case in addition to the equations of equilibrium two additional relationships involving the deformation of the beam must be utilized. The two conditions utilized are that the sum of the angle changes between A and C must be zero and that the deflection of one end with respect to the tangent at the other must equal zero.

These conditions yield the following relationships for the elastic case:

$$M_A = \frac{Pab^2}{L^2}$$

$$M_C = \frac{Pa^2b}{L^2}$$

The dotted lines in Fig. 54 show the behavior of the beam when bending alone is considered. The first hinge forms at A, next at B, and last at C. The maximum load is 320 kips. The deflection curve has the two distinct breaks which are characteristic of continuous beams under bending alone.

For bending and shear the expressions for the moments become only slightly more complicated. In this case the angle change expression is not altered since the algebraic sum of the shear angle changes will always be zero if statics is satisfied. However, there are added terms in the deflection relationship.

The two expressions are:

$$\frac{1}{EI}\left[\frac{Pab}{2} - \frac{M_A L}{2} - \frac{M_{BC} L}{2}\right] = 0$$

$$\frac{1}{EI}\left[\frac{-Pab}{2}\left(\frac{L+b}{3}\right) + \frac{M_A L^2}{3} + \frac{M_{BC} L^2}{6}\right] + \gamma_{AB}\, a - \gamma_{BC}\, b = 0$$

For the elastic case these reduce to:

$$M_A = \frac{Pab}{L} - M_{BC}$$

$$M_{BC} = \frac{\frac{Pa^2b}{6} + \frac{Pab}{KL}}{\frac{L^2}{6} + \frac{2}{K}}$$

As a check we note that if $a = b = \frac{L}{2}$ (the load is in the center of the beam), then $M_A = M_{BC} = \frac{PL}{8}$, which is the same expression as for bending alone.

There is a slight redistribution of moment in the elastic range as shown by the solid lines. At a load of 158 kips, shear yielding begins in section AB. At this point there is a marked redistribution of moment, and for the example chosen M_C reaches the hinge moment first,

next M_B, and last M_A. M_A drops off slightly during the process and then picks up again. As the portion AB yields, more and more of the load is transferred toward C.

The equations given with the examples are for the initial response only and obviously have to be altered as the hinges form or the sections yield in shear.

For many obvious reasons it would not be expected that the results of these analyses could be exactly duplicated experimentally. The important point to be drawn from the examples is that high shear forces can cause a redistribution of the moments and slopes for cases of unsymmetrical loading. This fact must be kept in mind by anyone planning tests and performing analyses where shear forces are high enough to be of importance.

14. General Observations

The field of plastic or limit design and its possible application to structural practice has been the subject matter of numerous papers (many of which are included in the bibliography). A full discussion of the subject is beyond the scope of this report. In general the economy to be gained by plastic design procedures occurs in cases in which there is a difference in magnitude of the bending moments between the load points and reactions of structures, a condition commonly characteristic of redundant structures. The first yielding which occurs at the point of highest moment generally does not cause failure. The deflection of

the redundant beam at this yield load is considerably less than that for the comparable simple beam of the same span at its initial yield load. Also, the redundant beam still retains considerable reserve strength after reaching the initial yield load. Therein lies the background for the basis of plastic design of beams.

Obviously there are many limitations in utilizing the reserve strength, two of the more serious ones being local flange and web buckling. Flange or web buckling may seriously impair the rotation capacity of the member. This subject of desirable section properties evidently is under study at another institution at the present time. Thick flanges and webs tend to cut down the possibility of buckling and this probably will be the trend where large rotation capacities are desirable. Thick flanges will provide greater moment capacity, especially as the strain hardening capacity is utilized. This larger moment capacity indicates higher shear forces. Thus the possibility of shear yielding in the web and its corresponding effect on the behavior of the structure must be kept in mind when desirable section properties are studied. Also, the strengthening of beams by adding cover plates will necessarily require shear to be taken into consideration.

As a general rule shear will be of primary importance in only unusual loading conditions. The most obvious example is a concentrated load near the end of a beam as might occur in the use of offset columns in buildings. Since general shear yielding in the webs will cause excessive deflections, the recommended practice is to avoid high shear

when possible. However, when high shear forces are encountered, the data presented in this report will permit an estimate of the shear deflection to be made.

The ratio of total span length to depth for which shear is of importance in plastic design is variable and depends on the boundary conditions and moment gradient. For a 12WF120 beam fixed at both ends and loaded at the center, general shear yielding in the web will occur at or before the yield moment is reached at the support or load point (both moments are equal in this case) for a span to depth ratio of about 11. This emphasizes the fact that the span depth ratio need not be extremely small for shear deformation to be of importance. Shear deflections in the elastic range are also of importance. It is generally accepted that shear deflections should be considered when the span to depth ratios for simply supported beams is eight or less. For the same beam section as above, simply supported and with a span eight times the depth, the elastic shear deflection represents about 25 per cent of the total deflection. Since this particular beam will yield in flexure before yielding in shear, the percentage of total deflection caused by shear will decrease following flexural yielding. Of course, for beams in which shear yielding occurs before flexural yielding, there will be an increase in the percentage of total deflection attributable to shear.

V. SUMMARY

As far as is known from the literature, the tests described in this report represent the first large-scale tests of continuous beams loaded far into the plastic range in which extremely high shear forces are present. On the basis of these tests it is concluded that no measurable reduction in the moment capacity (for the section and span used) was indicated.

Data for computing the shear deflection of wide flange steel beams in the plastic range were obtained from the tests.

Theroetical examples are presented which show that moment and slope redistribution take place in unsymmetrically loaded beams when shear is considered. This redistribution may be of major importance when shear yielding of the web occurs.

BIBLIOGRAPHY

1. Baker, J. F., "A Review of Recent Investigations into the Behaviour of Steel Frames in the Plastic Range," Journ. Instn. Civil Engrs., vol. 31, 1949, pp. 188-240

2. Baker, J. F., and Roderick, J. W., "Investigation into the Behaviour of Welded Rigid Frame Structures. Second Interim Report," Trans. Inst. of Welding, vol. 3, 1940, pp. 83-92

3. Fife, W. M., and Wilbur, J. B., Theory of Statically Indeterminate Structures, McGraw-Hill Book Co., Inc., New York, 1937, p. 27

4. Hendry, A. W., "An Investigation of the Strength of Certain Welded Portal Frames in Relation to the Plastic Method of Design," The Structural Engineer, vol. 28, 1950, pp. 311-326

5. Horne, M. R., "The Plastic Theory of Bending of Mild Steel Beams with Particular Reference to the Effect of Shear Forces," Proceedings Roy. Soc. London, Ser. A., vol. 207, 1951, pp. 216-228.

6. Johnston, B. G., Yang, C. H., and Beedle, L. S., "An Evaluation of Plastic Analysis as Applied to Structural Design. Progress Report No. 8," The Welding Journal, vol. 32, 1953, Research Supplement, pp. 224-s-239-s

7. Knudson, K. E., Yang, C. H., Johnston, B. G., and Beedle, L. S., "Plastic Strength and Deflections of Continuous Beams. Progress Report No. 9," The Welding Journal, vol. 32, 1953, Research Supplement, pp. 240-s-256-s

8. Leth, C.-F. A., "The Effect of Shear Stresses on the Carrying Capacity of I-Beams," Tech. Report All-107 of Brown University to ONR under Contract N7onr-35801, March, 1954, pp. 1-70

9. Luxion, W. W., and Johnston, B. G., "Plastic Behavior of Wide Flange Beams. Progress Report No. 1," The Welding Journal, vol. 27, 1948, Research Supplement, pp. 538-s-554-s

10. Lyse, I., and Godfrey, H. J., "Shearing Properties and Poisson's Ratio of Structural and Alloy Steels," ASTM Proc., vol. 33, 1933, pp. 274-292

11. Maier-Leibnitz, H., "Versuche, Ausdeutung und Anwendung der Ergebnisse," Prelim. Publication, English Edition, Second Cong., Int. Assoc. of Bridge and Struct. Engineering, 1936, pp. 97-130

12. Newmark, N. M., "Numerical Procedure for Computing Deflections, Moments, and Buckling Loads," Trans. ASCE, vol. 108, 1943, pp. 1161-1234

13. Roderick, J. W., and Phillips, I. H., "Carrying Capacity of Simply Supported Mild Steel Beams," Engineering Structures (Colston Papers, vol. II), Academic Press, Inc., New York, 1949, pp. 9-48

14. Timoshenko, S., Strength of Materials, D. Van Nostrand, New York, Part II, 2nd Ed., 1941, p. 362

15. Van den Broek, J. A., Theory of Limit Design, John Wiley and Sons, Inc., New York, 1948

16. Yang, C. H., Beedle, L. S., and Johnston, B. G., "Plastic Design and the Deformation of Structures. Progress Report No. 3," The Welding Journal, vol. 30, 1951, Research Supplement, pp. 348-s-356-s

17. Yang, C. H., Beedle, L. S., and Johnston, B. G., "Residual Stress and the Yield Strength of Steel Beams. Progress Report No. 5," The Welding Journal, vol. 31, 1952, Research Supplement, pp. 205-s-229-s

APPENDIX A

COMPUTATION OF KEY POINTS FOR DRAWING THE MOMENT-CURVATURE DIAGRAM FOR THE PURE BENDING OF A WIDE FLANGE BEAM

Experience indicates that at the most five points are needed in order to be able to sketch the shape of the moment-curvature (M-φ) diagram up to the beginning of the strain hardening region. Since the strain distribution is assumed to be linear, the stress blocks, which are used to compute the moments, actually consist of the stress-strain curve with the strain axis (to the strain in question) superimposed on one-half the depth of the beam. Figure 7 shows the stress blocks for different assumed depths of yielding. The moments are computed by taking into account the stress, effective area, and the appropriate moment arm about the neutral axis. The curvatures are computed from the strains.

The five points which are used to sketch the moment-curvature diagram are shown in Fig. 8 and are listed below with a statement of the conditions represented:

$M_1 - \varphi_1$ Yielding impending in outer fiber (Fig. 7b)

$M_2 - \varphi_2$ Yielding penetrated to inside of flange (Fig. 7c)

$M_3 - \varphi_3$ Yielding penetrated to 1/4 h

$M_4 - \varphi_4$ Yielding penetrated to 5/12 h

$M_5 - \varphi_5$ Strain hardening strain impending in outer fiber (Fig. 7d)

$M_{shr} - \varphi_{shr}$ Outer fiber strain in strain hardening region (Fig. 7e)

The distance from the neutral axis to the depth of yielding is denoted by y (see Fig. 7 for notation). Then, y_1, y_2, etc., refer to the conditions represented by $M_1 - \varphi_1$, $M_2 - \varphi_2$, etc. The following notation is also used:

Z_1 = first moment of entire beam section = $bt(h-t) + wy_2^2$

Z_2 = first moment of web area corresponding to $\pm y_2 = wy_2^2$

Z_3 = first moment of web area corresponding to $\pm y_3 = wy_3^2$

Z_4 = first moment of web area corresponding to $\pm y_4 = wy_4^2$

The expressions for moment and curvature can be derived using this notation and are as follows:

$$M_1 = \frac{\sigma_{yp} I}{y_1} \qquad \varphi_1 = \frac{\sigma_{yp}}{EI_y}$$

$$M_2 = (Z_1 - Z_2)\sigma_{yp} + \frac{2}{3} Z_2 \sigma_{yp} \qquad \varphi_2 = \frac{\sigma_{yp}}{Ey_2}$$

$$M_3 = (Z_1 - Z_3)\sigma_{yp} + \frac{2}{3} Z_3 \sigma_{yp} \qquad \varphi_3 = \frac{\sigma_{yp}}{Ey_3}$$

$$M_4 = (Z_1 - Z_4)\sigma_{yp} + \frac{2}{3} Z_4 \sigma_{yp} \qquad \varphi_4 = \frac{\sigma_{yp}}{Ey_4}$$

Computations will show that the moment M_5 is generally within a fraction of one per cent of the value of the fully plastic moment which facilitates its computation as follows:

$$M_5 = M_{fp} = Z_1 \sigma_{yp} \qquad \varphi_5 = \frac{2\epsilon_{sh}}{h} = \frac{\epsilon_{sh}}{y_1}$$

In the strain hardening region the computations are only slightly more complicated. The procedure consists in first selecting the outer fiber strain, drawing the stress block, and computing the forces and moment arms in order to find the moment. The curvatures are found by dividing the outer fiber strain by one-half the depth of the section.

APPENDIX B

NOTATION

The following notation is used in this report:

A_w = web area used to obtain the average shear stress across the web = $w(h-t)$

a,b = distance between support and load, or between loads, as indicated in figures

b = flange width of a wide flange beam (see Fig. 7) or width of cross-section at the point where the shear stress is being computed by the formula VQ/Ib

ϵ = tensile or compressive strain

E = modulus of elasticity of steel

γ = shear strain

G = modulus of elasticity in shear = $\frac{E}{2(1+\mu)}$

h = over-all depth of beam

I = moment of inertia of the cross-section of a beam about its centroidal axis

K = constant appearing in moment expressions in Section 13 = $A_w G/EI$

L = span length of beam

M = moment

P = concentrated load

φ = curvature

Q = the statical moment about the neutral axis of the part of the cross-section between the point where the shearing stress is wanted and the outside of the beam

σ = tensile or compressive stress

τ = shear stress

t = flange thickness

V = shear force

w = web thickness

y = distance measured from neutral axis (see Fig. 7)

Z = statical moment of cross-section of beam (see Appendix A and Table 1)

fp = subscript denoting "fully plastic"

sh = subscript denoting moment, strain, or curvature values when strain hardening is impending on the top or bottom of the beam

shr = subscript denoting moment or curvature values when strains are in the strain hardening region

yp = subscript denoting yield point

TABLE 1 SECTION PROPERTIES OF BEAM TEST SPECIMENS

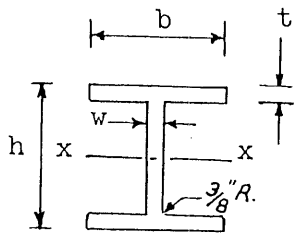

Beams B1 and B2
8WF58 As-rolled Sections

Beam	Depth h in.	Web Thickness w in.	Flange Width b in.	Flange Thickness t in.	Area in.^{2}	I_x in.^{4}	Z_x in.^{3}
Measured*							
B1	8.85	.518	8.132	.840	17.50	237	61.80
B2	8.82	.519	8.136	.824	17.25	232	60.68
AISC Handbook	8.75	.510	8.222	.808	17.06	227.3	-----
Per Cent Variation							
B1	+1.1	+1.6	-1.1	+4.0	+2.6	+4.3	-----
B2	+0.8	+1.8	-1.0	+2.0	+1.1	+4.7	-----

*Average of values taken at two locations on beam

TABLE 2 TENSILE TEST COUPON DATA

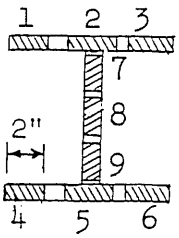

Tension Test Coupon No.	σ_{yp} k/sq.in	$\sigma_{max.}$ k/sq.in. x 10^{-3}	ϵ^*_{sh} in./in.	E k/sq.in. x 10^{-3}	Per Cent Elong.
B1					
1	34.5	61.3	.014	----	34
2	31.7	59.4	.010	32.1	34
3	34.9	61.4	.014	31.5	35
4	34.0	61.2	.014	32.7	32
5	31.9	60.2	.010	30.8	34
6	34.9	61.2	.012	31.6	33
7	34.9	60.9	.015	31.8	32
8	36.1	61.0	.017	32.5	32
9	35.4	60.6	.015	32.5	33
Avg. Wtd. Value**	33.8	----	.012	31.8	--
B2					
1	35.9	62.2	.014	30.5	32
2	34.3	63.7	.010	31.6	32
3	35.2	62.2	.013	31.5	35
4	36.5	62.4	.013	32.3	33
5	34.2	63.2	.009	35.6	31
6	35.4	62.6	.014	28.4	33
7	36.6	63.0	.015	28.0	29
8	38.6	63.2	.019	30.4	31
9	36.4	63.0	.014	30.9	33
Avg. Wtd. Value**	35.5	----	.012	31.5	--

*Estimated strain at beginning of strain hardening region

**Individual coupon data weighted for (1) area represented and (2) distance from neutral axis

TABLE 3 LOAD - SHEAR - MOMENT DATA FOR BEAM B1

Central Load 2P Kips	Shear - Kips				Moment (Kip-in.)			
	West Cantilever	West V-M (A)	East V-M (B)	East Cantilever	West Reaction	West Ld.Pt.	East Ld.Pt.	East Reaction
0	0	0	0	0	0	0	0	0
17.5	3.8	9.3	8.2	2.7	-204	+131	+151	-144
40	9.7	20.9	19.1	7.8	514	239	272	416
50.5	11.5	26.3	24.2	9.4	611	335	372	499
59.5	14.4	31.2	28.3	11.5	762	360	411	610
66.5	15.3	34.5	32.0	12.8	811	430	474	679
81.5	18.3	42.1	39.4	15.5	968	547	595	823
100	23.1	51.4	48.6	20.3	1224	626	676	1075
113	26.5	57.6	55.4	24.3	1402	670	708	1289
132	30.6	67.1	64.9	28.3	1620	796	837	1499
142	32.5	71.5	70.5	31.4	1721	854	874	1663
150.5	33.0	76.2	74.3	31.1	1752	991	1026	1649
164	35.1	82.8	81.2	33.5	1862	1119	1149	1774
176	36.2	88.4	87.6	35.3	1917	1266	1282	1871
195	37.2	97.8	97.2	36.6	1972	1549	1559	1940
216	39.1	108.7	107.3	37.6	2071	1842	1868	1995
235	42.4	119.1	115.9	39.2	2247	2039	2096	2078
246	45.4	123.3	122.7	44.7	2404	2036	2047	2369
269	52.5	134.1	134.9	53.3	2783	2044	2030	2827

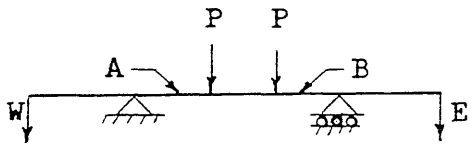

TABLE 4 LOAD - SHEAR - MOMENT DATA FOR BEAM B2a

Central Load 2P Kips	Shear - Kips				Moment (Kip-in.)			
	West Canti-lever	West V-M (A)	East V-M (B)	East Canti-lever	West Reaction	West Ld.Pt.	East Ld.Pt.	East Reaction
0	0	0	0	0	0	0	0	0
30	4.3	14.4	15.6	4.5	-226	+34	+42	-238
65.5	10.3	32.8	32.7	9.5	546	43	88	501
100	15.9	49.9	50.1	15.1	844	54	113	789
130	21.4	65.8	64.2	19.8	1134	50	106	1050
160	26.3	79.8	80.2	26.0	1390	46	68	1376
185	28.8	92.2	92.8	28.5	1525	134	161	1510
199	29.7	100.0	99.0	29.7	1573	228	208	1573
211	31.5	105.8	105.2	30.9	1666	238	260	1633
230	33.0	116.3	113.7	32.0	1748	345	350	1697
254	34.9	127.3	126.7	33.9	1847	444	488	1793
282	36.6	141.2	140.8	35.9	1939	602	634	1901
317	39.0	158.5	158.5	38.6	2065	788	808	2045
352	41.7	176.1	175.9	40.6	2210	959	1021	2146
398	45.9	199.2	198.8	42.5	2432	1154	1326	2252

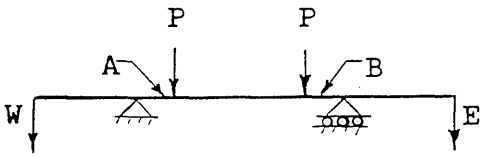

TABLE 5 LOAD - DEFLECTION DATA FOR BEAM B1

Central Load 2P Kips	Deflections* - in.								
	1	2	3	4	5	6	7	8	9
0	0	0	0	0	0	0	0	0	0
17.5	0.026	0.014	0.020	0.028	0.033	0.027	0.019	0.010	0.003
40	0.025	0.026	0.036	0.049	0.055	0.045	0.030	0.014	0.041
50.5	0.050	0.028	0.042	0.058	0.066	0.054	0.035	0.016	0.062
59.5	0.062	0.034	0.050	0.070	0.079	0.065	0.043	0.019	0.071
66.5	0.081	0.035	0.053	0.076	0.086	0.070	0.046	0.020	0.090
81.5	0.141	0.032	0.054	0.080	0.091	0.076	0.048	0.020	0.134
100	0.176	0.037	0.063	0.095	0.108	0.091	0.058	0.024	0.184
113	0.212	0.041	0.070	0.109	0.122	0.106	0.065	0.028	0.224
132	0.275	0.049	0.085	0.134	0.150	0.132	0.079	0.036	0.287
142	0.296	0.062	0.117	0.175	0.193	0.169	0.108	0.052	0.321
150.5	0.349	0.178	0.385	0.516	0.533	0.506	0.372	0.162	0.357
164	0.368	0.237	0.507	0.694	0.717	0.686	0.491	0.220	0.376
176	0.395	0.300	0.643	0.894	0.919	0.885	0.628	0.284	0.405
195	0.488	0.417	0.894	1.260	1.293	1.254	0.884	0.303	0.449
216	1.197	0.602	1.297	1.848	1.893	1.842	1.287	0.486	0.576
235	1.909	0.803	1.741	2.486	2.556	2.490	1.723	0.697	1.309
246	3.085	1.039	2.238	3.193	3.317	3.209	2.218	0.932	2.363
269	4.944	1.364	2.947	4.204	4.442	4.211	2.894	1.217	3.977

* Zero base line is through supports; all of above deflections are vertically downward from this base line.

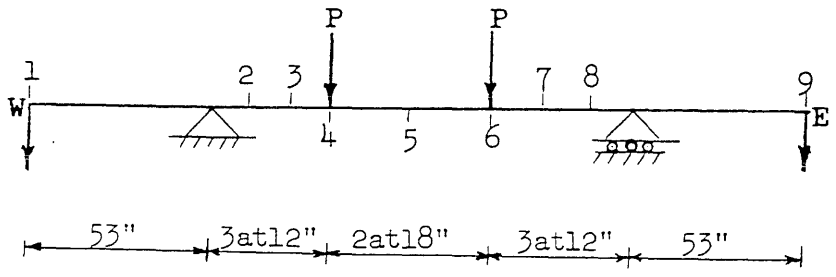

TABLE 6 LOAD - DEFLECTION DATA FOR BEAM B2a

Central Load 2P Kips	Deflections* - in.										
	1	2	3	4	5	6	7	8	9	10	11
0	0	0	0	0	0	0	0	0	0	0	0
30	0.039	0.005	0.003	0.005	0.011	0.012	0.010	0.005	0.002	0.006	0.044
65.5	0.100	0.013	0.005	0.010	0.016	0.024	0.019	0.012	0.007	0.012	0.090
100	0.172	0.023	0.008	0.014	0.024	0.031	0.028	0.018	0.010	0.020	0.155
130	0.245	0.034	0.012	0.021	0.035	0.040	0.038	0.025	0.014	0.030	0.221
160	0.341	0.050	0.041	0.099	0.130	0.132	0.134	0.104	0.039	0.049	0.326
185	0.385	0.058	0.092	0.221	0.293	0.307	0.297	0.224	0.087	0.058	0.373
199	0.416	0.063	0.131	0.307	0.412	0.429	0.419	0.309	0.123	0.062	0.400
211	0.442	0.067	0.142	0.335	0.452	0.474	0.463	0.342	0.137	0.065	0.421
230	0.472	0.073	0.192	0.451	0.611	0.646	0.621	0.455	0.183	0.070	0.445
254	0.550	0.088	0.260	0.614	0.833	0.876	0.846	0.616	0.247	0.083	0.509
282	0.685	0.116	0.376	0.886	1.219	1.257	1.213	0.880	0.350	0.104	0.614
317	1.378	0.246	0.560	1.332	1.811	1.862	1.795	1.304	0.506	0.197	1.045
352	2.575	0.440	0.958	2.257	2.954	3.052	3.003	2.165	0.805	0.345	1.653
398	3.659	0.631	1.330	3.109	3.984	4.095	4.086	2.998	1.086	0.472	2.179

*Zero base line is through supports; all of above deflections are vertically downward from this base line.

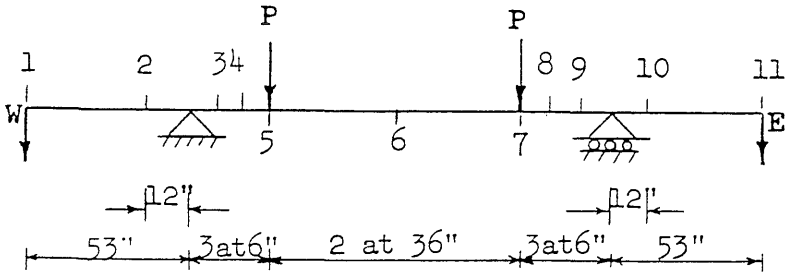

TABLE 7 COMPARISON OF SHEAR STRESS VALUES IN THE ELASTIC RANGE

Beam B1

Load Kips	Shear Kips	τ_{xy} from Rosettes* No. 2	No. 4	No. 5	$\frac{VQ}{Ib}$	$\frac{V}{A_w}$	τ_{xy} from Rosettes* No. 1	No. 3	$\frac{VQ}{Ib}$
17.5	9.3	2,550	2,880	2,670	2,340	2,240	2,550	2,730	2,290
40	20.9	6,030	5,780	6,030	5,250	5,040	6,100	5,710	5,150
50.5	26.3	8,430	7,260	7,900	6,600	6,350	7,810	8.560	6,370
59.5	31.2	10,720	8,410	9,260	7,830	7,500	9,310	16,670	7,680
66.5	34.5	12,650	9,400	10,660	8,650	8,300	11,590	----	8,500
81.5	42.1	14,890	11,450	13,440	10,500	10,150	15,370	----	10,400
100	51.4	----	13,870	----	12,900	12,400	----	----	----
113	57.6	----	15,530	----	14,400	13,900	----	----	----

Beam B2a

		No. 7	No. 9				No. 6	No. 8	
30	14.4	3,570	2,150		3,630	3,500	3,720	3,630	3,540
65.5	32.8	8,310	11,560		8,260	7,900	11,820	8,470	8,070
100	49.9	14,060	----		12,580	12,000	----	15,200	12,300
130	65.8	16,540	----		16,600	15,900	----	----	16,200

*For gage numbers and locations see Fig. 33.

Note: All shear stress values are in units of lb./sq.in.

TABLE 8 LONGITUDINAL STRAIN DISTRIBUTION SHEAR-MOMENT SECTIONS
BEAMS B1 and B2a

Load (2P) Kips	Shear Kips	Moment Kip-in.	ϵ_1	ϵ_2	ϵ_3	ϵ_4	ϵ_5
(a) Beam B1 - Section 12" E of W Reaction							
17.5	9.3	- 92	+100	+ 30	+ 0	- 43	- 110
40.0	20.9	- 263	+188	+ 62	+ 12	- 68	- 200
50.5	26.3	- 296	+230	+ 78	+ 15	- 85	- 258
59.5	31.2	- 388	+275	+ 92	+ 24	- 93	- 292
66.5	34.5	- 397	+300	+ 102	+ 24	- 105	- 327
81.5	42.1	- 463	+360	+ 132	+ 39	- 115	- 395
100.0	51.4	- 607	+430	+ 161	+ 69	- 118	- 484
113.0	57.6	- 711	+475	+ 202	+ 107	- 91	- 552
132.0	67.1	- 815	+505	+ 287	+ 229	- 25	- 625
142.0	71.5	- 863	+568	+ 147	+ 332	- 272	- 675
150.5	76.2	- 838	+659	+ 267	+ 177	- 500	- 669
164	82.8	- 868	+655	+ 117	+ 156	- 480	- 630
176	88.4	- 856	+635	- 128	+ 214	- 493	- 595
195	97.8	- 798	+602	- 320	+ 356	- 488	- 532
216	108.7	- 767	+580	- 630	+ 683	- 388	- 470
235	119.1	- 784	+590	-1040	+1151	- 345	- 427
246	123.3	- 924	+615	-1338	+1790		- 440
269	134.1	-1193	+675		+2751		- 482

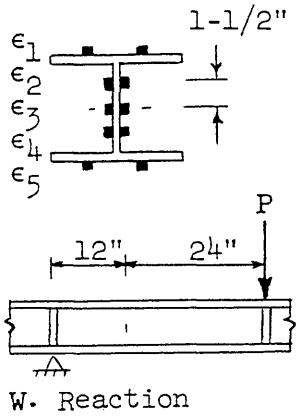

Load (2P) Kips	Shear Kips	Moment Kip-in.	ϵ_1	ϵ_2	ϵ_3	ϵ_4	ϵ_5
(b) Beam B2a - Section 13" E of W Reaction							
30	14.4	- 39	+ 25	+ 192	+ 1	- 10	- 32
65.5	32.8	- 121	+144	+ 413	+ 16	- 24	- 92
100.0	49.9	- 196	+220	+ 800	+ 66	- 20	- 160
130	65.8	- 279	+259	+1188	+ 16	- 28	- 207
160	79.8	- 353	-220	+1355	- 88	+1207	+ 304
185	92.2	- 327	-440	+1636	+ 293	+ 908	+ 524
199	100.0	- 273	-507	+1756	+ 240	- 235	+ 615
211	105.8	- 291	-500	+2136	+ 234	- 416	+ 636
230	116.3	- 238	-565	+2740	- 308	- 891	+ 755
254	127.3	- 192	-630	+3758	- 499	-1446	+ 905
282	141.2	- 104	-702	+6198		-2097	+ 1156
317	158.5	- 5	-740			-2543	+ 1735
352	176.1	+ 80	-750				+ 6125
398	199.2	+ 159	-795				+ 11,625

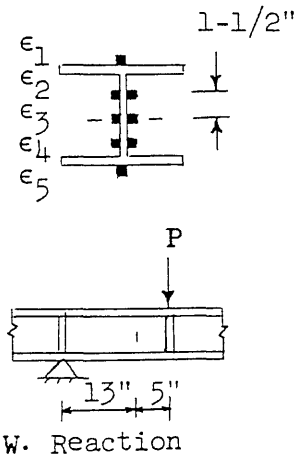

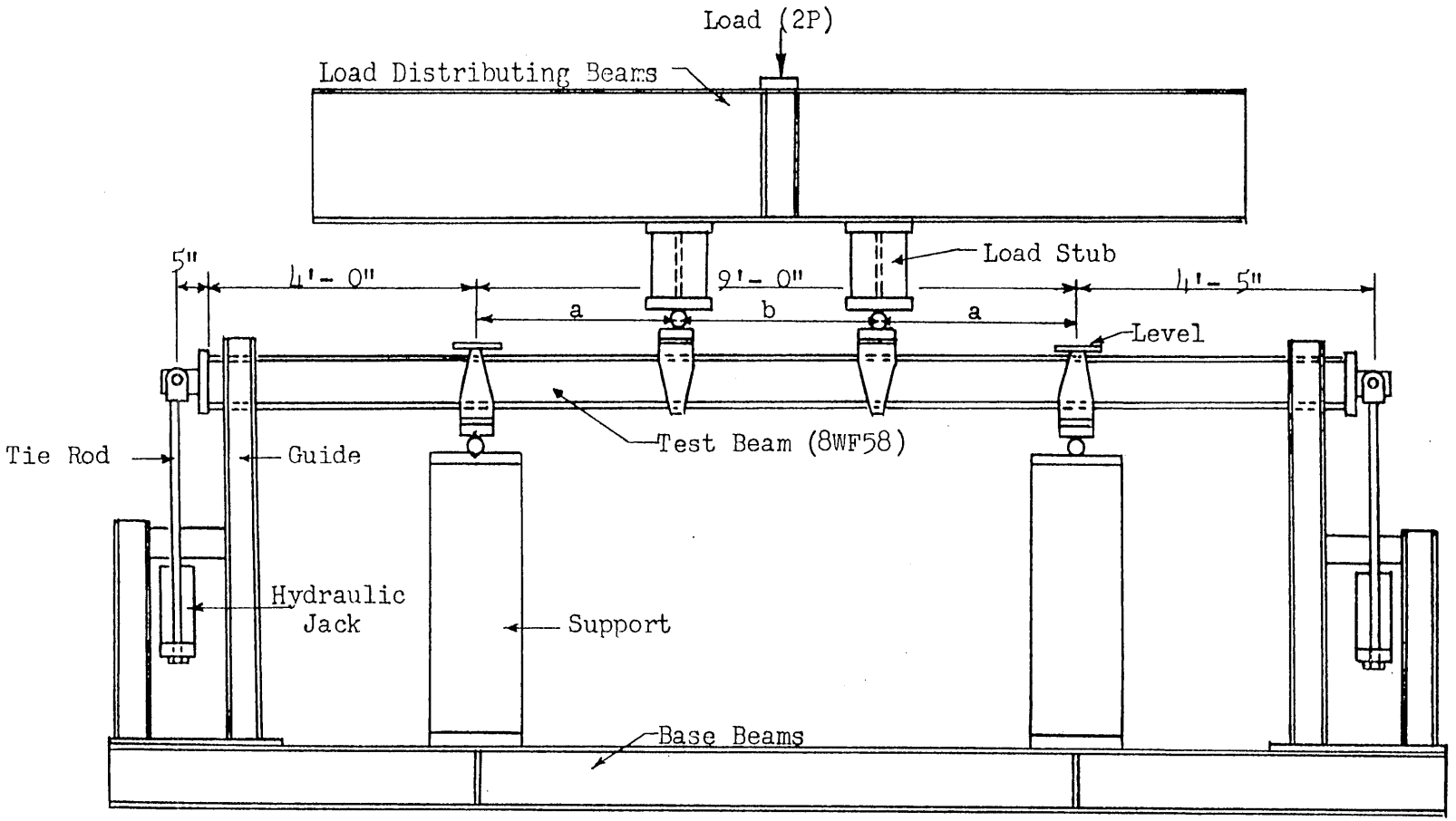

Beam	a	b
B1	36"	36"
B2	18"	72"

FIG. 1 SCHEMATIC VIEW OF CONTINUOUS BEAM TEST SETUP

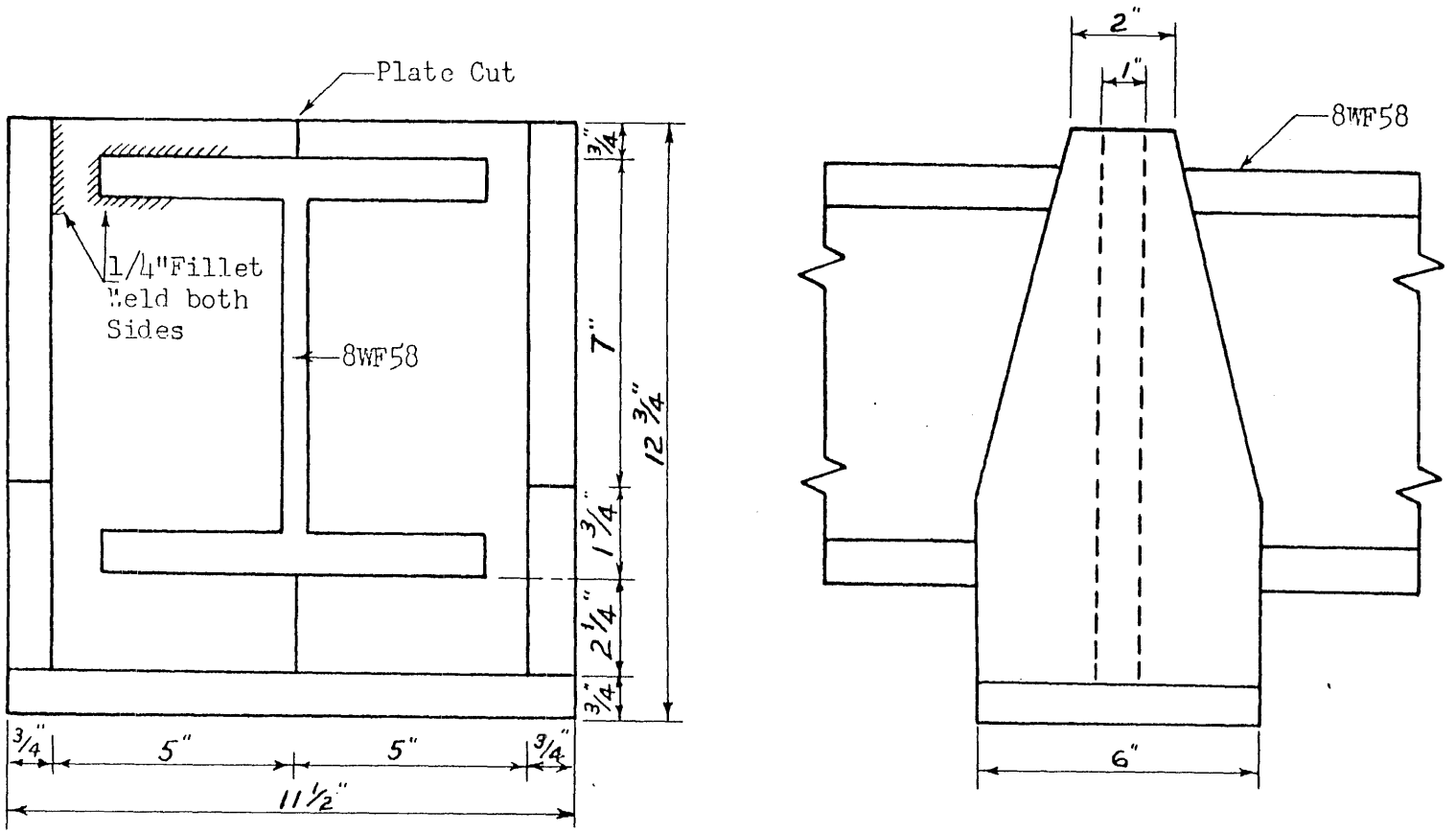

FIG. 2 DETAIL OF LOAD AND REACTION BRACKET

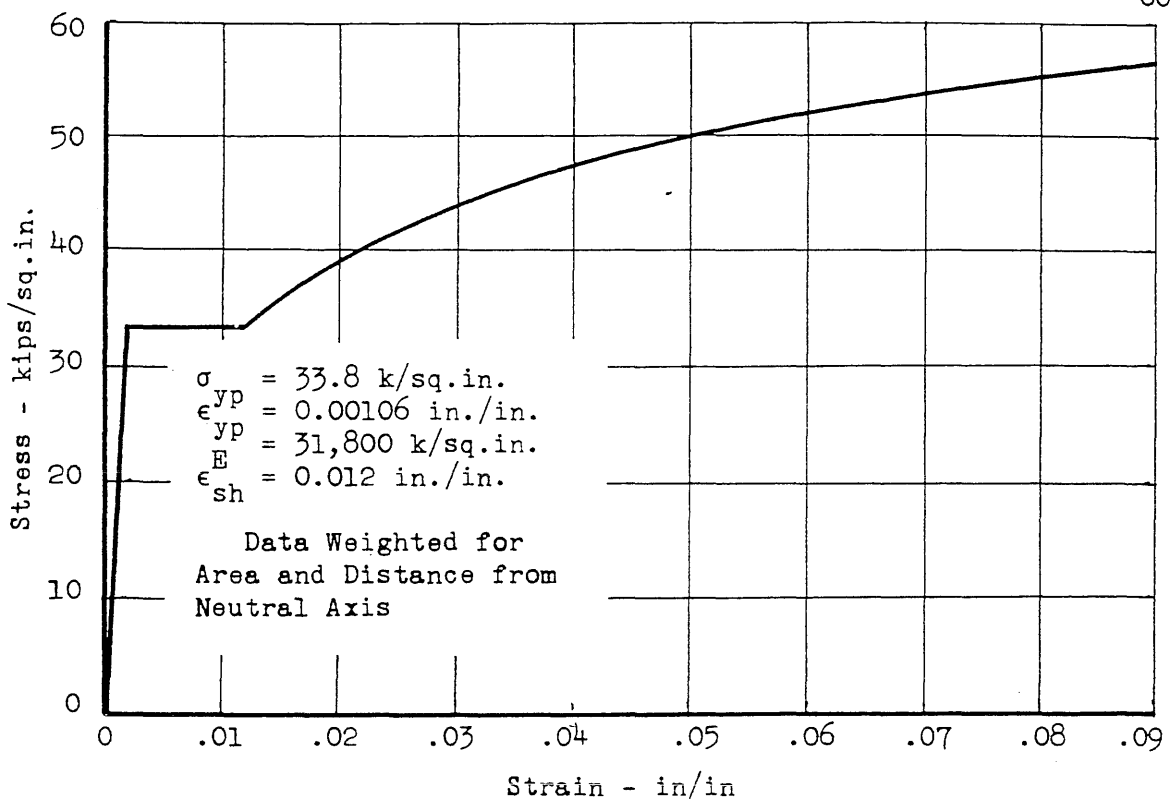

FIG. 3 STRESS-STRAIN DIAGRAM FOR BEAM B1

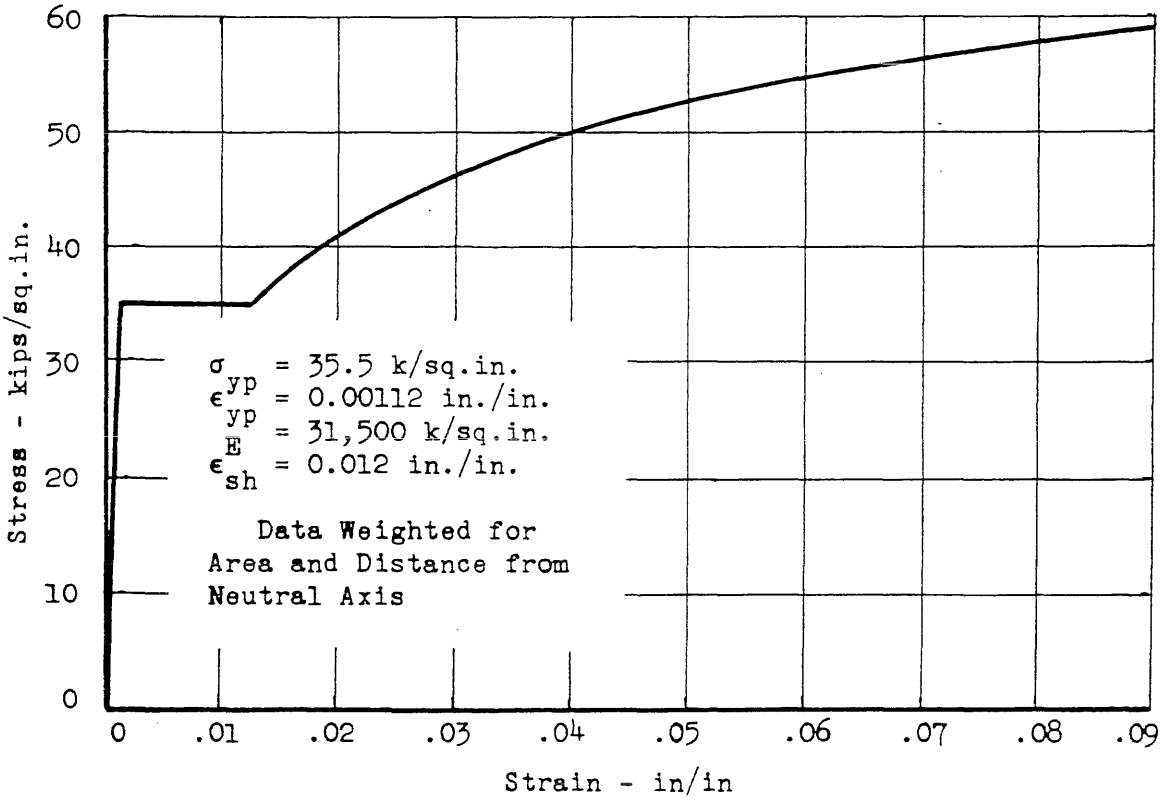

FIG. 4 STRESS-STRAIN DIAGRAM FOR BEAM B2

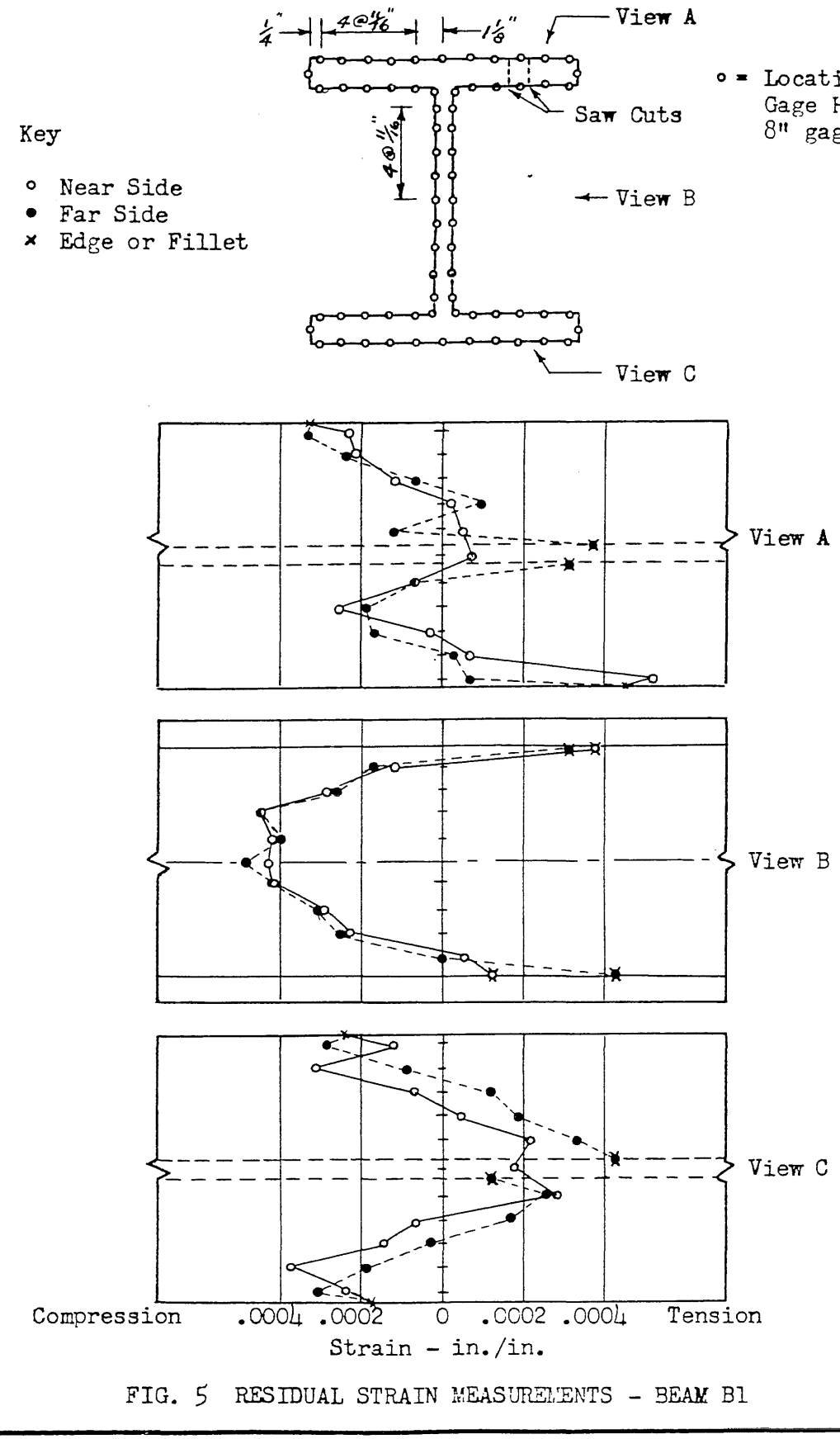

FIG. 5 RESIDUAL STRAIN MEASUREMENTS - BEAM B1

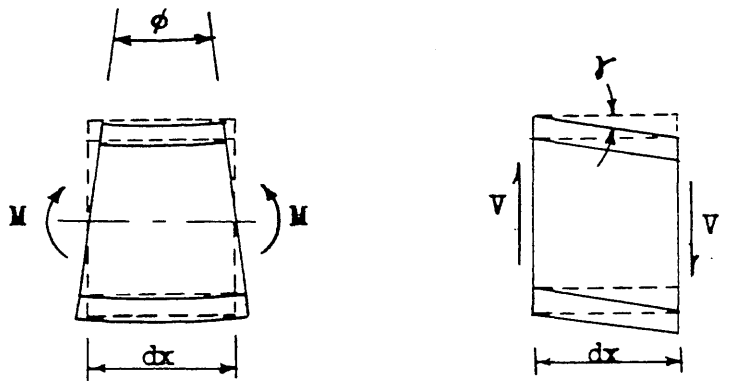

FIG. 6 DEFORMATION OF A BEAM SECTION DUE TO BENDING MOMENT AND SHEAR

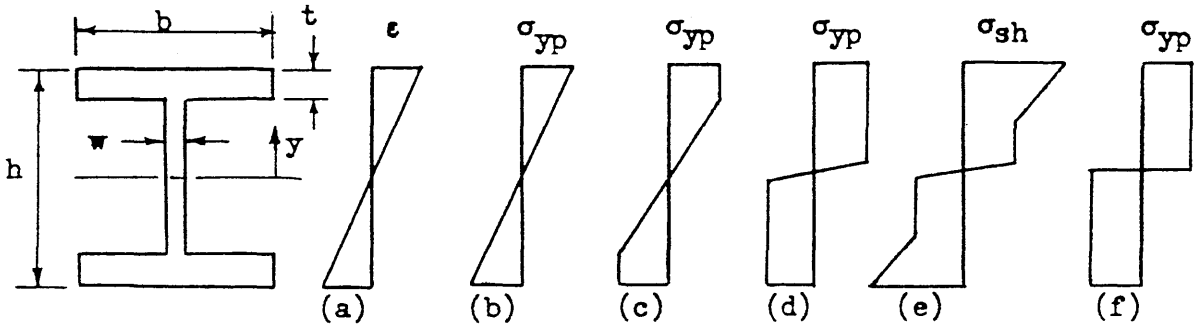

FIG. 7 FORMATION OF STRESS BLOCKS

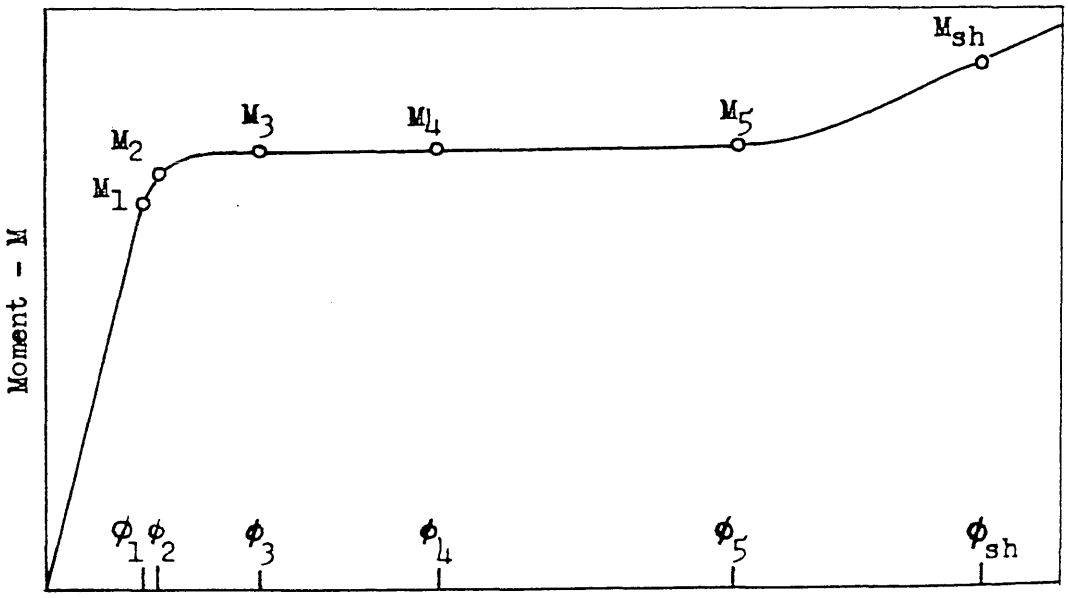

FIG. 8 TYPICAL MOMENT-CURVATURE DIAGRAM

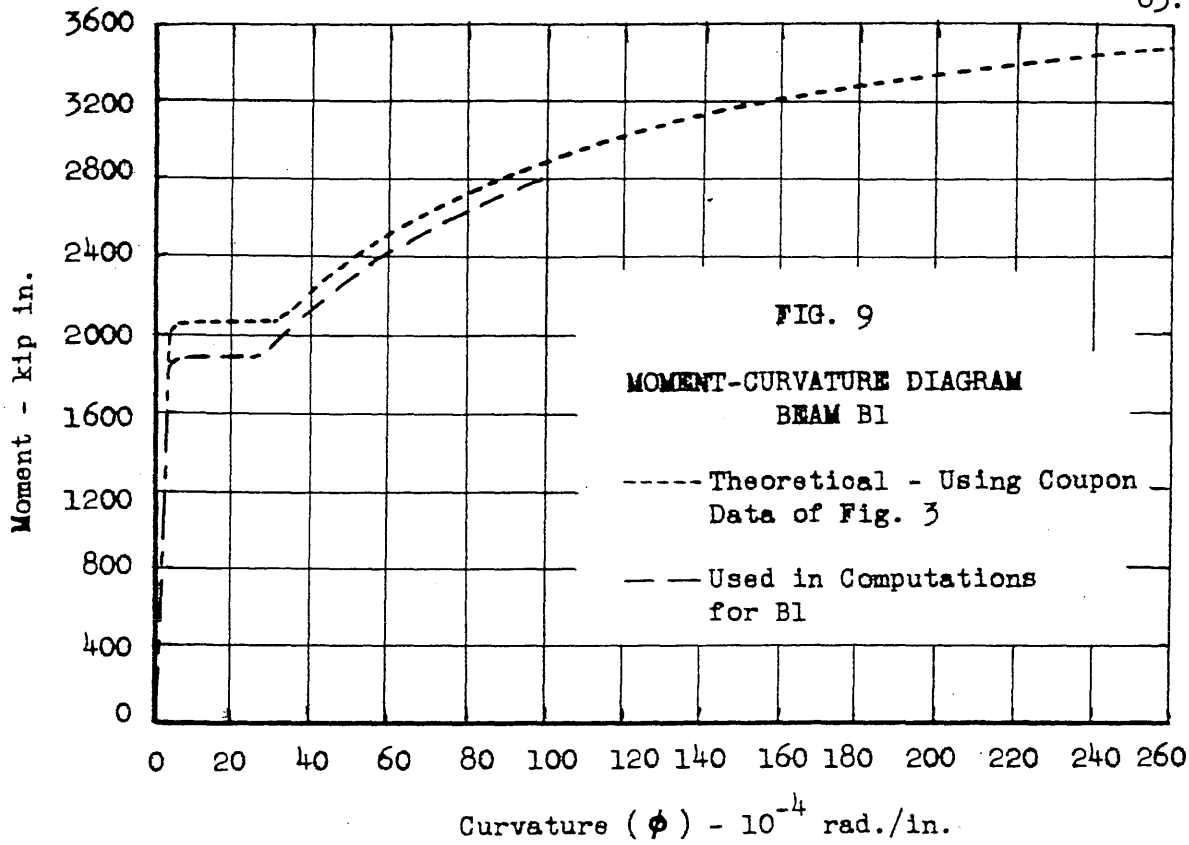
Moment - kip in.
3600
3200
2800
2400
2000
1600
1200
800
400
0
0 20 40 60 80 100 120 140 160 180 200 220 240 260
Curvature (ϕ) - 10^-4 rad./in.
FIG. 9
MOMENT-CURVATURE DIAGRAM
BEAM B1
----- Theoretical - Using Coupon Data of Fig. 3
— — Used in Computations for B1

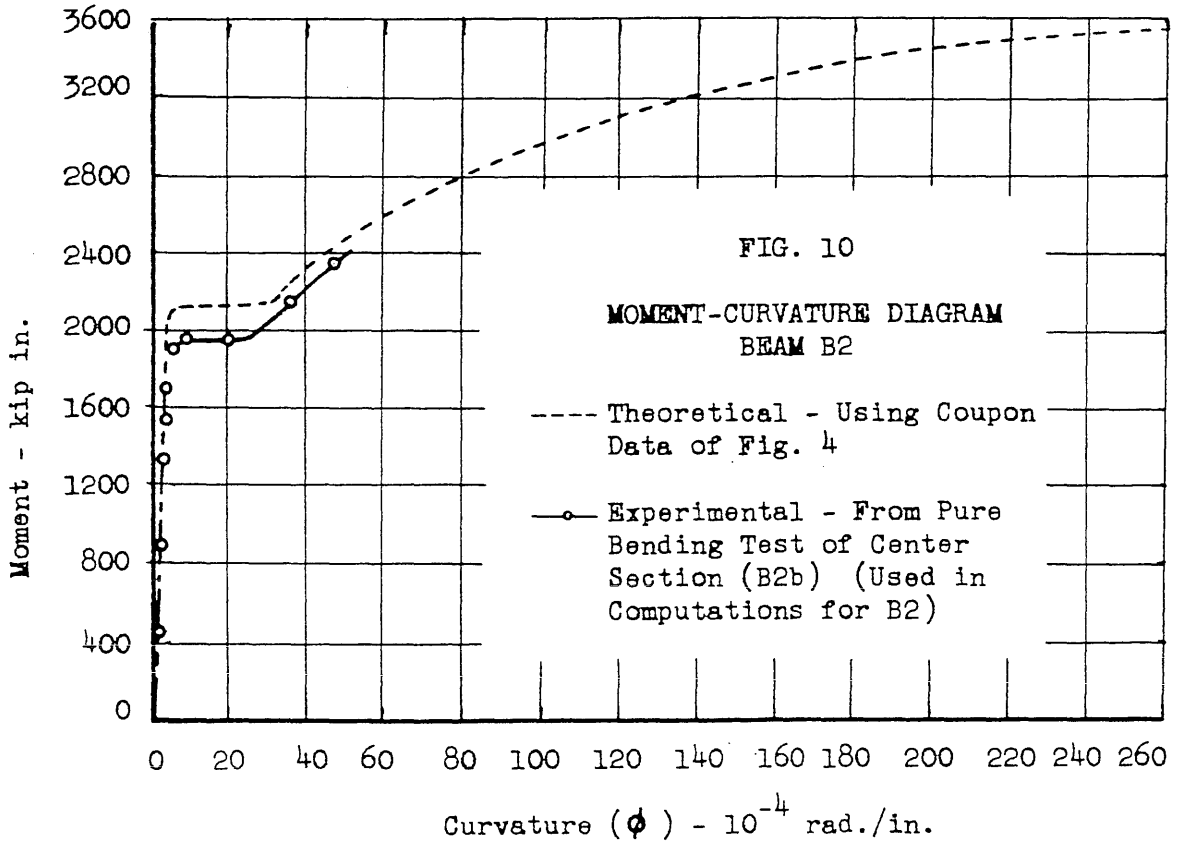
Moment - kip in.
3600
3200
2800
2400
2000
1600
1200
800
400
0
0 20 40 60 80 100 120 140 160 180 200 220 240 260
Curvature (ϕ) - 10^-4 rad./in.
FIG. 10
MOMENT-CURVATURE DIAGRAM
BEAM B2
---- Theoretical - Using Coupon Data of Fig. 4
—o— Experimental - From Pure Bending Test of Center Section (B2b) (Used in Computations for B2)

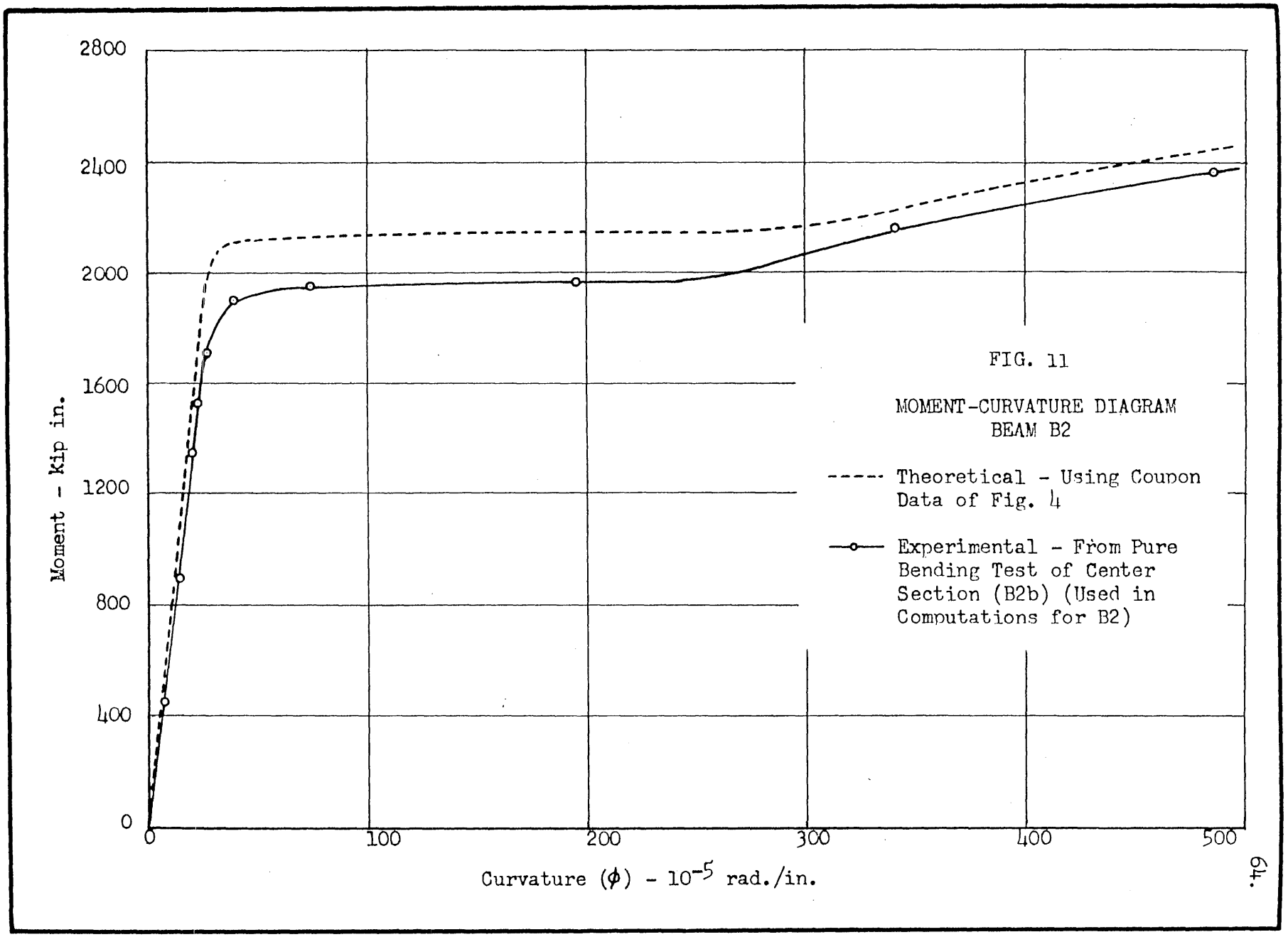

FIG. 11

MOMENT-CURVATURE DIAGRAM
BEAM B2

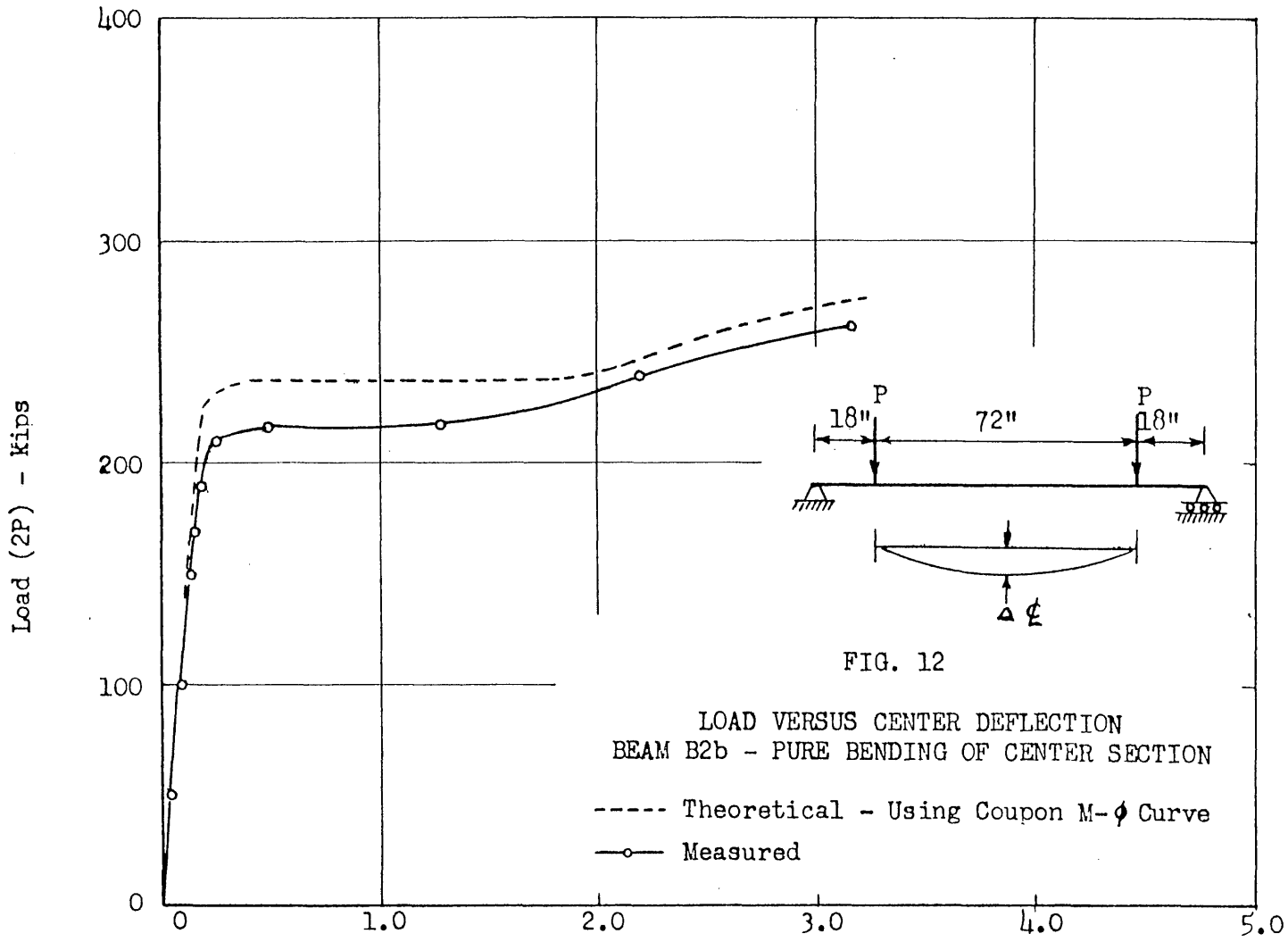

FIG. 12

LOAD VERSUS CENTER DEFLECTION
BEAM B2b - PURE BENDING OF CENTER SECTION

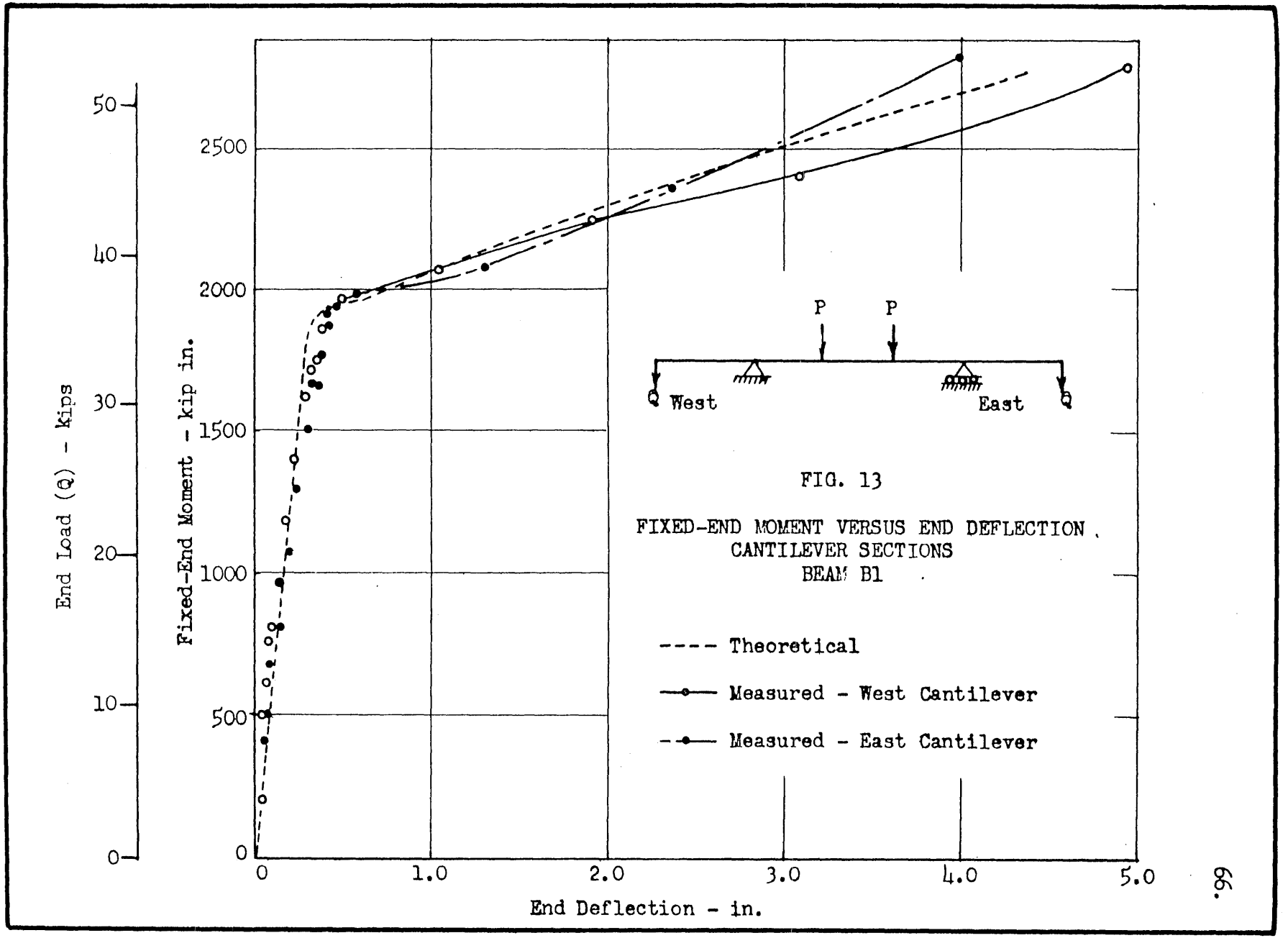

FIG. 13

FIXED-END MOMENT VERSUS END DEFLECTION
CANTILEVER SECTIONS
BEAM B1

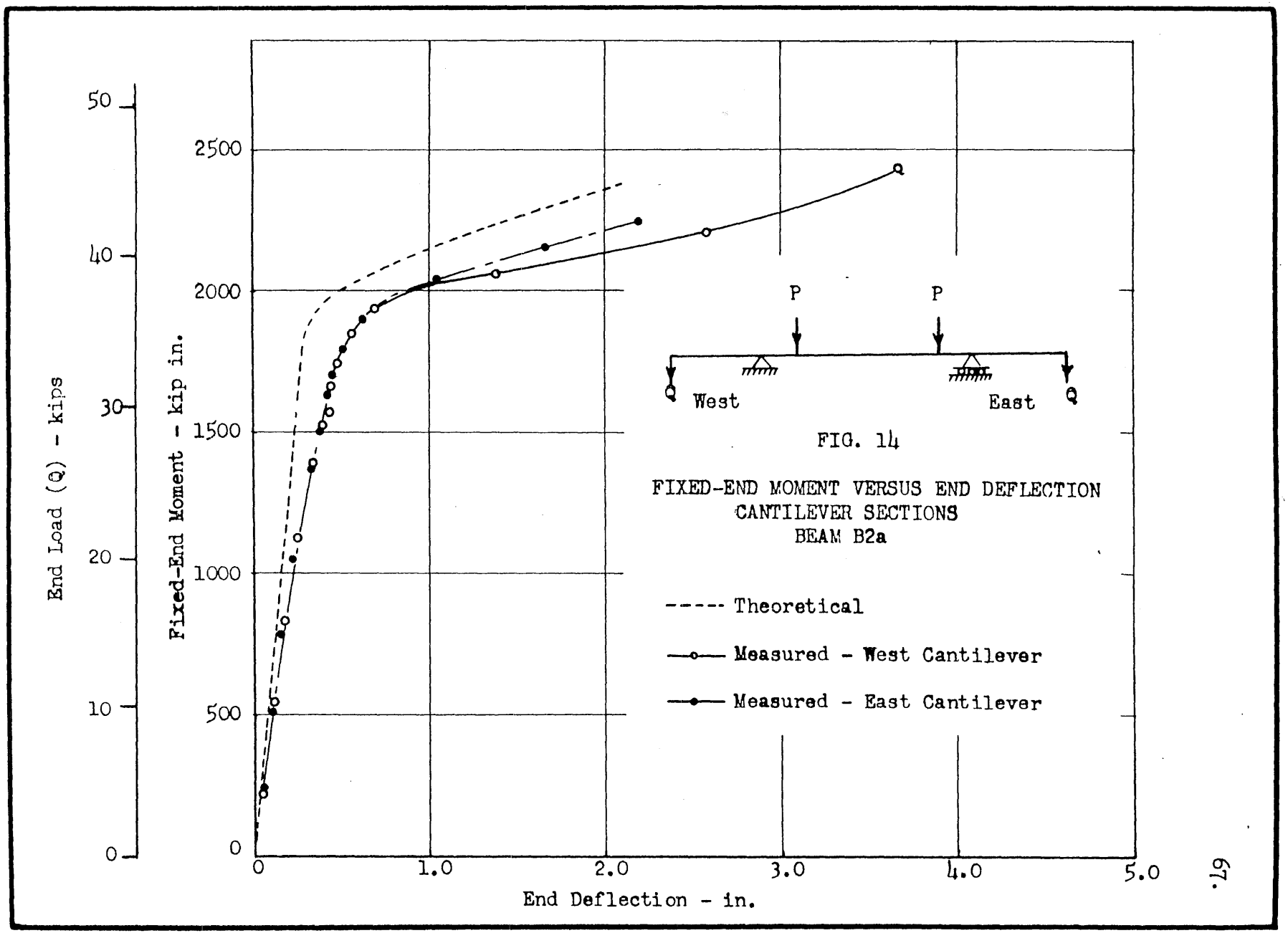

FIG. 14

FIXED-END MOMENT VERSUS END DEFLECTION
CANTILEVER SECTIONS
BEAM B2a

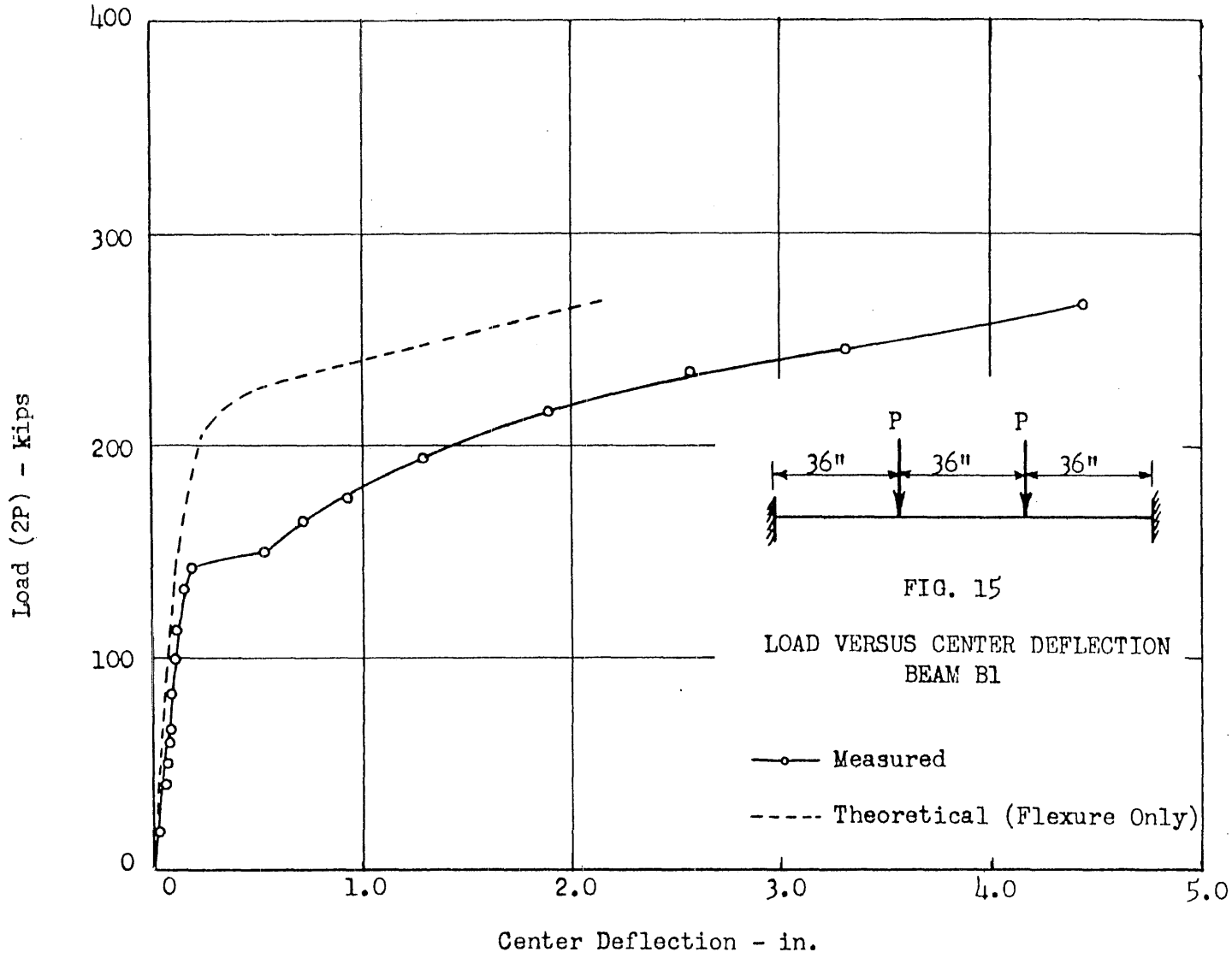

FIG. 15

LOAD VERSUS CENTER DEFLECTION
BEAM B1

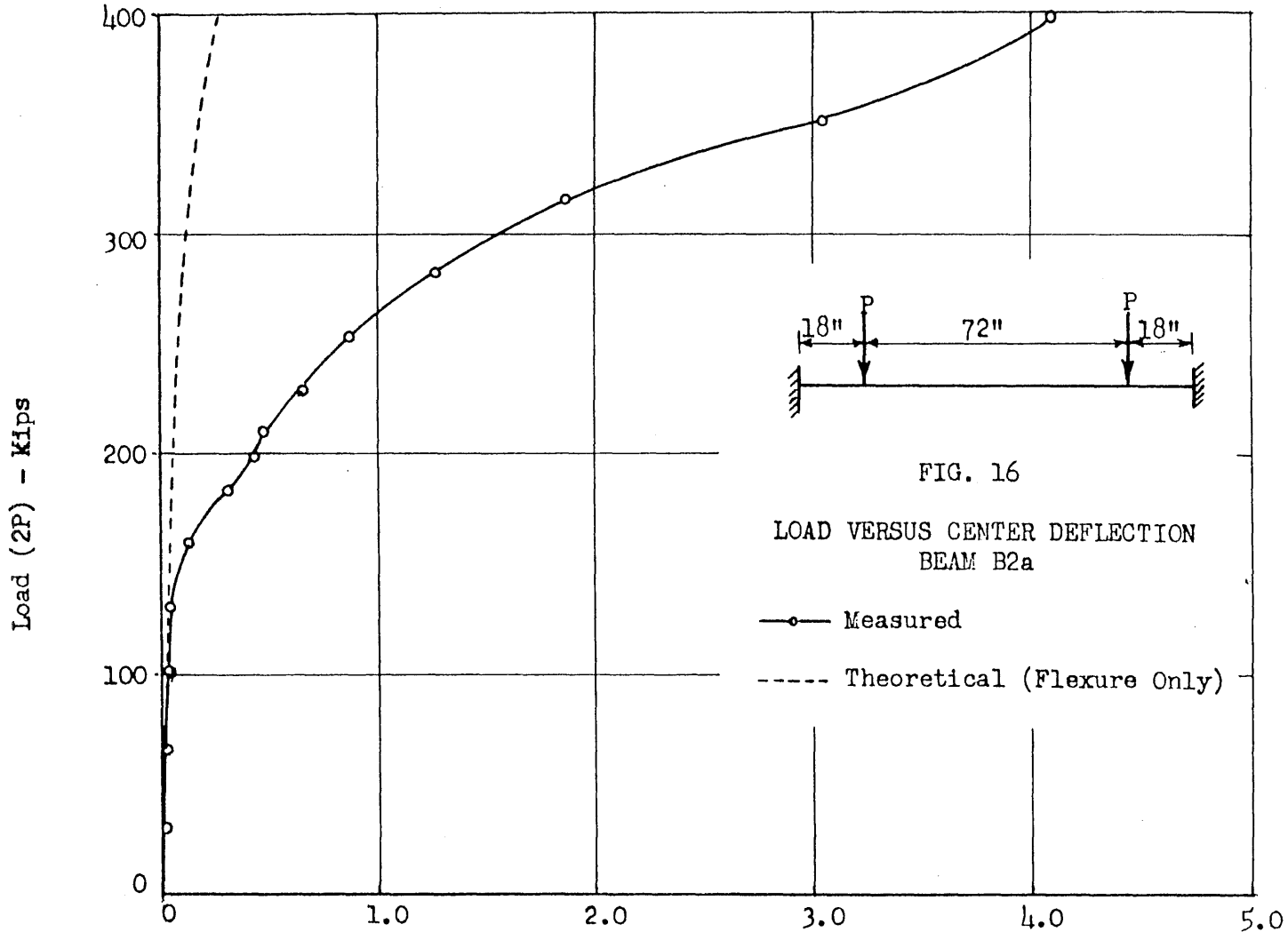

FIG. 16

LOAD VERSUS CENTER DEFLECTION
BEAM B2a

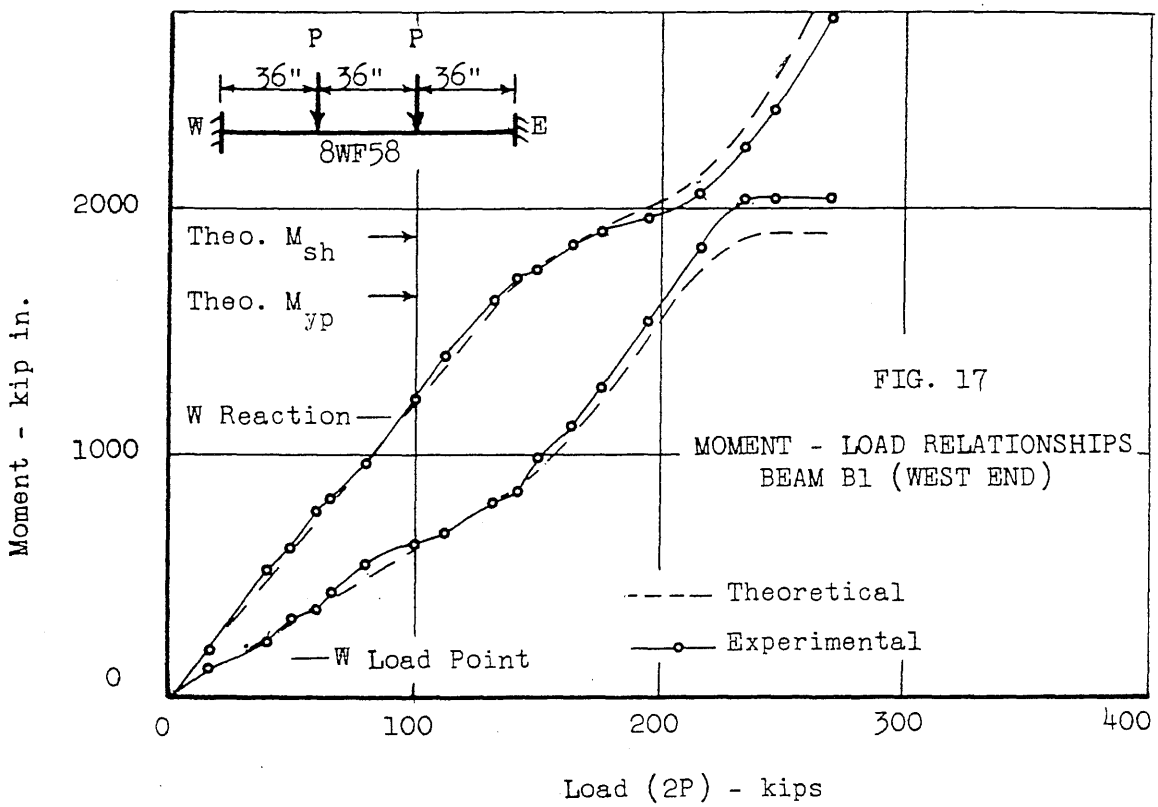

FIG. 17

MOMENT - LOAD RELATIONSHIPS
BEAM B1 (WEST END)

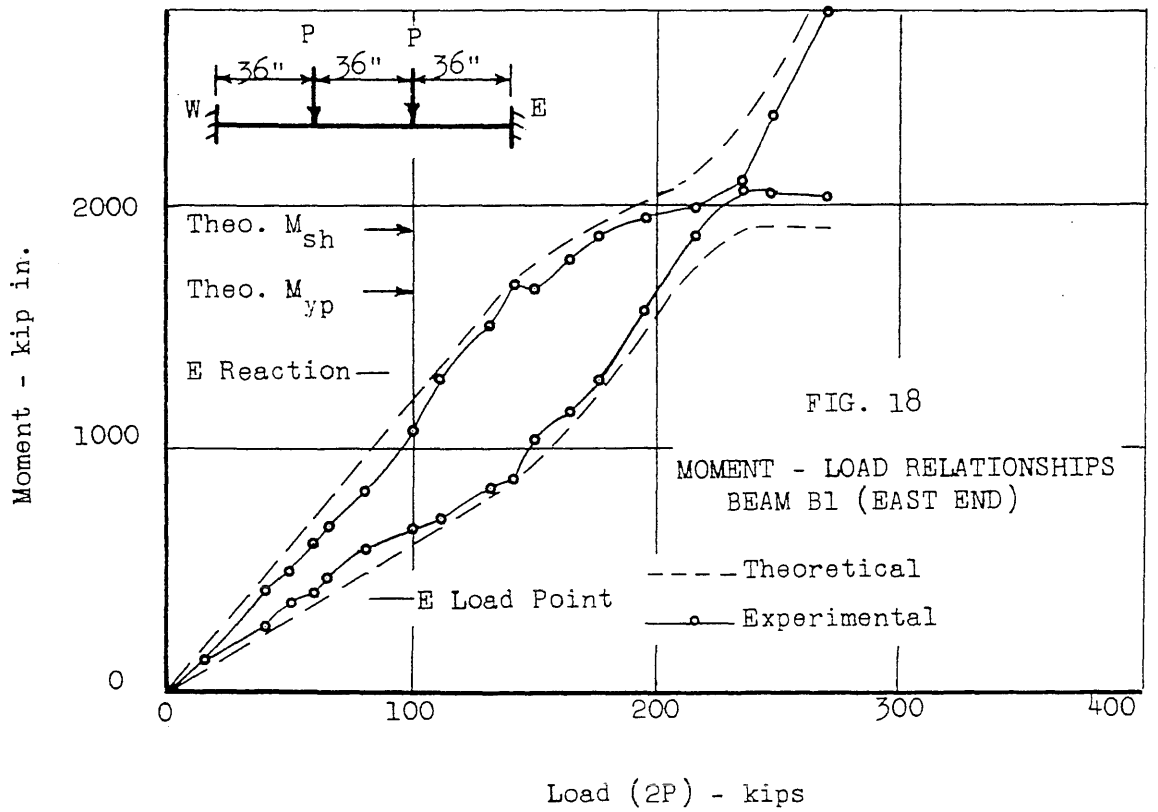

FIG. 18

MOMENT - LOAD RELATIONSHIPS
BEAM B1 (EAST END)

FIG. 19

MOMENT - LOAD RELATIONSHIPS
BEAM B2a (WEST END)

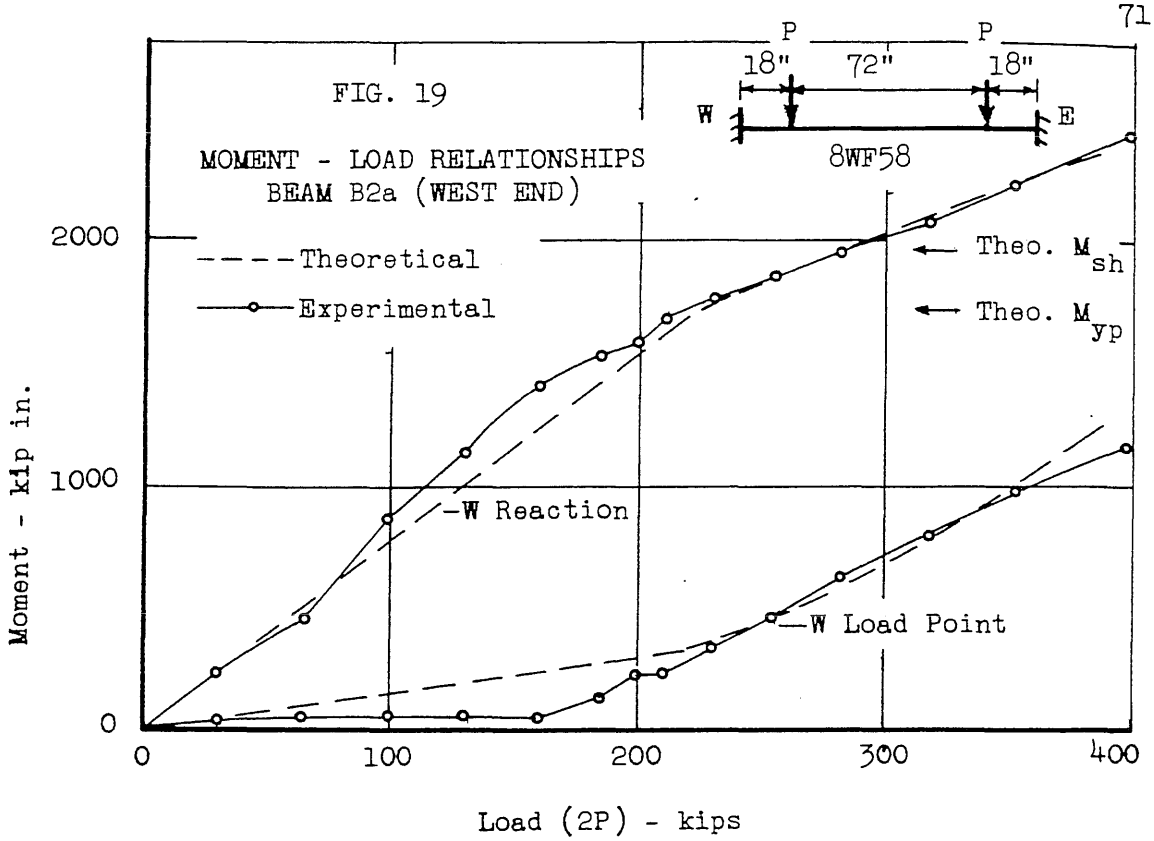

FIG. 20

MOMENT - LOAD RELATIONSHIPS
BEAM B2a (EAST END)

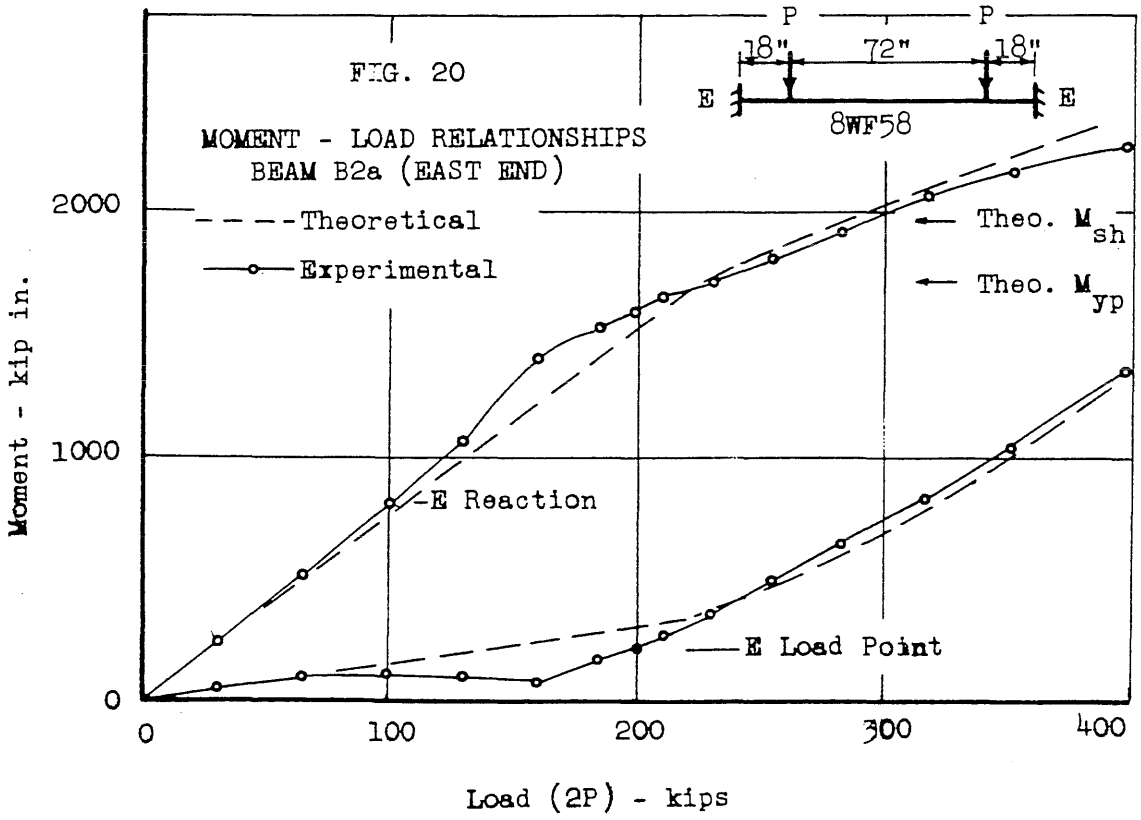

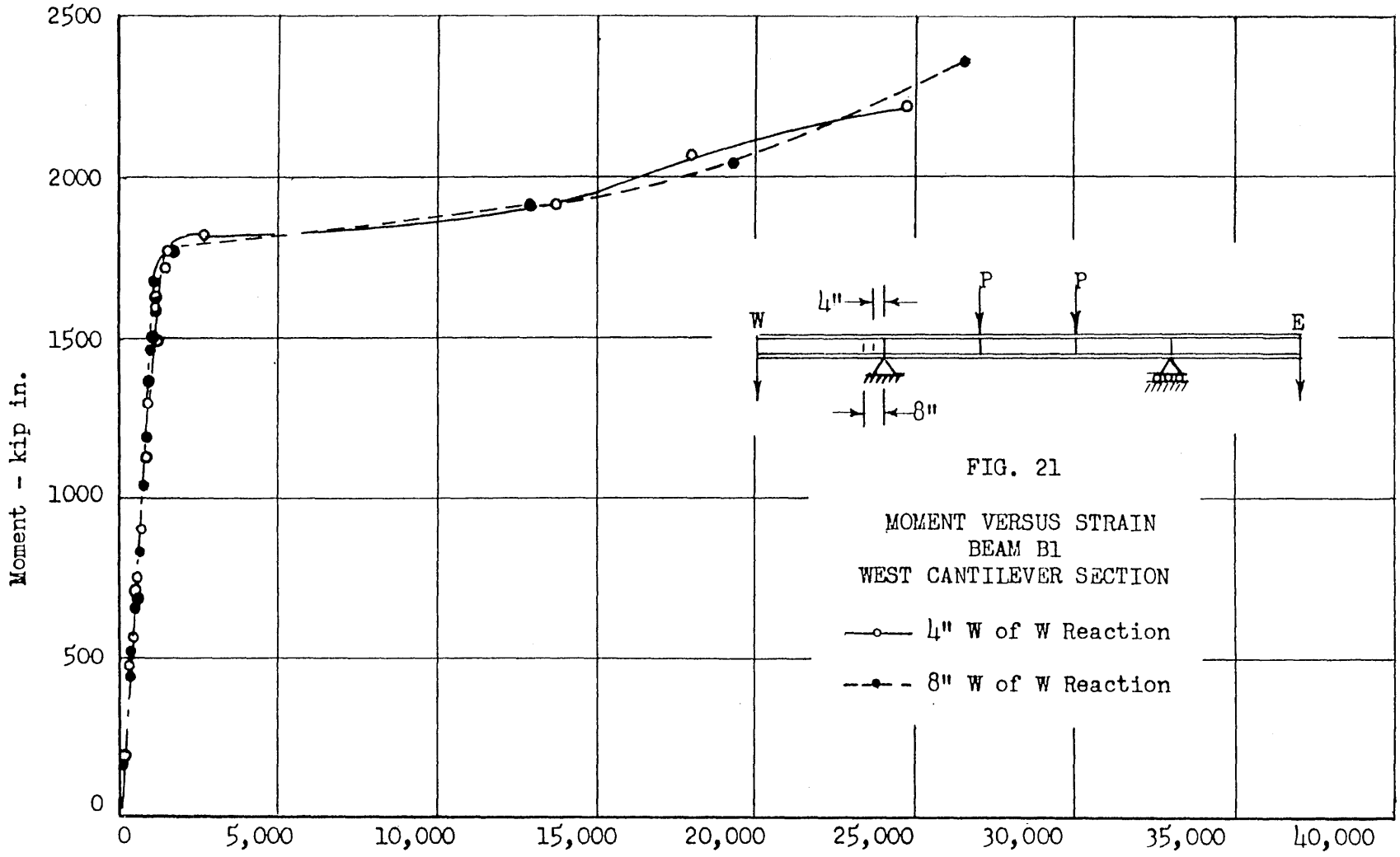

FIG. 21

MOMENT VERSUS STRAIN
BEAM B1
WEST CANTILEVER SECTION

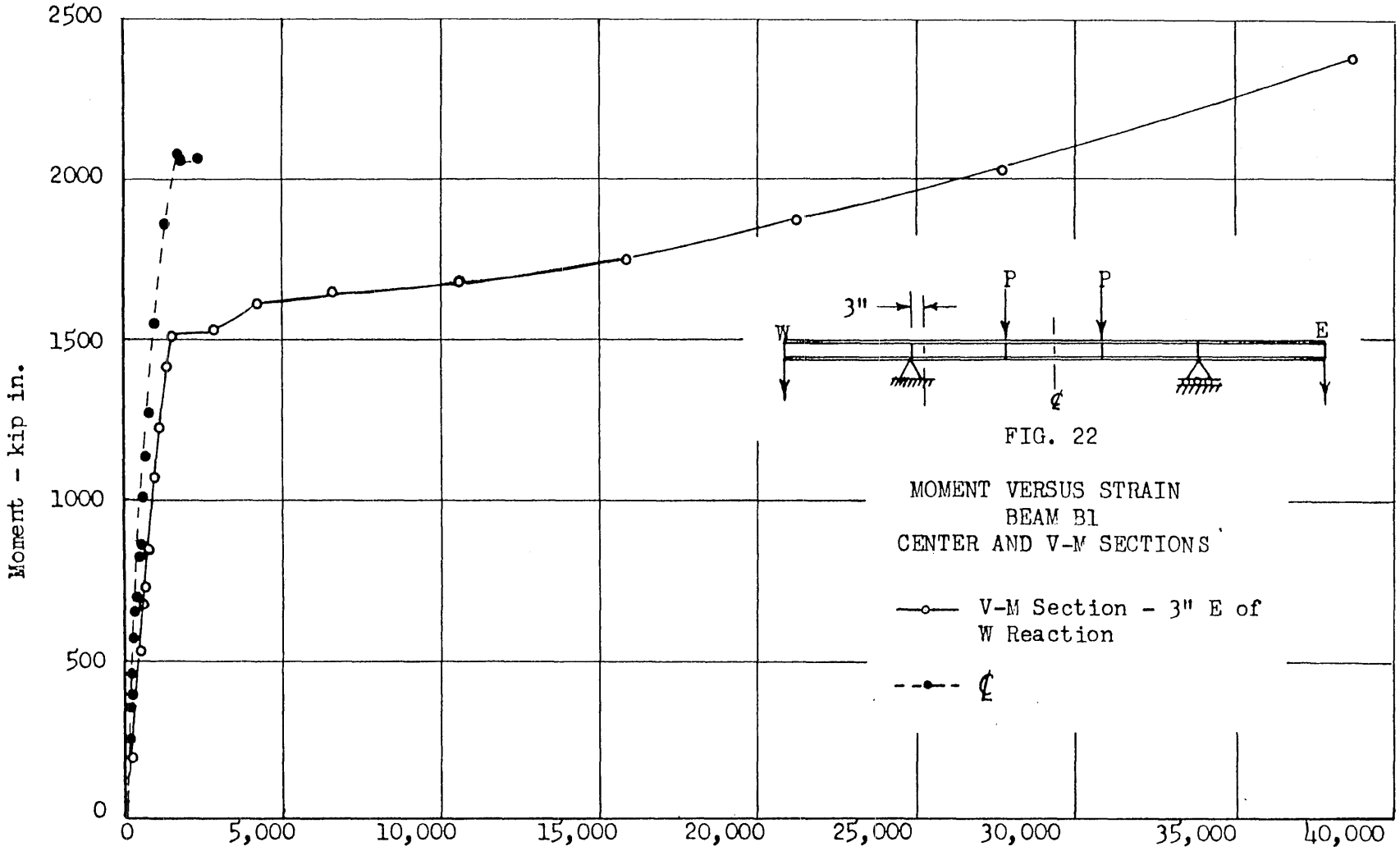
2500
2000
1500
1000
500
0
Moment - kip in.
0
5,000
10,000
15,000
20,000
25,000
30,000
35,000
40,000
Strain - micro in./in.
3"
P
P
W
E
℄
MOMENT VERSUS STRAIN
BEAM B1
CENTER AND V-M SECTIONS
V-M Section - 3" E of W Reaction
℄

FIG. 22

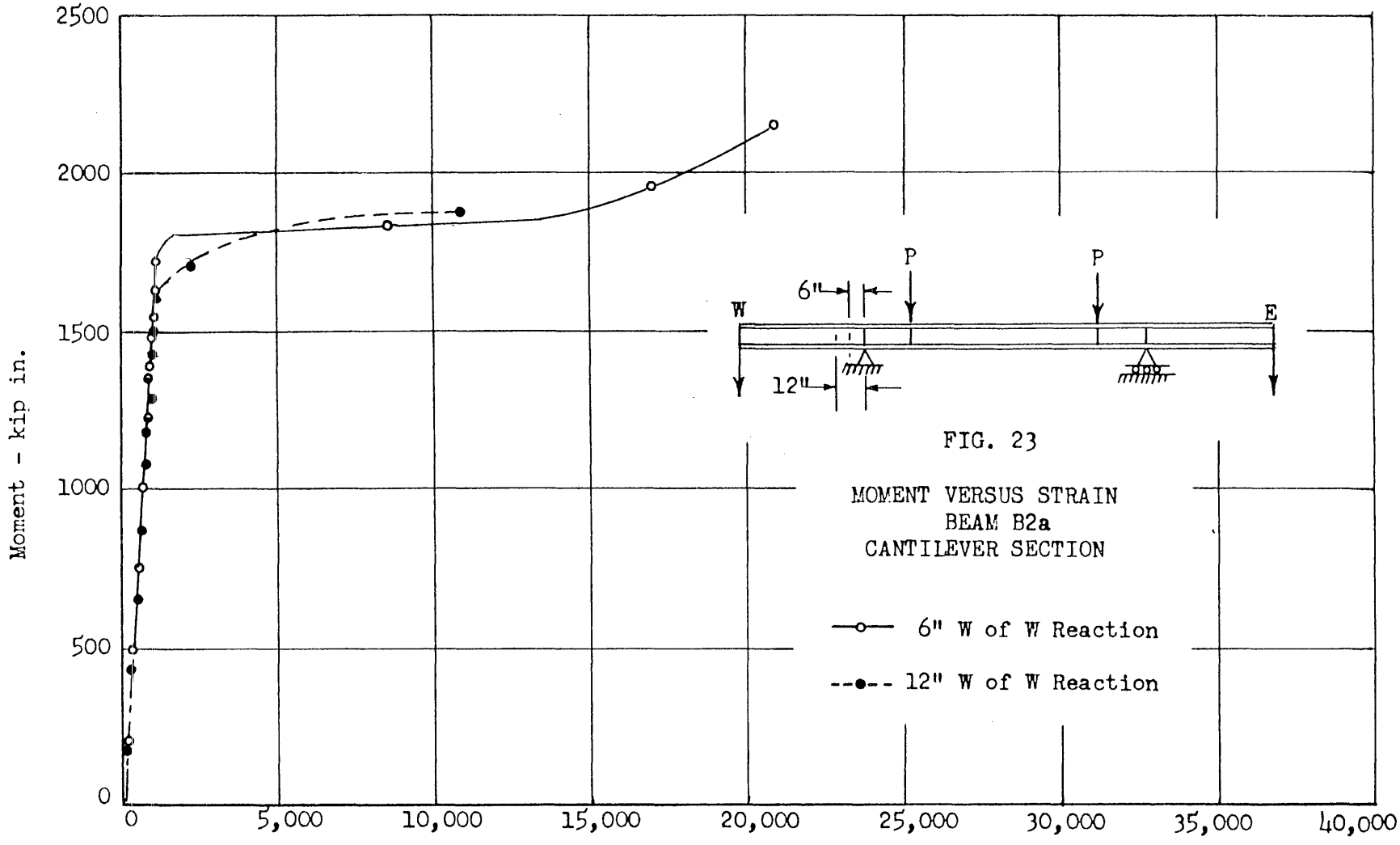

FIG. 23

MOMENT VERSUS STRAIN
BEAM B2a
CANTILEVER SECTION

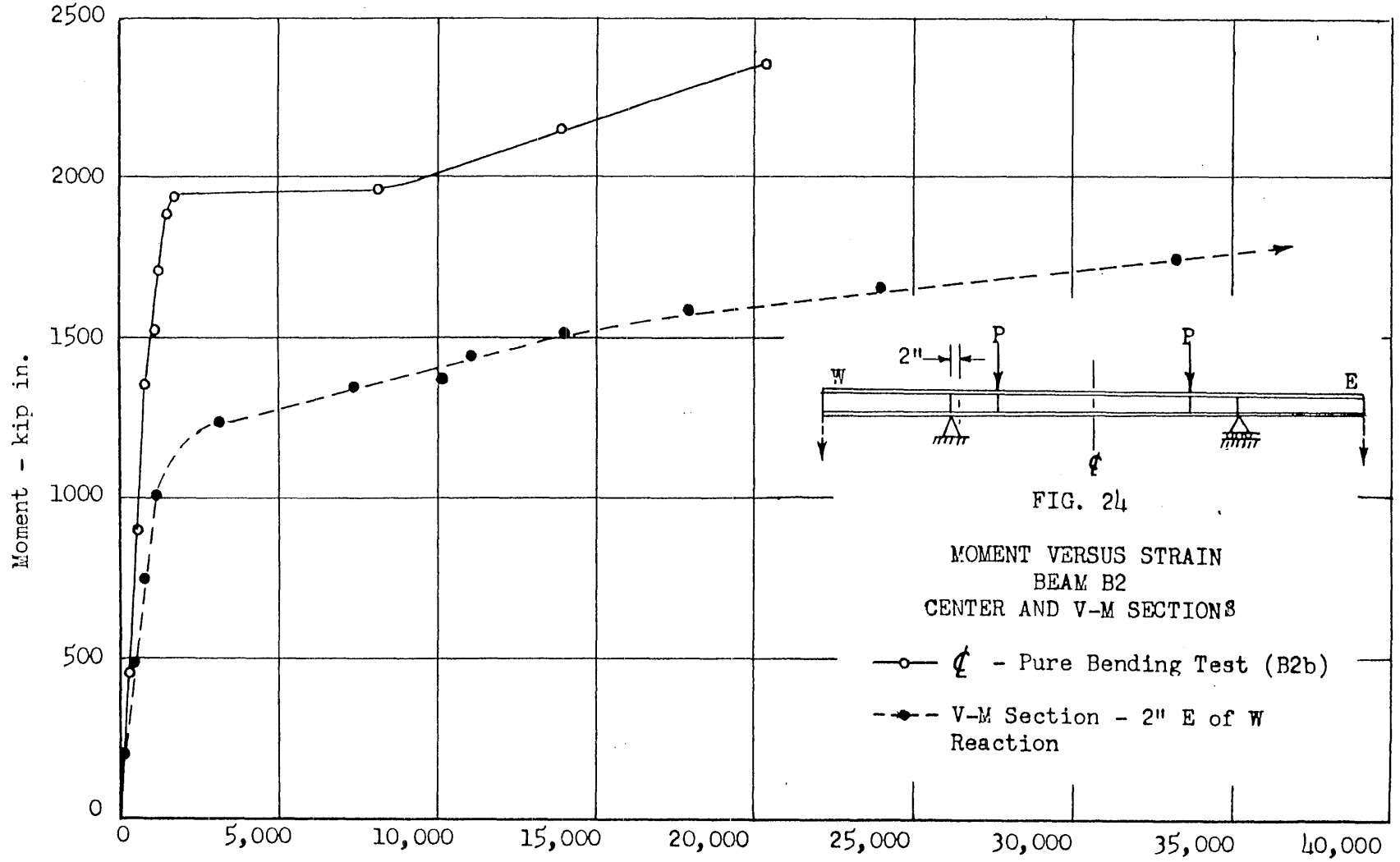

FIG. 24

MOMENT VERSUS STRAIN
BEAM B2
CENTER AND V-M SECTIONS

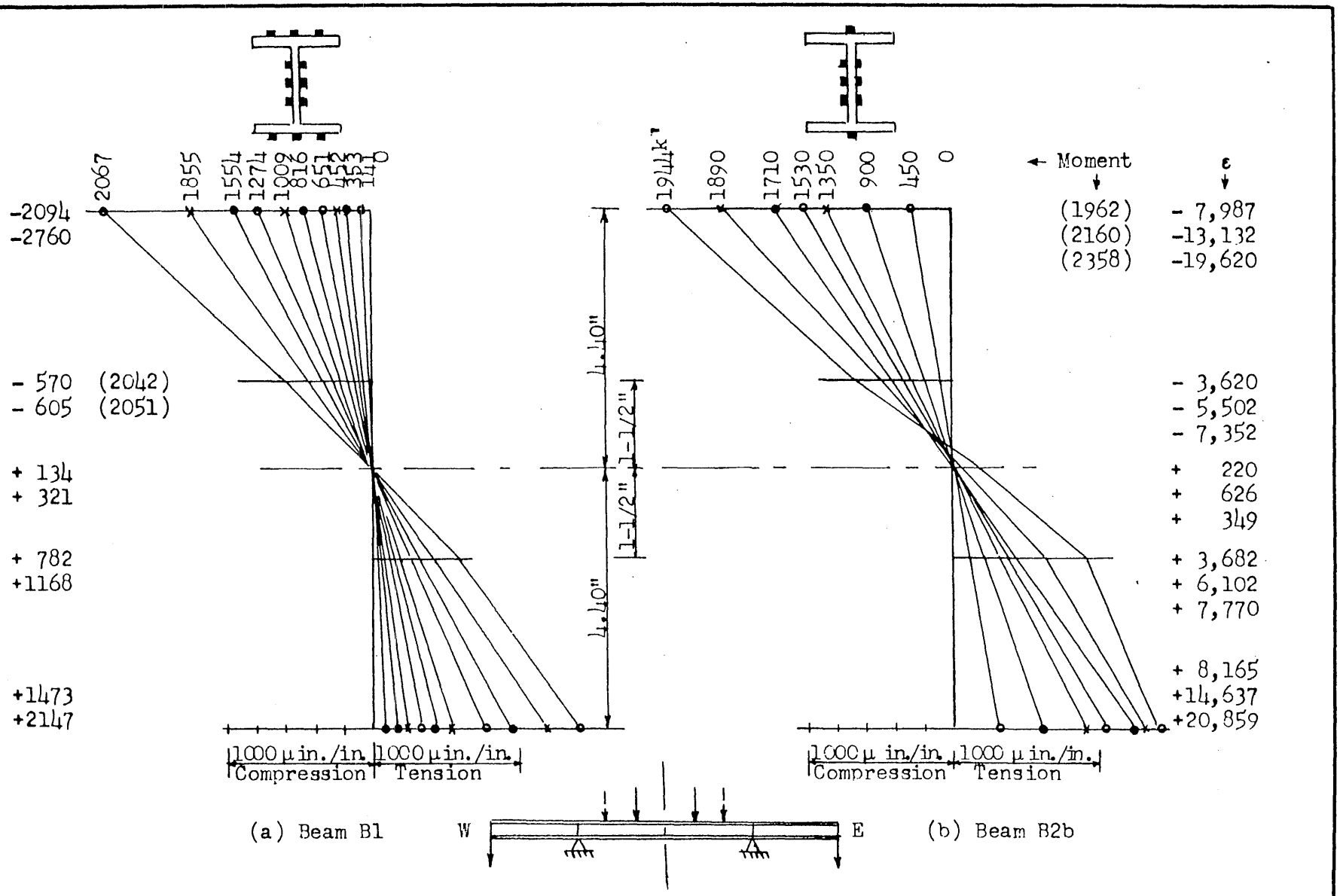

FIG. 25 STRAIN DISTRIBUTION AT CENTER OF BEAMS

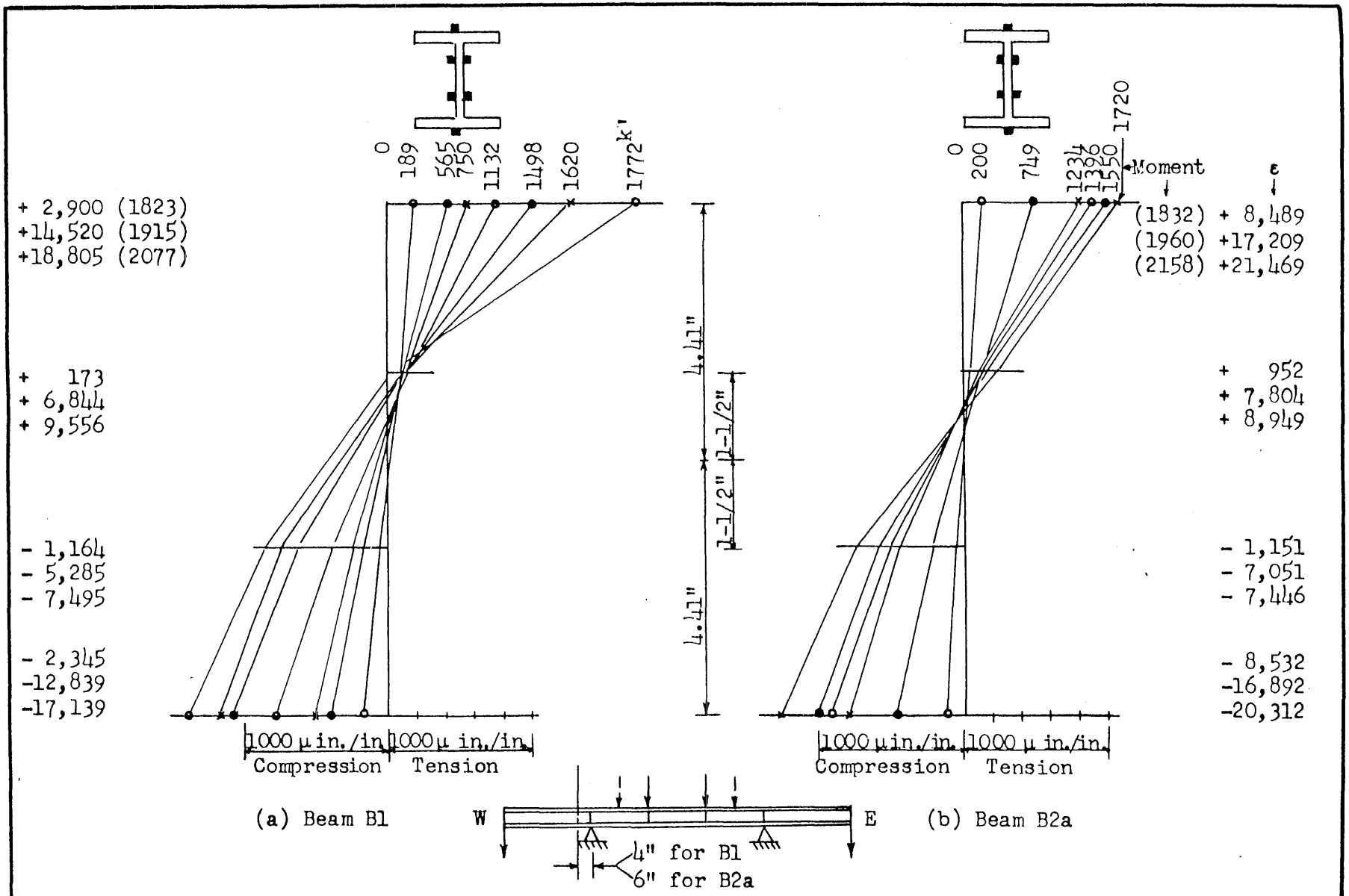

FIG. 26 STRAIN DISTRIBUTION IN CANTILEVER SECTIONS

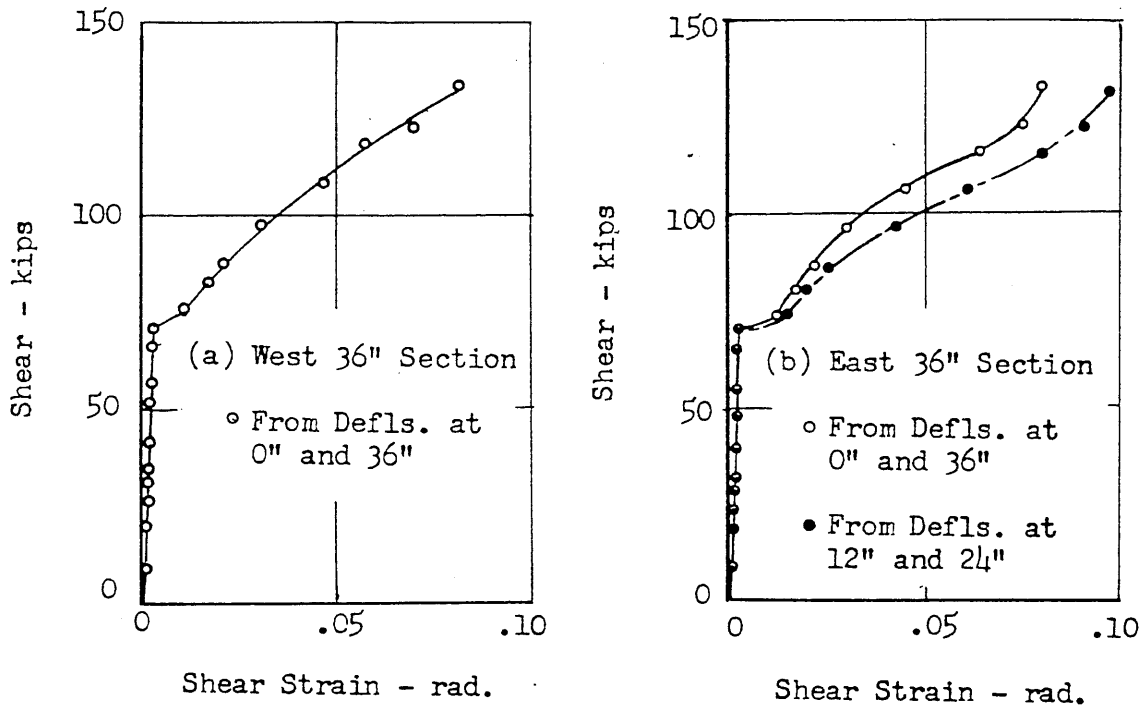

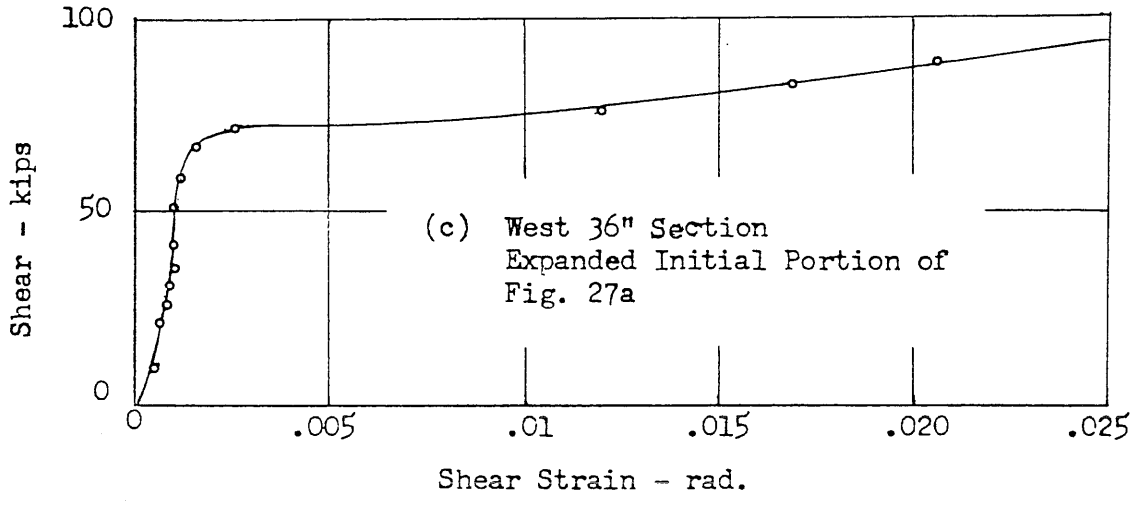

FIG. 27 SHEAR VERSUS SHEAR STRAIN - BEAM B1

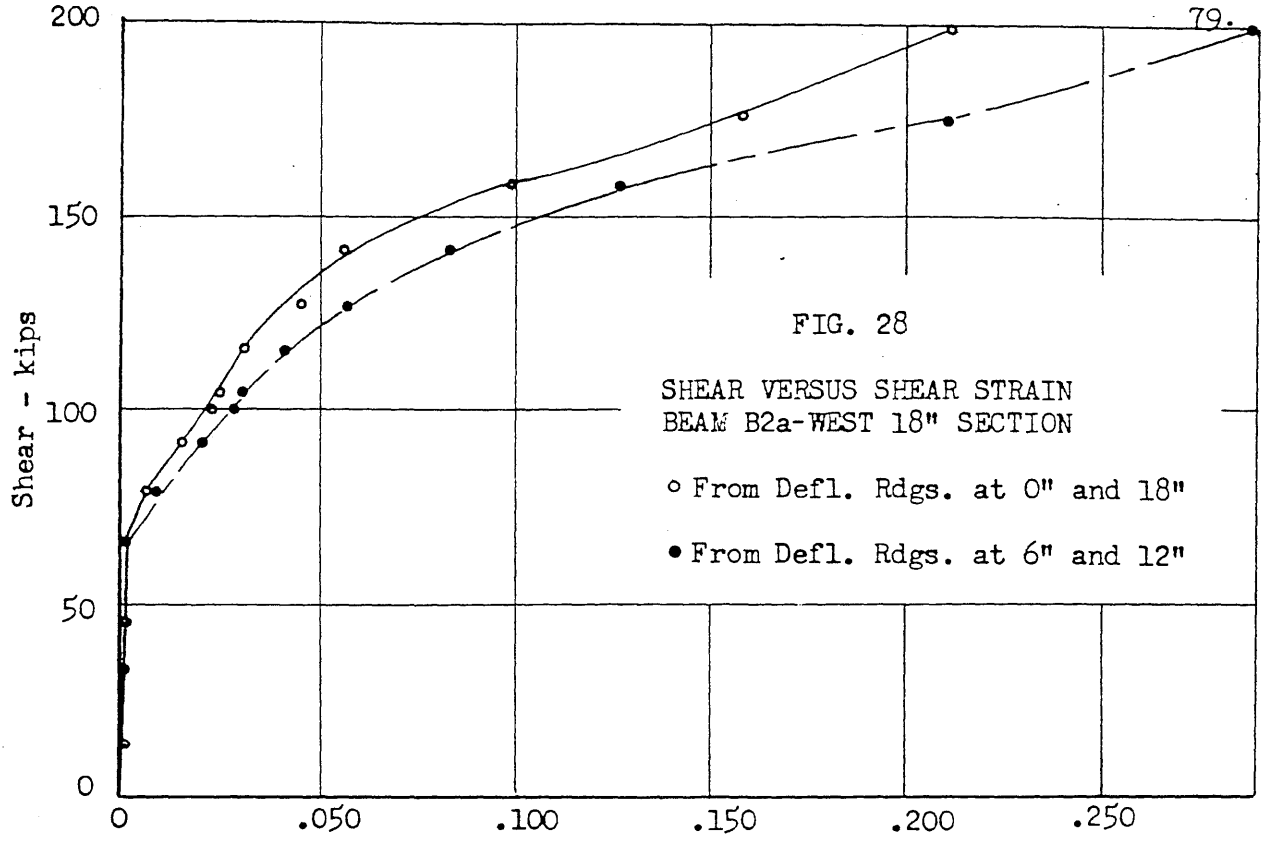

FIG. 28

SHEAR VERSUS SHEAR STRAIN
BEAM B2a-WEST 18" SECTION

○ From Defl. Rdgs. at 0" and 18"

● From Defl. Rdgs. at 6" and 12"

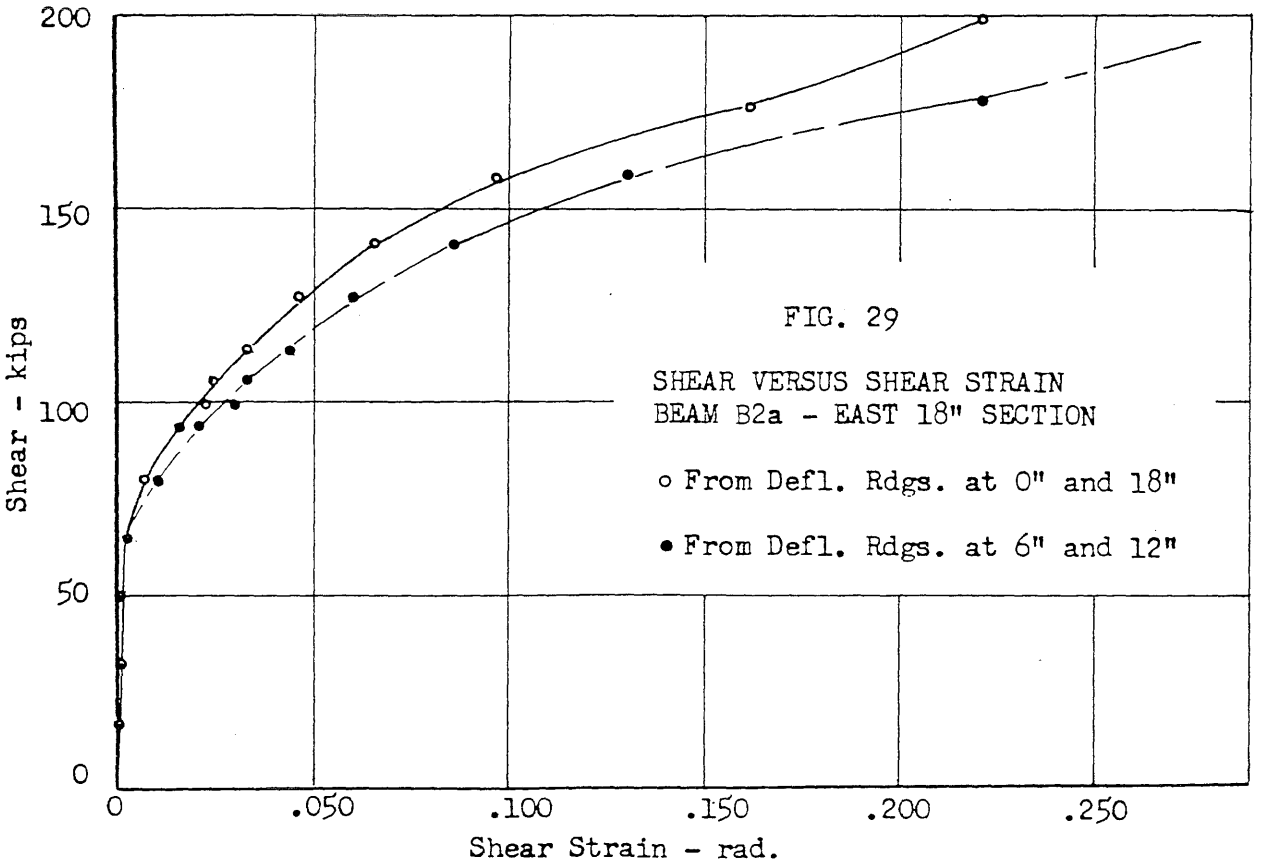

FIG. 29

SHEAR VERSUS SHEAR STRAIN
BEAM B2a - EAST 18" SECTION

○ From Defl. Rdgs. at 0" and 18"

● From Defl. Rdgs. at 6" and 12"

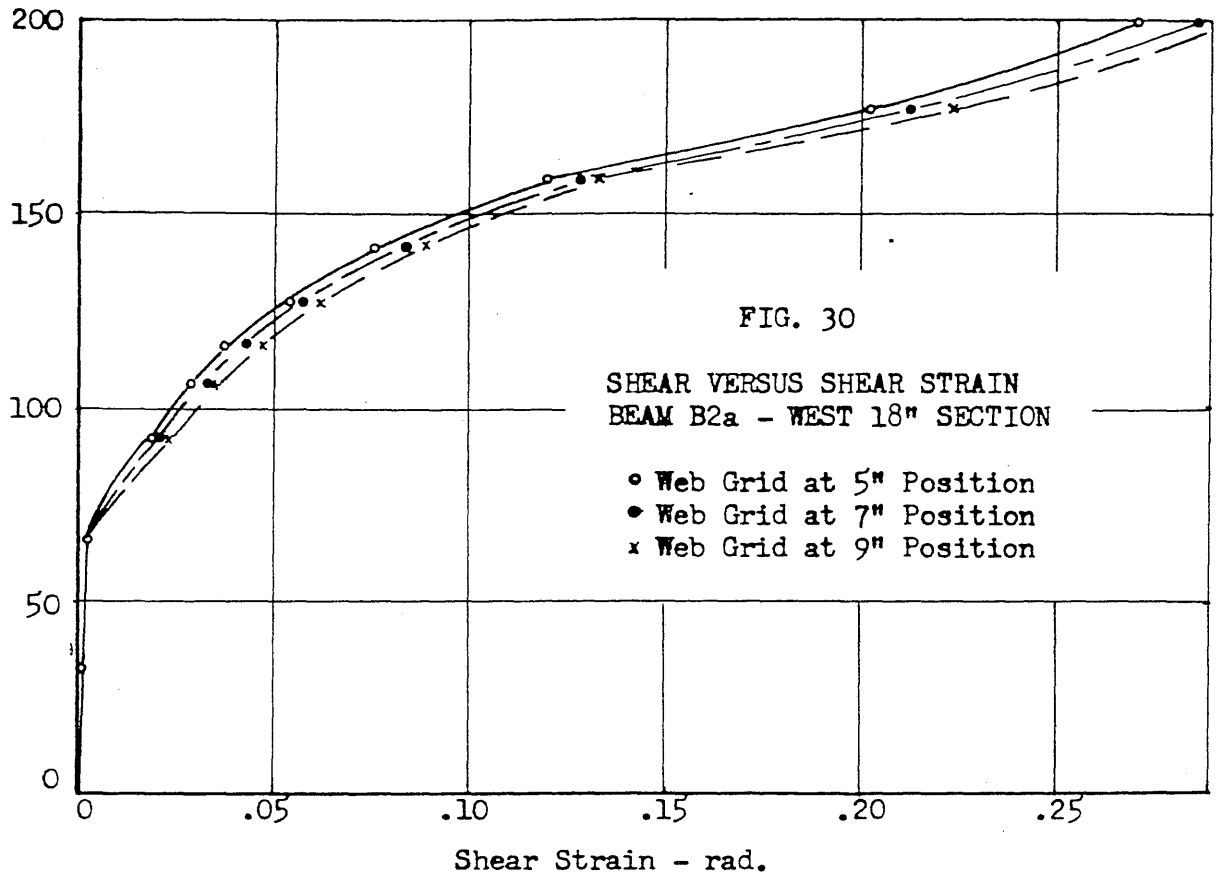

FIG. 30

SHEAR VERSUS SHEAR STRAIN
BEAM B2a - WEST 18" SECTION

- ∘ Web Grid at 5" Position
- • Web Grid at 7" Position
- x Web Grid at 9" Position

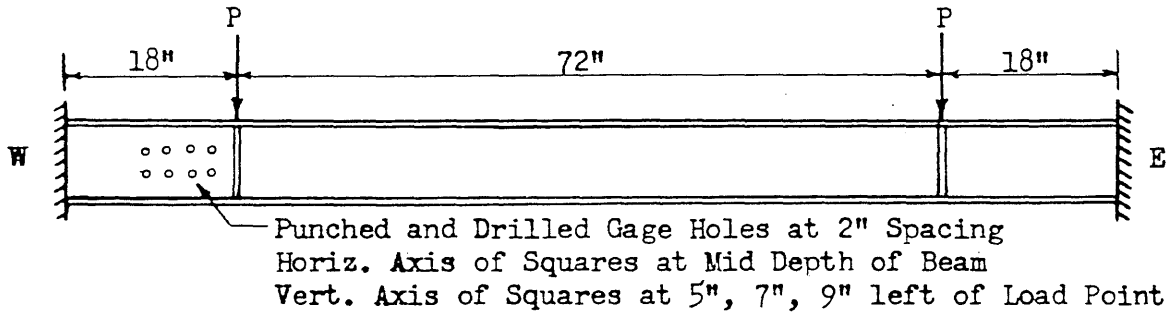

Punched and Drilled Gage Holes at 2" Spacing
Horiz. Axis of Squares at Mid Depth of Beam
Vert. Axis of Squares at 5", 7", 9" left of Load Point

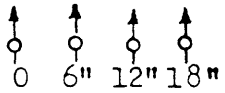

Deflection Gages (Distances are from reaction on W and E end of Beam)

Note: For Beam B1, Defl. Gages at 0, 12", 24", 36" were used in Computations.

FIG. 31 BEAM B2a - GRID AND DEFLECTION GAGE LAYOUT USED IN OBTAINING THE SHEAR STRAIN DATA

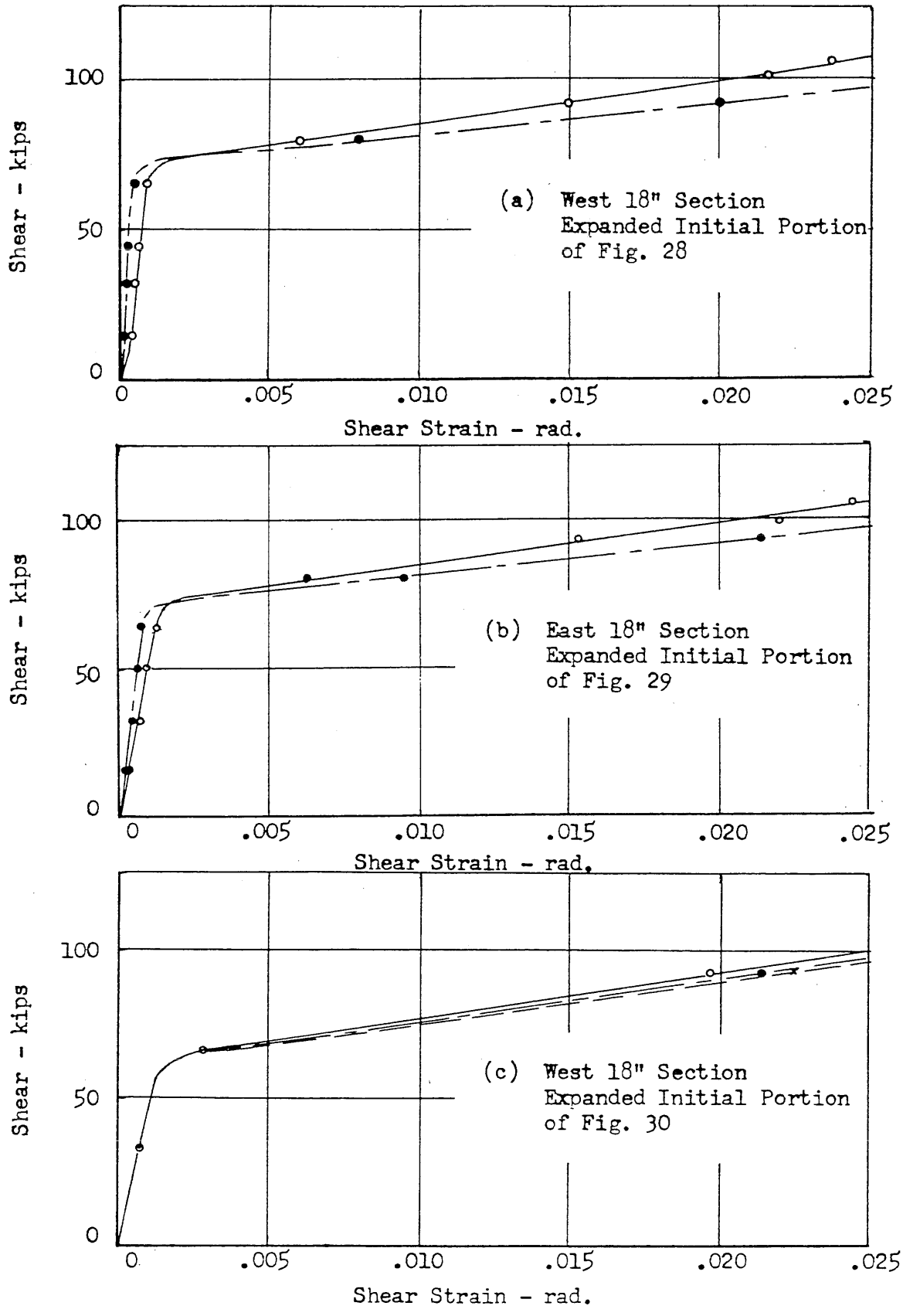

FIG. 32 SHEAR VERSUS SHEAR STRAIN - BEAM B2a

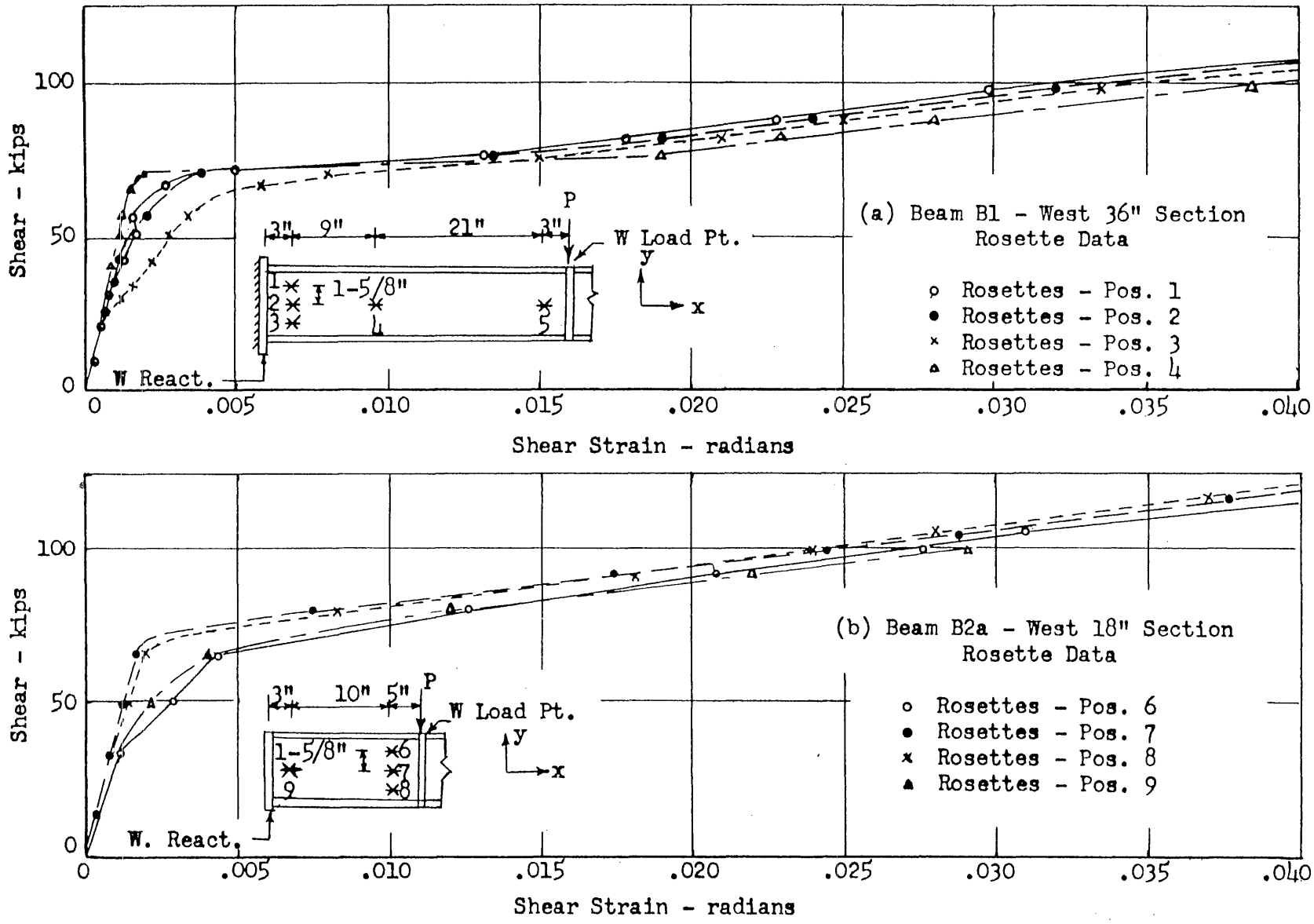

FIG. 33 SHEAR VERSUS SHEAR STRAIN - BEAMS B1 AND B2a - ROSETTE DATA

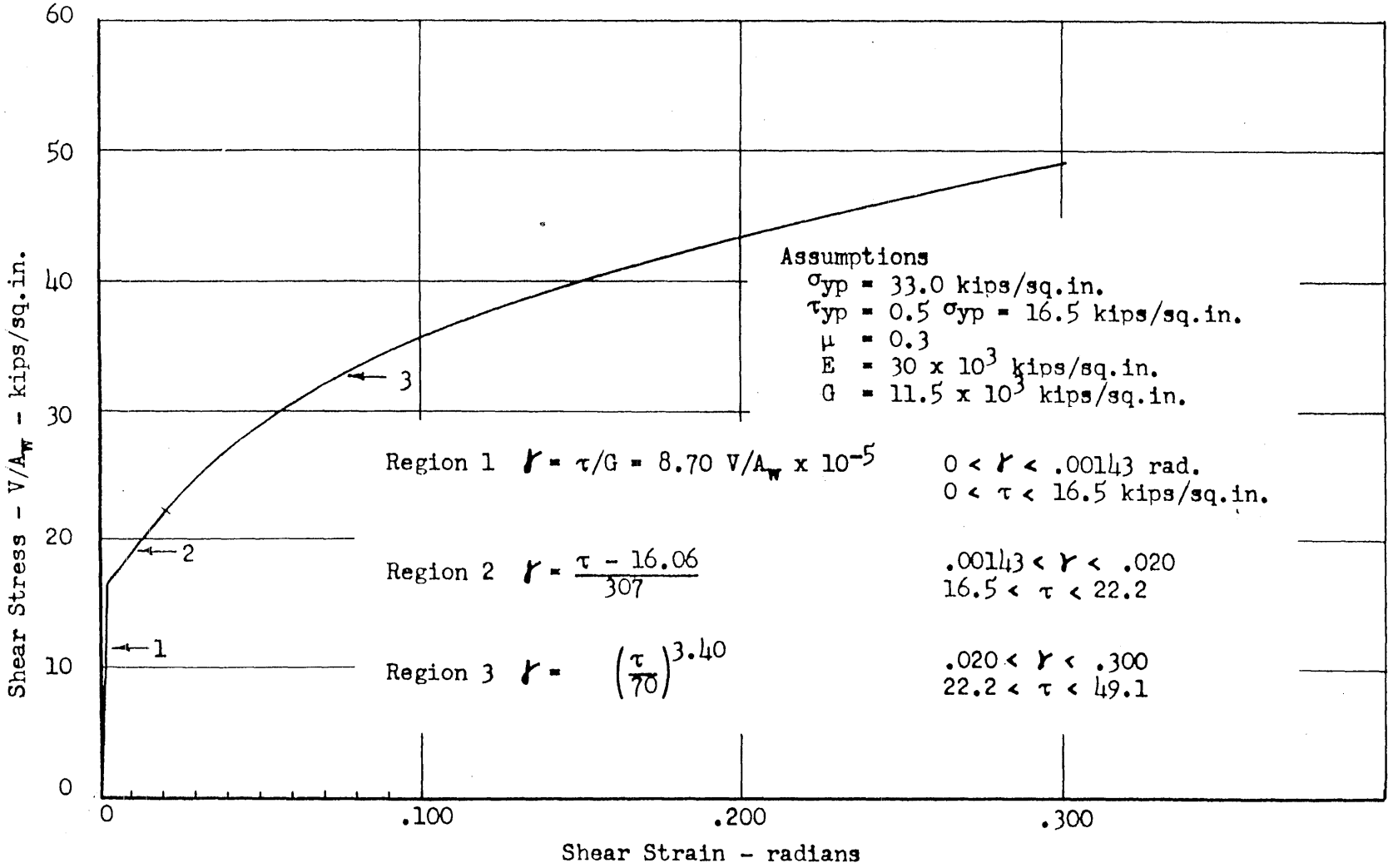

FIG. 34 SHEAR STRESS-STRAIN DIAGRAM

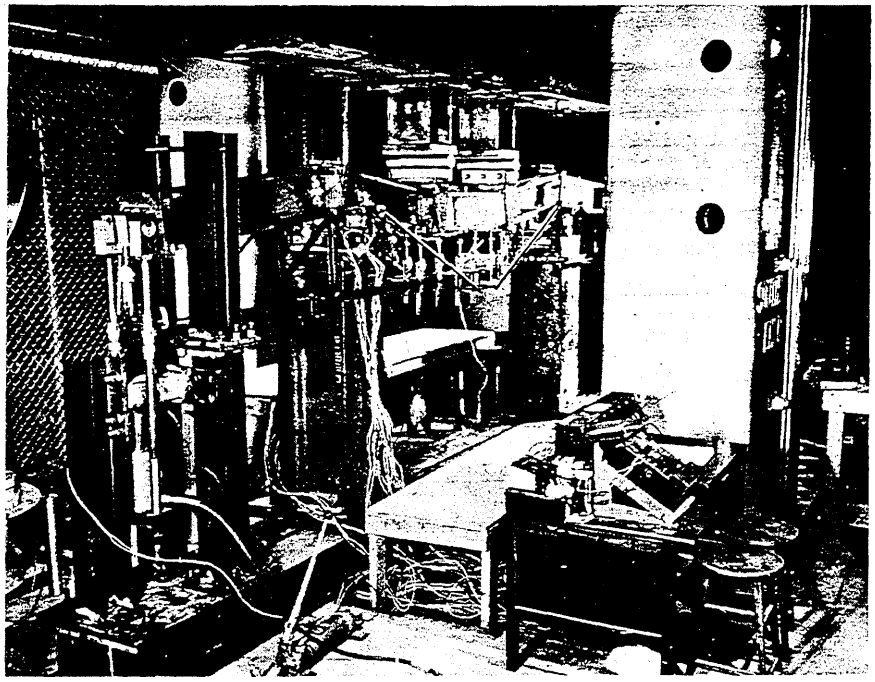

FIG. 35 BEAM B1 AFTER TEST

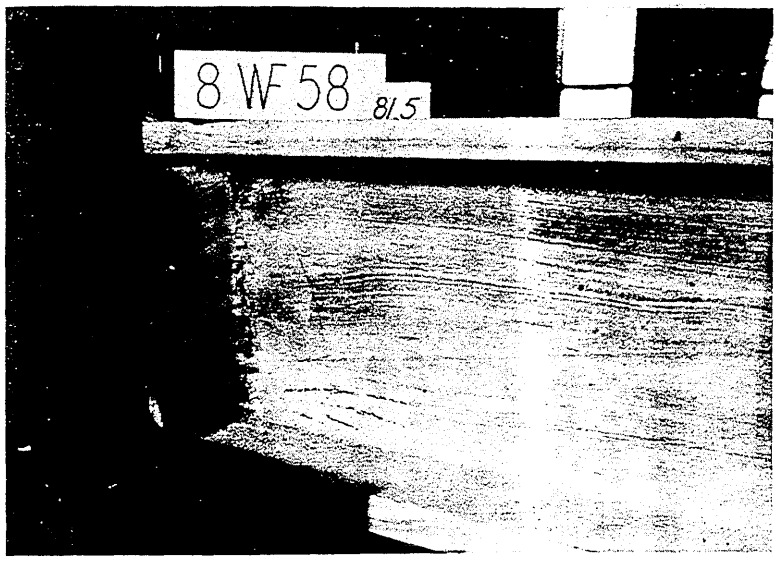

FIG. 36 BEAM B1 - V-M SECTION - LOAD = 81.5 KIPS
(REACTION ON LEFT)

FIG. 37 BEAM B1 - V-M SECTION - LOAD = 100 KIPS
(REACTION ON RIGHT)

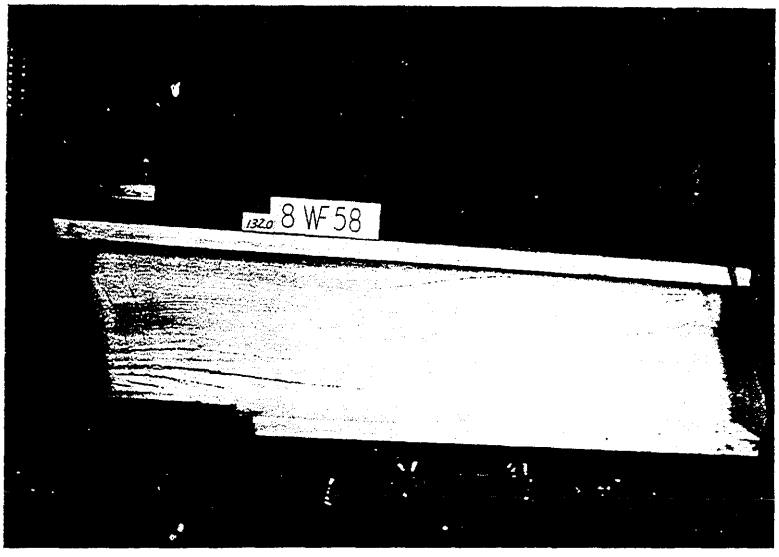

FIG. 38 BEAM B1 - V-M SECTION - LOAD = 132 KIPS
(REACTION ON LEFT)

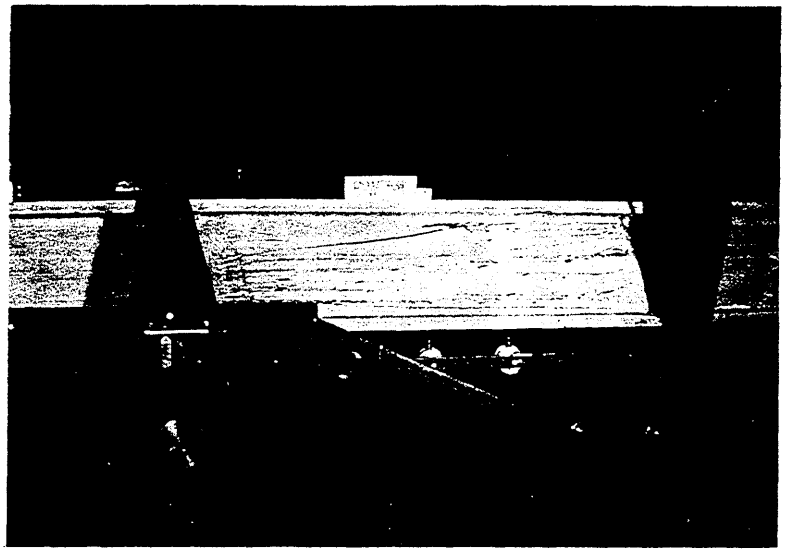

FIG. 39 BEAM B1 - V-M SECTION - LOAD = 150.5 KIPS
(REACTION ON LEFT)

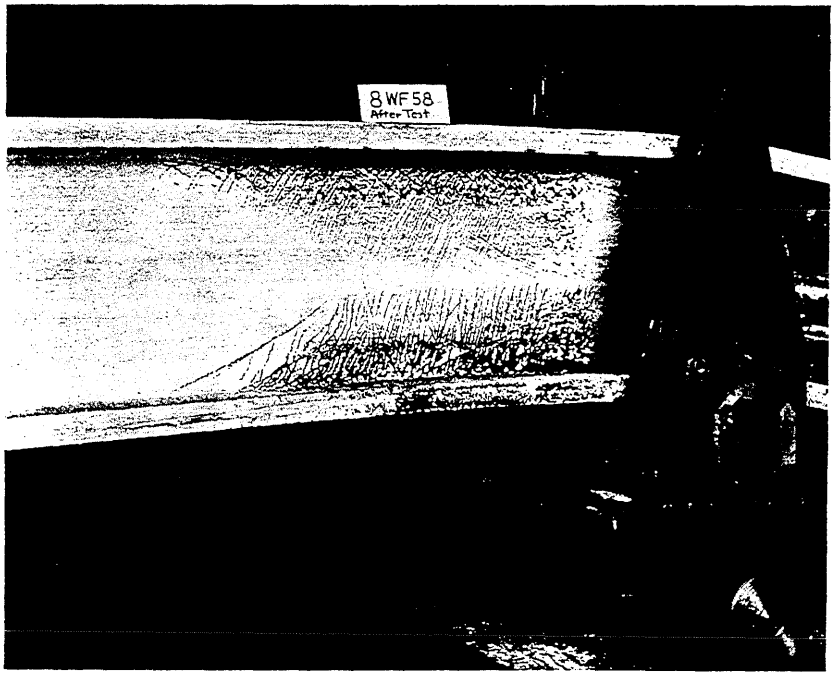

FIG. 40 BEAM B1 - CANTILEVER SECTION - AFTER TEST
(REACTION AT RIGHT)

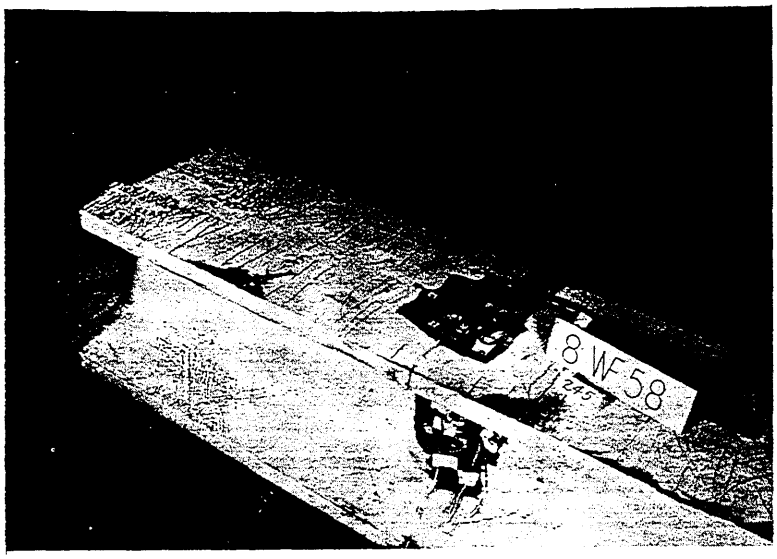

FIG. 41 BEAM B1 - CENTRAL SECTION - LOAD = 245 KIPS

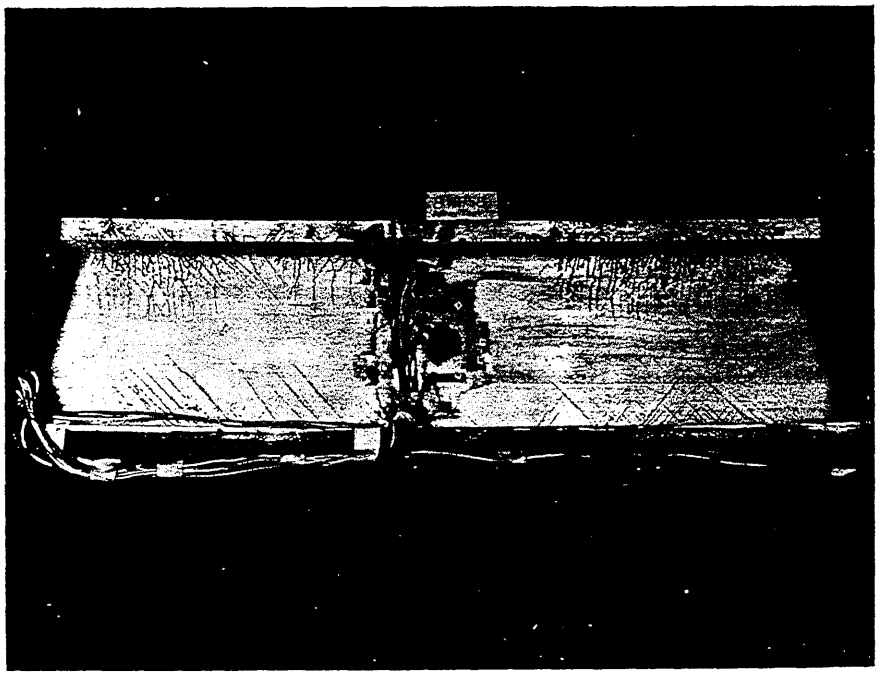

FIG. 42 BEAM B1 - CENTRAL SECTION - AFTER TEST

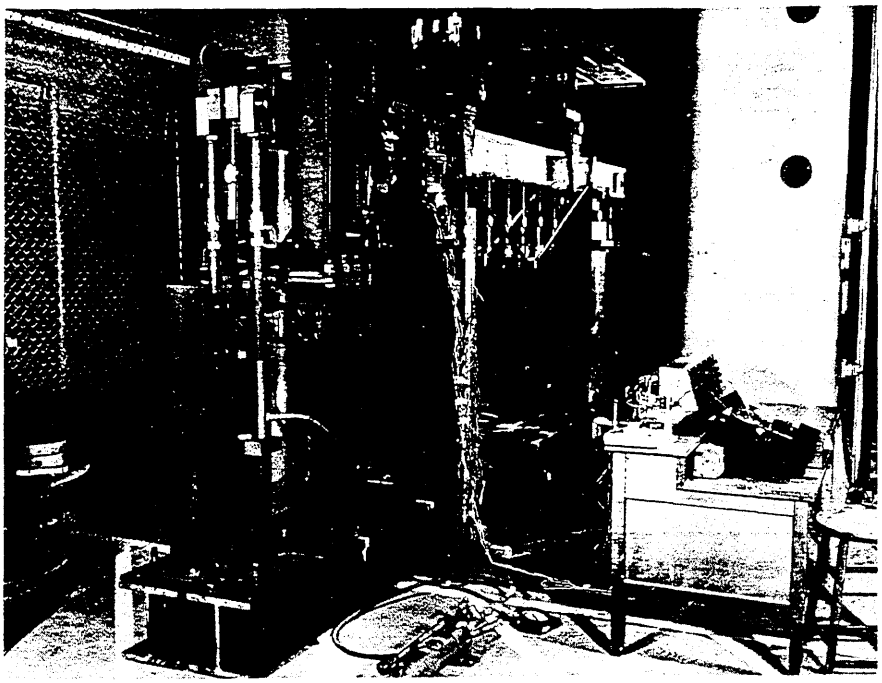

FIG. 43 BEAM B2 BEFORE TEST

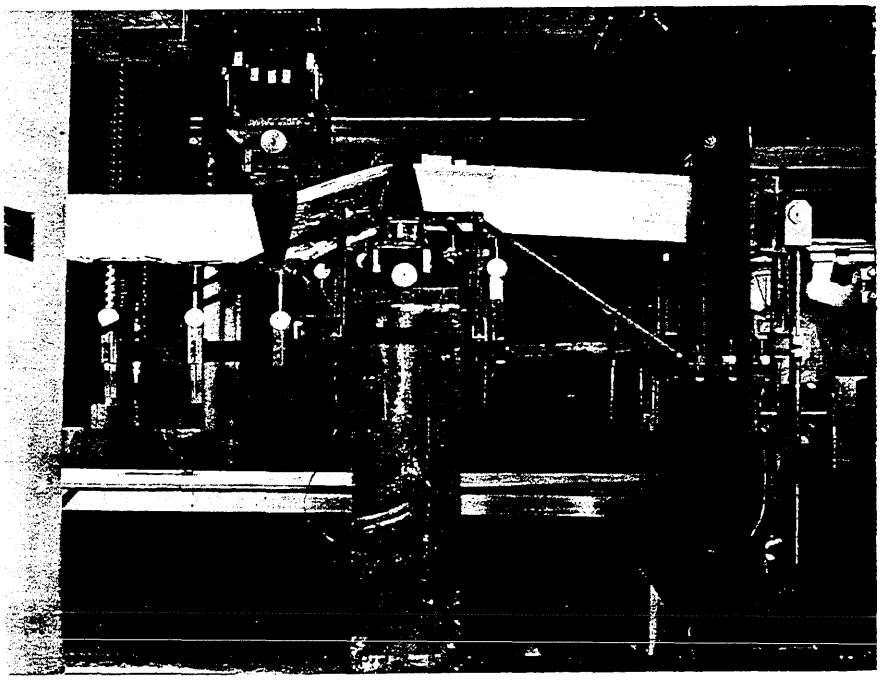

FIG. 44 BEAM B2a - SHOWING SHEAR DEFORMATION - AFTER TEST

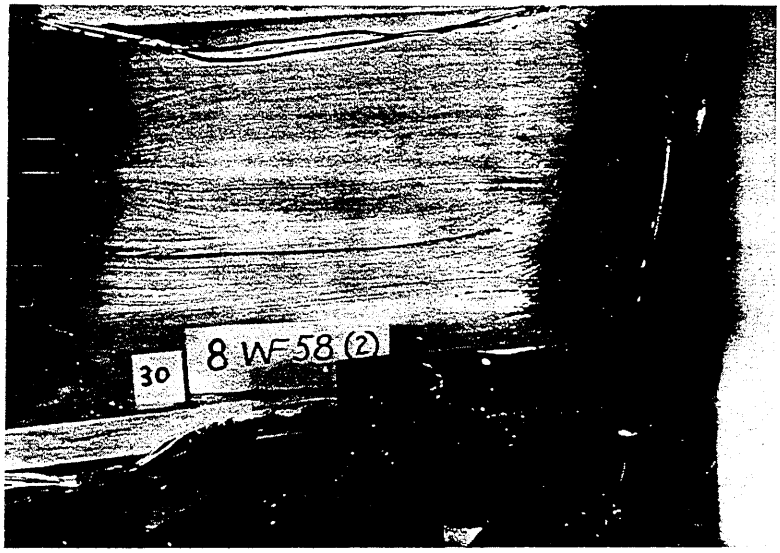

FIG. 45 BEAM B2a - V-M SECTION - LOAD = 30 KIPS
(REACTION ON RIGHT)

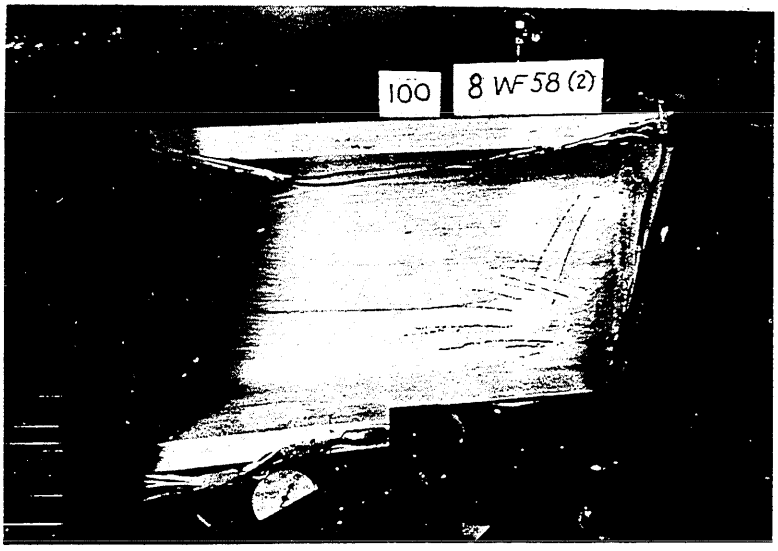

FIG. 46 BEAM B2a - V-M SECTION - LOAD = 100 KIPS
(REACTION ON RIGHT)

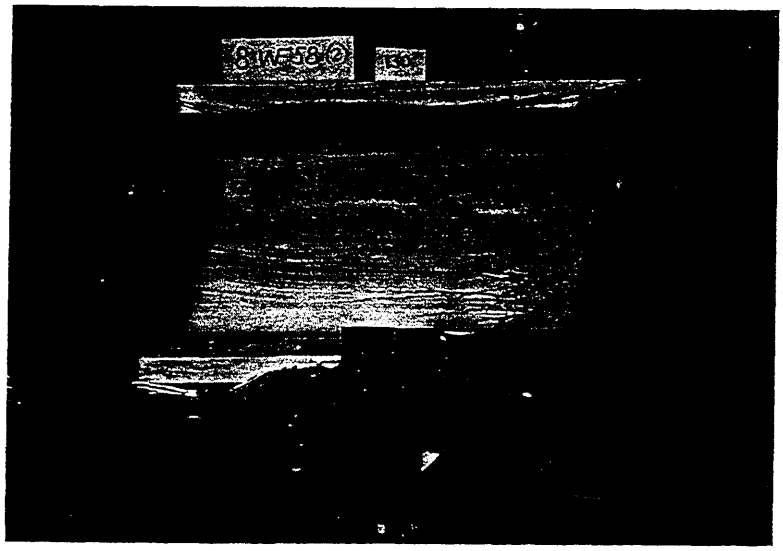

FIG. 47 BEAM B2a - V-M SECTION - LOAD = 130 KIPS
(REACTION ON RIGHT)

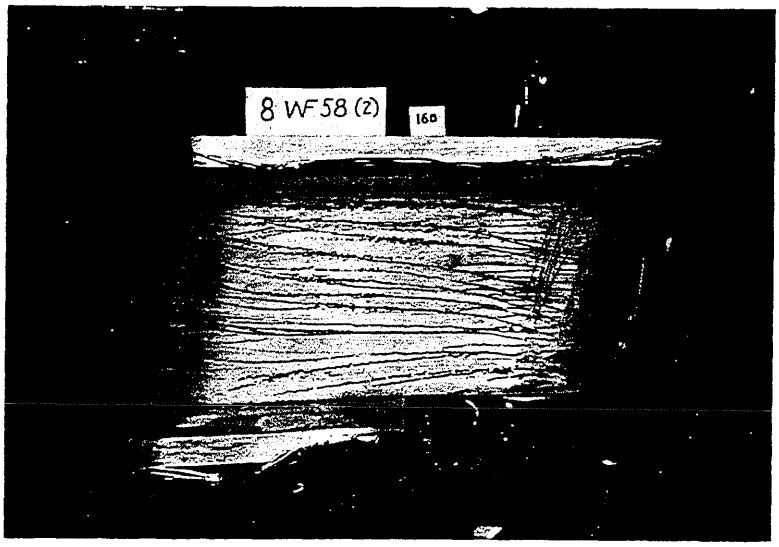

FIG. 48 BEAM B2a - V-M SECTION - LOAD = 160 KIPS
(REACTION ON RIGHT)

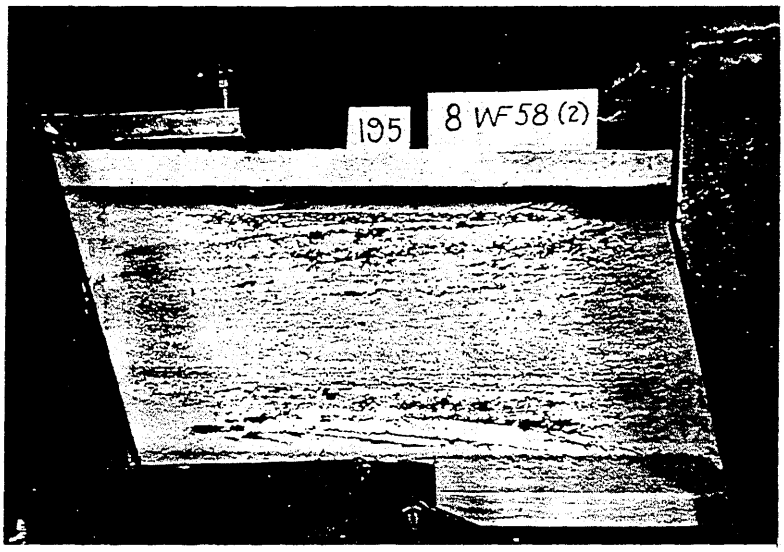

FIG. 49 BEAM B2a - V-M SECTION - LOAD = 195 KIPS (REACTION ON LEFT)

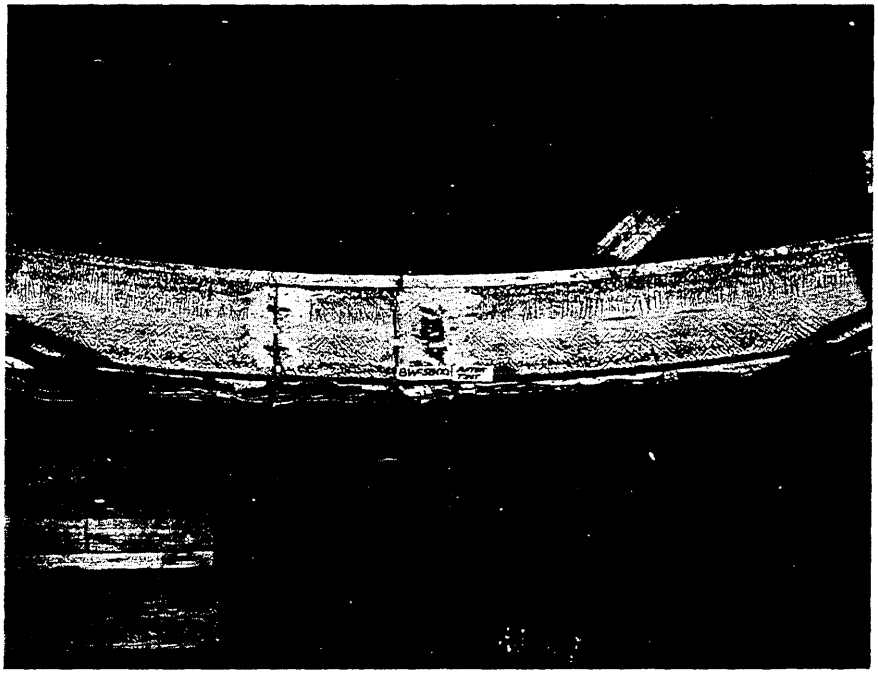

FIG. 50 BEAM B2b - CENTRAL SECTION AFTER PURE BENDING TEST

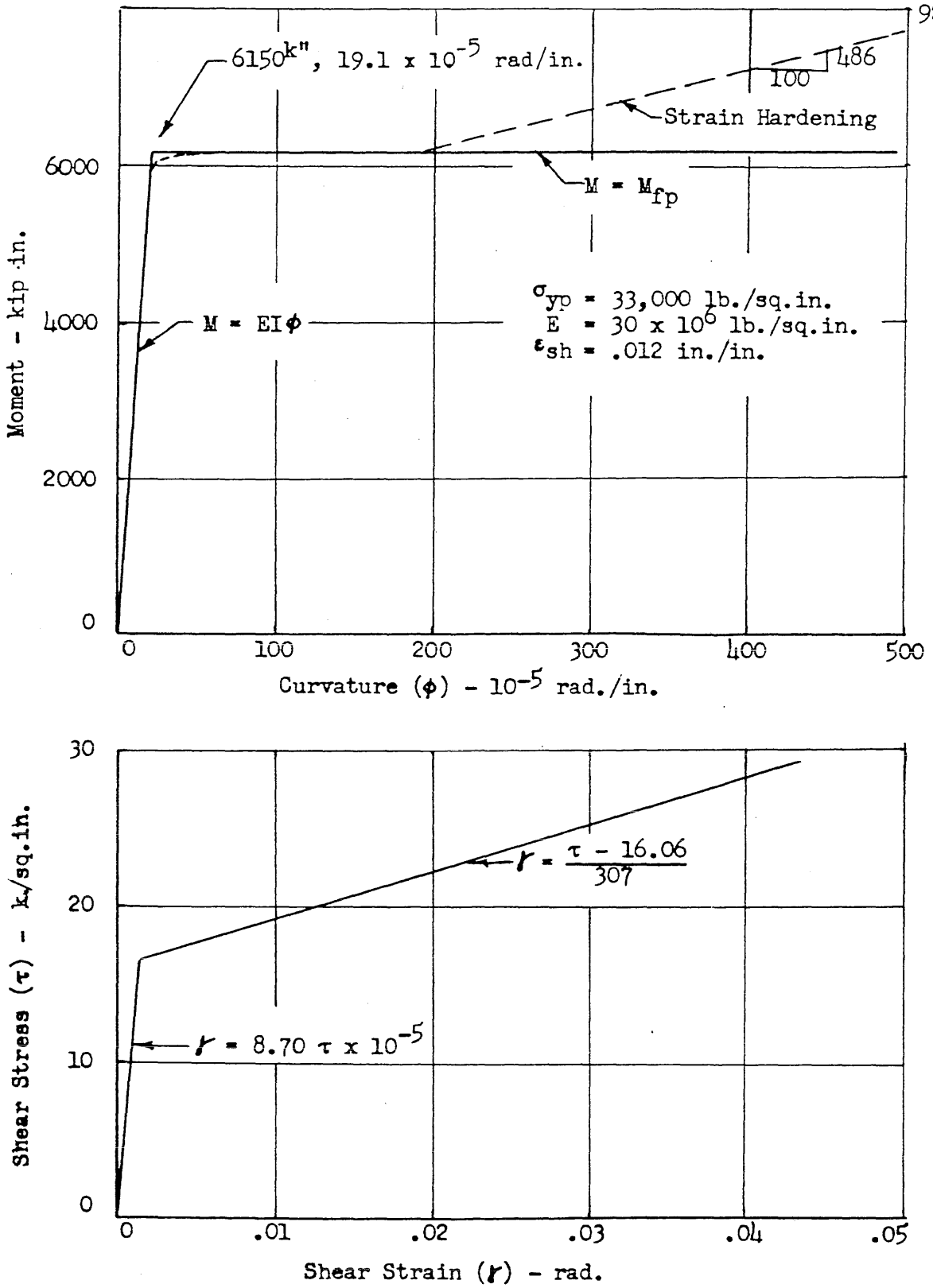

FIG. 51 M-φ AND τ-γ CURVES USED IN COMPUTATIONS FOR 12WF120 BEAM

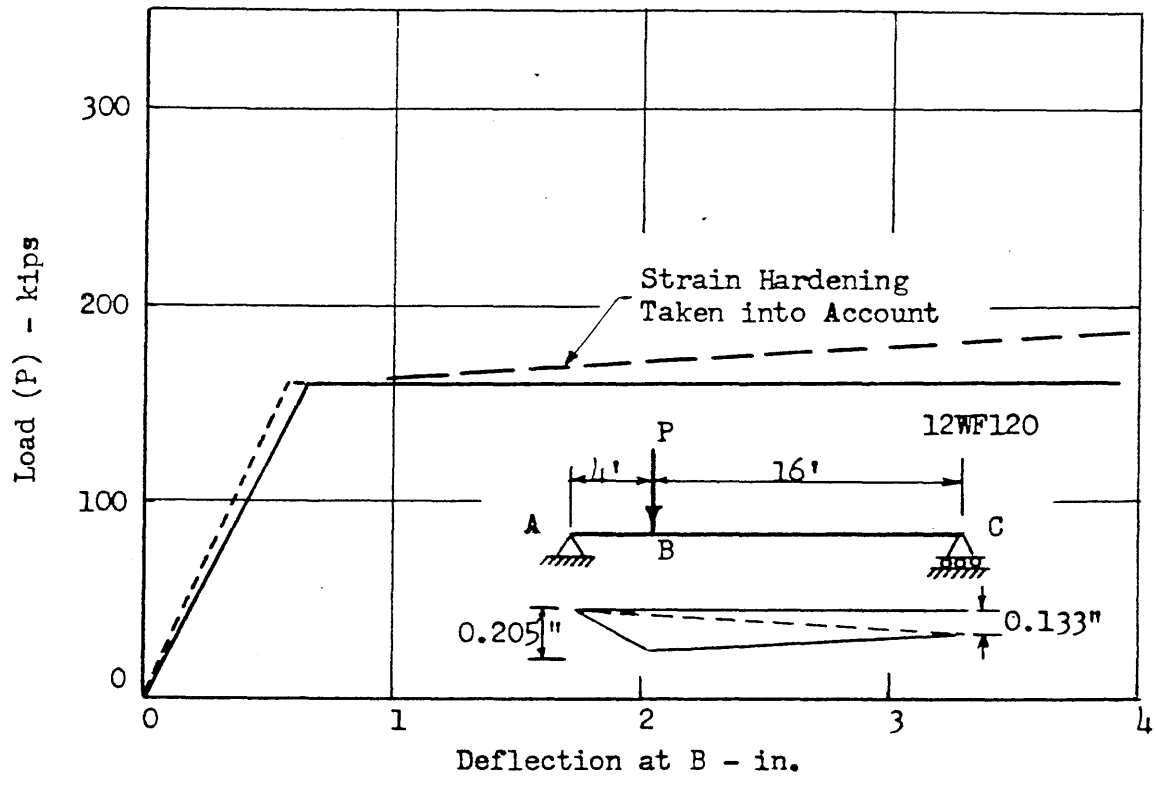

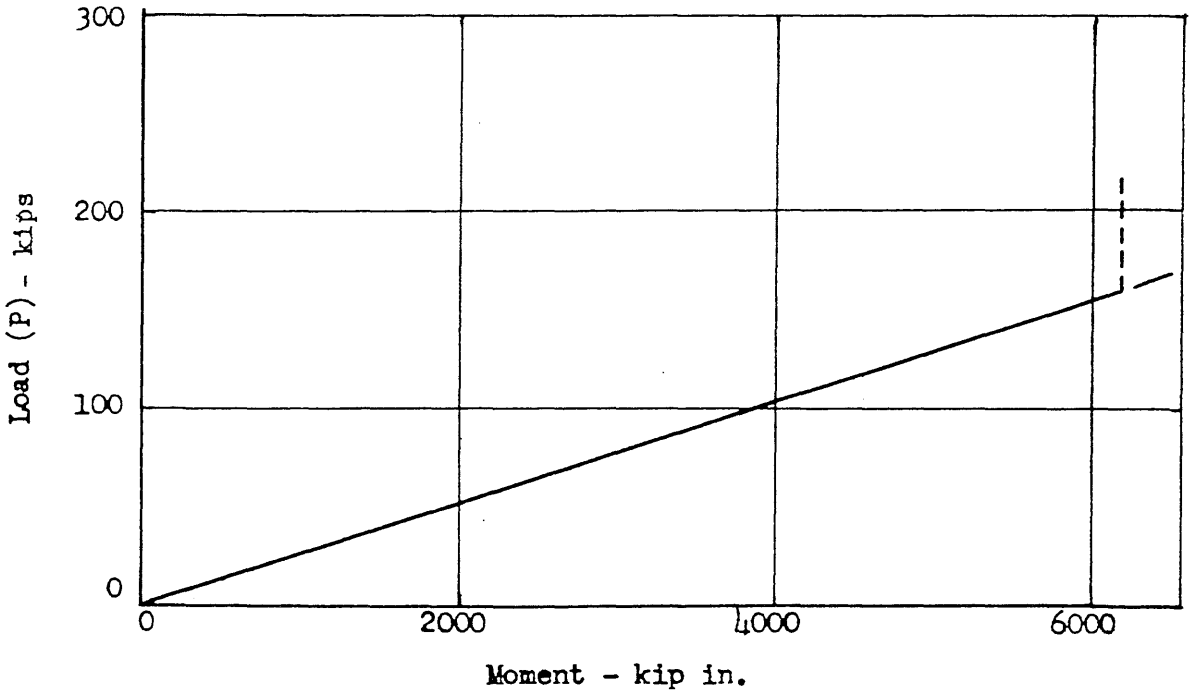

FIG. 52 LOAD - DEFLECTION - MOMENT RELATIONSHIPS FOR AN UNSYMMETRICALLY LOADED SIMPLE BEAM

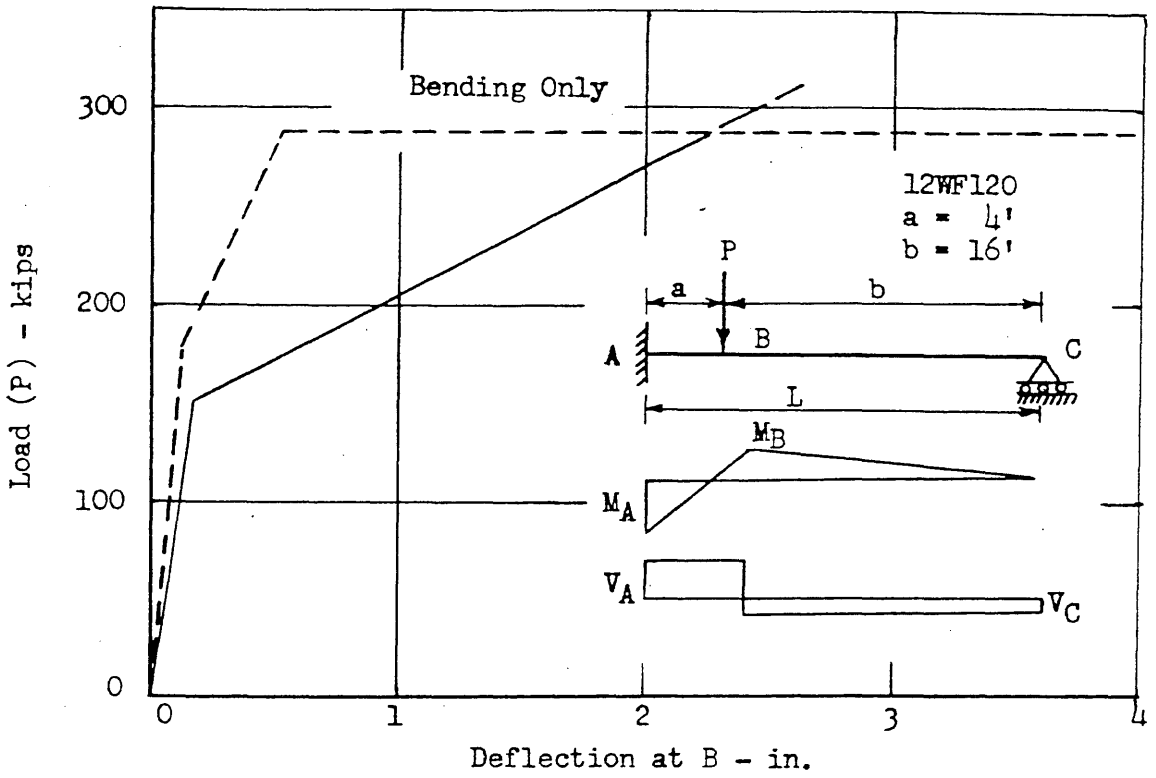

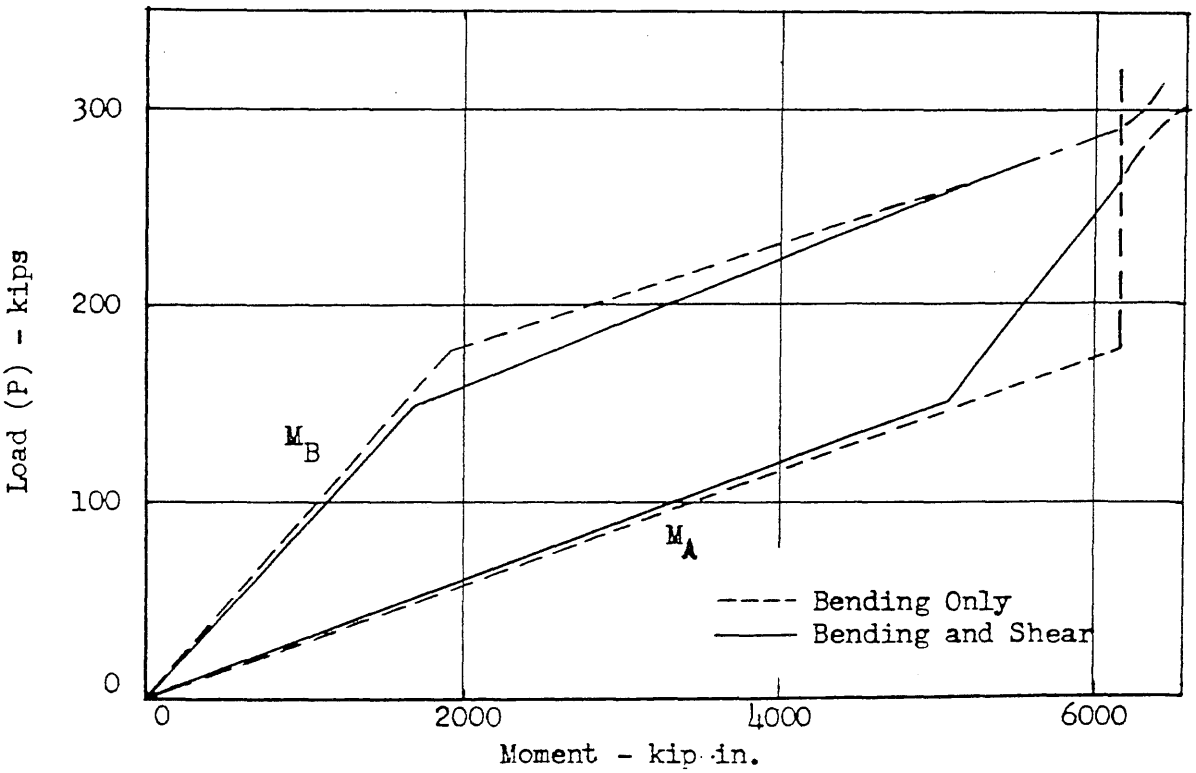

FIG. 53 LOAD - DEFLECTION - MOMENT RELATIONSHIPS FOR AN UNSYMMETRICALLY LOADED BEAM WITH ONE END FIXED

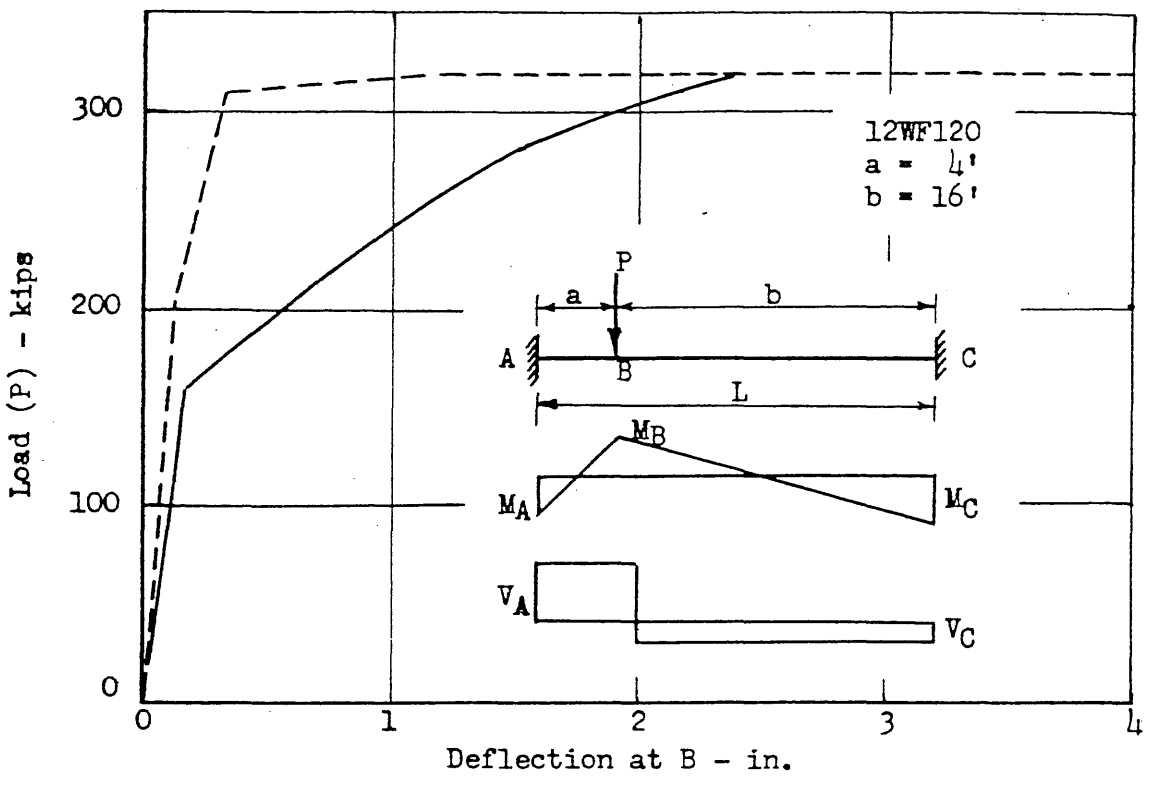

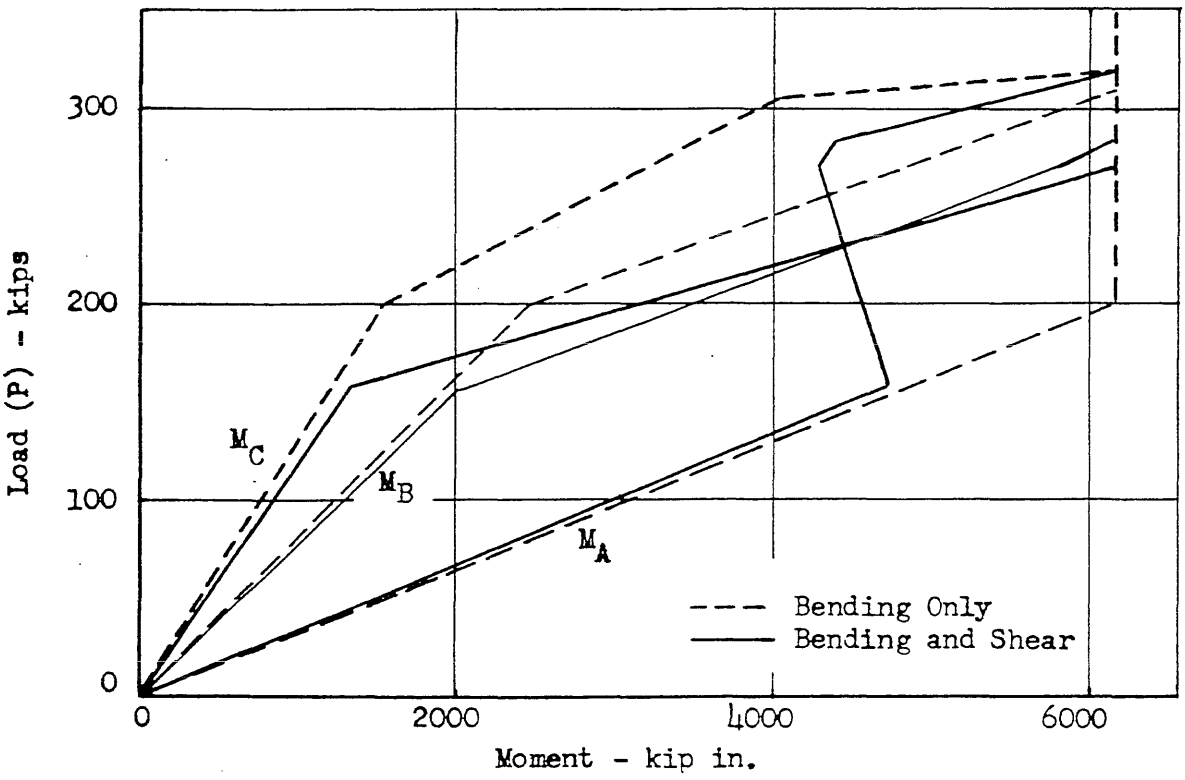

FIG. 54 LOAD - DEFLECTION - MOMENT RELATIONSHIPS FOR AN UNSYMMETRICALLY LOADED BEAM WITH BOTH ENDS FIXED

DISTRIBUTION

Contract No. AF 33(616)-170

Commanding General, Headquarters
Air Materiel Command
Wright-Patterson Air Force Base
Dayton, Ohio
Attn: MCAIEB (5)

The Chief,
Armed Forces Special Weapons Project
Washington 25, D. C.
Attn: Weapon Effects Division (1)

Director of Intelligence
Headquarters USAF
Washington 25, D. C.
Attn: Mr. R. G. Grassy - AFOIN-3B (1)

Commander
Wright Air Development Center
Wright-Patterson Air Force Base
Dayton, Ohio
Attn: Maj. Andrew Boreske, WCOES-2 (1)

The Rand Corporation
1700 Main Street
Santa Monica, California
Attn: Dr. Marc Peter (1)

Massachusetts Institute of Technology
Department of Civil and Sanitary Engineering
Room 1-232
Cambridge 39, Massachusetts
Attn: Dr. Charles Norris (1)

Drexel Institute
Philadelphia, Pennsylvania
Attn: Prof. Harry Bowman (1)

Armour Research Foundation
35 W. 33rd Street
Chicago 16, Illinois
Attn: Dr. S. J. Fraenkel (1)

DISTRIBUTION (Continued)

American Machine and Foundry Co.
Mechanics Research Department
1104 South Wabash Avenue
Chicago 5, Illinois
Attn: Mr. J. E. Fitzgerald (1)

Document Service Center (DSC)
U. B. Building
Dayton, Ohio (1)

Dean W. L. Everitt
University of Illinois (1)

Professor N. M. Newmark
University of Illinois (2)

Professor W. H. Munse
University of Illinois (1)

N. Brooks, Project Supervisor of
AF 24994, University of Illinois (1)

Project Supervisor (2)

Project Staff and Files (12)